2020

Investigating the coordinate regulation of stem cell proliferation and differentiation by FBF proteins

Xiaobo Wang

Investigating the coordinate regulation of stem cell proliferation and differentiation by FBF proteins

By

Xiaobo Wang

M.S., Shanghai Veterinary Research Institute, CAAS, Shanghai, China, 2010

Dissertation/Thesis

presented in partial fulfillment of the requirements for the degree of

Doctor of Philosophy

in Cellular, Molecular and Microbial Biology, Cellular and Developmental Biology

The University of Montana

Missoula, MT

Official Graduation Date (anticipated) August 2020

Submitted for approval by:

Scott Whittenburg, Dean of the Graduate School

Dr. Ekaterina Voronina, Research Advisor

Division of Biological Sciences

Dr. J. Stephen Lodmell, Committee Chair
Division of Biological Sciences

Dr. Jesse Hay

Division of Biological Sciences

Dr. Sarah Certel

Division of Biological Sciences

Dr. Kasper Hansen

Division of Biological Sciences

Wang, Xiaobo, Ph. D., May 2020 Cellular, Molecular and Microbial Biology

Abstract Title: Investigating the coordinate regulation of stem cell proliferation and differentiation by FBF proteins

Chairperson: Dr. Stephen Lodmell

Research Advisor: Dr. Ekaterina Voronina

Balance of stem cell proliferation and differentiation is important for maintaining tissue homeostasis, and uncovering the mechanisms regulating the balance of proliferation and differentiation of stem cells helps us understand the causative factors for ageing, cancer and various degenerative disorders. Pumilio and FBF (PUF) family RNA-binding proteins are conserved mRNA regulators controlling stem cell development in eukaryotes. FBF-1 and FBF-2, two PUF family proteins in *C. elegans*, are expressed in the mitotic region of the germline and are important for maintaining germline stem cells. FBF-1 and FBF-2 are very similar in primary sequence and share most of the target mRNAs, but they localize to distinct RNA granules and have different effects on target mRNAs and stem cell maintenance. This dissertation studies how FBFs mediate the coordinate regulation of germline stem cell proliferation and differentiation and the mechanisms allowing differential activities of FBF homologs in stem cells. This work has, for the first time, demonstrated that FBF-1 and FBF-2 have distinct effects on stem cell dynamics: FBF-1 restricts the rate of stem cell meiotic entry, while FBF-2 promotes both rates of proliferation and meiotic entry. Based on our findings, we propose that FBFs' coordinate regulation contributes to maintaining the balance of stem cell proliferation and differentiation in the germline. In addition, this work has also identified CCR4-NOT deadenylation machinery as an FBF-1-specific cofactor, DLC-1 as an FBF-2-specific cofactor, and five splicing factors as potential specific cofactors for FBF-2.

PUF proteins are conserved stem cell regulators in eukaryotes, from yeast to humans, and they share conserved mechanisms that affect stem cell proliferation and differentiation. This dissertation offers new mechanistic insights into PUF function in *C. elegans* that are likely relevant for other organisms.

Acknowledgements

I would like to first express my deepest and most sincere gratitude to my mentor Dr. Ekaterina (Katya) Voronina who has been working so hard supervising, instructing, and encouraging me during all kinds of trainings throughout my graduate school years. Katya is such a smart and knowledgeable scientist, whenever I was having trouble getting experiments to work or getting unexpected results, she was always so encouraging and helpful with some creative ideas helping me out of the "pits". In addition, thanks to her continuous and very patient instructions, I learned how to become an independent researcher which requires ability in independent data analysis, critical thinking, professional writing, and presentation of research work to the public. Overall, I could not have achieved what I have accomplished without her whole-heartedly instructions and encouragements. I want to say, Katya has raised me up to the best that I can be. In addition to her support for my academic development, Katya was also very understanding and supportive whenever I had to take off because of my family or my personal health reasons. I don't have better words than "THANKS" to express my gratitude regarding what she has done for me. I feel very lucky and honored to have Dr. Katya Voronina as my mentor, not only because she is my mentor, but because she showed me how to become an excellent mentor as well.

I want to express my great THANKS to all my previous and current lab members for their time and efforts contributed to my thesis project, and my research could not have gone such smoothly without their help. Especially thanks to Mary Ellenbecker for being such a supportive friend in the lab, not only because she was a very dedicated collaborator to my project, but also because she was such a good listener at those depressive time points of my life.

I am very thankful to all my dissertation committee advisors, Dr. J. Stephen Lodmell, Dr. Sarah Certel, Dr. Jesse Hay, and Dr. Kasper Hansen, for their guidance, advice and supports regarding my annual committee meeting, progressive research reports and dissertation. Thanks to Dr. Sarah Certel and Steve Lodmell for providing recommendation letters for my application of the GSA travel award and the AHA predoctoral fellowship. I especially appreciate all committee advisors for their support of my dissertation defense plan considering my special personal situation. Their time and efforts are deeply appreciated.

I also would like to thank the Graduate Education Committee (GEC) for their valuable time and guidance of programmatic requirements in the progress of my graduate school years.

As a trainee, I warmly thank all my graduate course/seminar instructors, Dr. J. Stephen Lodmell, Dr. Mark Grimes, Dr. John McCutcheon, Dr. Jeffery Good, Dr. Jesse Hay, Dr. Brent Ryckman, Dr. Klara Briknarova, Dr. Kasper Hansen, Dr. Ekaterina Voronina, Dr. J.B. Alexander (Sandy) Ross, Dr. Scott Wetzel, and Dr. Liz Putnam. Additionally, I am thankful to have opportunities to seek advice and collaborations with other scientists when presenting my research work at the membrane dynamics seminar, especially the Annual CBSD retreat supported by Dr. Stephen Sprang. I want to express special thanks to Dr. Stephen Sprang for his valuable time of becoming the chair of my comprehensive exam committee, and his recommendation letter for my application of the AHA predoctoral fellowship. I truly appreciate such a supportive academic environment created by all faculty of the CMMB program.

My sincere thanks to Dr. Gretchen McCaffrey for allowing me to join in the writing workshop and her very helpful instructions in my proposal writings. Also thanks to Miss Laure Pengelly Drake for her time instructing me in my application for the Bertha Morton Scholarship, and other tutors at the writing center for their help with my writings.

I also wish to thank others at the University of Montana:

Dr. Mike Minnick and Jim Driver for their guidance during my TA experience, and Sarah Weldon for assisting with material preparation for the lab courses that I taught.

Dr. Jim Battisti for his assistance with my application for the Student Research Grant Program provided by the Montana Academy of Sciences.

Minnick lab, Hay lab, Lodmell lab, Nunberg lab, and especially Sprang Lab and Ryckman Lab for sharing experimental materials and equipment.

Lou Herritt and Zifan Wang for assisting me during confocal microscopy imaging.

David Xing for training me to use the qPCR machine.

Jill Burke, Zooey Zephyr, Ruth Johnson, Rochelle Krahn and Janean Clark in the DBS office for all administrative services such as class room reservation, graduate program related information emails, and payroll/pay/travel expenses/forms.

Additional thanks to all the friends we met in Missoula who helped us get settled. Especially thanks to Qin Yu and her husband Wayne Davis for their support and care in our lives.

Last but not least, I would like to express my gratitude for the love and support from all my family members. My sincere and warm thanks to my husband Feng Yi for bringing me to the beautiful town of Missoula, his support in my studies and career development, and especially his love and care in my life. I deeply appreciate all the supports from my other family members back in China, my parents, my sister, and my grandpa who passed away a little before I started my graduate school. I felt ashamed that I could not come back when my grandpa was dying, but I wish they all would understand and feel proud of me for graduating.

TABLE OF CONTENTS

Chapter 1. Diverse Roles of PUF Proteins in Germline Stem and Progenitor Cell Development in *C. elegans*

(This chapter is a modified version of the manuscript published in Frontiers in cell and developmental biology, 06 February 2020, https://doi.org/10.3389/fcell.2020.00029)

Stem cell development depends on post-transcriptional regulation mediated by RNA-binding proteins (RBPs) (Zhang et al., 1997; Forbes and Lehmann, 1998; Okano et al., 2005; Ratti et al., 2006; Kwon et al., 2013). Pumilio and FBF (PUF) family RBPs are highly conserved post-transcriptional regulators that are critical for stem cell maintenance (Wickens et al., 2002; Quenault et al., 2011). The RNA-binding domains of PUF proteins recognize a family of related sequence motifs in the target mRNAs, yet individual PUF proteins have clearly distinct biological functions (Lu et al., 2009; Wang et al., 2018). The *C. elegans* germline is a simple and powerful model system for analyzing regulation of stem cell development. Studies in *C. elegans* uncovered specific physiological roles for PUFs expressed in the germline stem cells ranging from control of proliferation and differentiation to regulation of the sperm/oocyte decision. Importantly, recent studies started to illuminate the mechanisms behind PUF functional divergence. This review summarizes the many roles of FBF-1 and FBF-2 in germline stem and progenitor cells (SPCs) and discusses the factors accounting for their distinct biological functions. PUF proteins are conserved in evolution, and insights into PUF-mediated regulation provided by the *C. elegans* model system are likely relevant for other organisms.

Introduction

Post-transcriptional regulation of gene expression governs the rate of protein production through the control of key steps in mRNA life cycle. In eukaryotes, RNA-binding proteins (RBPs) play critical roles in mRNA biogenesis, stability, function, transport, and cellular localization essential for post-transcriptional regulation (Glisovic et al., 2008). RBPs expressed in stem cells contribute to the regulation of stem cell self-renewal and differentiation (Forbes and Lehmann, 1998; Kwon et al., 2013; Okano et al., 2005; Ratti et al., 2006; Zhang et al., 1997), while misregulation of RBP activity can lead to tumors (Degrauwe et al., 2016; Rezza et al., 2010). Post-

transcriptional regulation in stem cells relies on the combined activities of many RBPs (Arvola et al., 2017; Eckmann et al., 2004). Investigating the basic mechanisms of RBP function in stem cells will advance our understanding of abnormal post-transcriptional regulation relevant to human diseases, such as cancer.

PUF family RBPs are highly conserved eukaryotic posttranscriptional regulators (Quenault et al., 2011; Wickens et al., 2002). The name of this family comes from the first identified PUF proteins, Pumilio in *D. melanogaster* and *fem-3*-binding factor (FBF) in *C. elegans*. PUF proteins control diverse biological processes including oogenesis (Parisi and Lin, 1999), organelle biogenesis (García-Rodríguez et al., 2007), neuronal function (Mee et al., 2004), and memory formation (Dubnau et al., 2003; Zhang et al., 2017). In addition to these roles, PUF proteins share an evolutionarily conserved role in stem cell maintenance. Mutation of Pumilio induces loss of female germline stem cells in *Drosophila* due to differentiation to cystoblasts and then egg chambers (Forbes and Lehmann, 1998; Lin and Spradling, 1997). Similarly, loss of PUF proteins in *C. elegans* results in germline stem cells entering meiosis and undergoing spermatogenesis (Crittenden et al., 2002; Haupt et al., 2019b; Zhang et al., 1997) and knockdown of planarian homolog *DjPum* by RNA interference induces loss of totipotent stem cells called neoblasts (Salvetti et al., 2005). In mammals, PUM proteins contribute to stem cell maintenance across multiple tissues (Naudin et al., 2017; Shigunov et al., 2012; Zhang et al., 2017).

Canonical PUF proteins are characterized by a conserved RNA-binding domain (Pumilio homology domain, PUM-HD) with eight consecutive α-helical PUM repeats (Hall, 2016; Wang et al., 2001; Zamore et al., 1997; Zhang et al., 1997). Crystal structures of the classical PUM-HD uncover a crescent arrangement of PUM repeats. Single-stranded RNA binds to the inner concave surface of PUM-HD. Typically, one PUM repeat contacts one RNA base. A five-amino-acid motif in the second alpha helix of a PUM repeat determines the sequence specificity of RNA base recognition (Campbell et al., 2014; Cheong and Hall, 2006; Wang et al., 2002). Three key residues in the motif directly interact with RNA, thus comprising the tripartite recognition motifs (TRMs) (Campbell et al., 2014; Hall, 2016; Wang et al., 2002). Although individual PUF proteins preferentially associate with RNA motifs of distinct lengths and sequences, the canonical target motifs share the core UGU triplet (Lu et al., 2009; Wang et al., 2018).

PUF proteins control stability and translation of their target mRNAs by binding to their 3'UTRs (Zamore et al., 1997; Zhang et al., 1997). The best-documented mechanism of PUF-mediated regulation is through deadenylation of the target mRNAs that results in translational repression or mRNA decay (Goldstrohm et al., 2006; Kadyrova et al., 2007; Van Etten et al., 2012; Weidmann et al., 2014; Wreden et al., 1997). Alternatively, PUFs can interfere with recognition of cap structure by translation initiation factors through directly binding to the cap (Cao et al., 2010) or through recruiting cap-binding cofactors (Cho et al., 2006; Cho et al., 2005). Additionally, PUFs might attenuate translational elongation through an interaction with Argonaute family proteins (Friend et al., 2012). For all PUFs investigated to date, high-throughput approaches have suggested a large number of putative regulatory targets. Putative PUF target mRNAs have been identified in yeast, *Drosophila, C. elegans,* and humans by using RIP (RNA Immunoprecipitation)-Chip, RIP-seq, and CLIP (Cross-linking immunoprecipitation)-seq (Gerber et al., 2004; Gerber et al., 2006; Hafner et al., 2010; Morris et al., 2008; Porter et al., 2019; Prasad et al., 2016). The conservation of a number of PUF targets between nematodes and other species including humans was first reported in a microarray study (Kershner and Kimble, 2010) and then confirmed and expanded by CLIP-seq analysis (Porter et al., 2019; Prasad et al., 2016). The shared PUF target mRNAs are enriched for biological process GO terms such as cell cycle, cell division, and nuclear division. Cell cycle regulation is central to stem cell maintenance (Boward et al., 2016), and mRNA target conservation reflects PUF proteins' ancient role in stem cell maintenance.

The *C. elegans* germline is a powerful model that revealed many aspects of PUF protein function in germline stem cells. Ten PUF proteins identified in *C. elegans* are clustered into 4 subfamilies: PUF-8/9, FBF-1/2, PUF-3/11/4, and PUF-5/6/7 (Hubstenberger et al., 2012; Liu et al., 2012; Stumpf et al., 2008; Wickens et al., 2002). Among these PUF proteins, FBF-1 and FBF-2 that are enriched in germline stem cells support stem cell maintenance (Crittenden et al., 2002; Lamont et al., 2004; Voronina et al., 2012), yet each is functionally distinct. This chapter focuses on the contribution of FBF-1 and FBF-2 to germline stem and progenitor cell function. We then discuss recent advances in uncovering the determinants that regulate FBF biological functions.

The *C. elegans* germline is a powerful model that revealed many aspects of PUF protein function in germline stem cells. Ten PUF proteins identified in *C. elegans* are clustered into 4 subfamilies:

PUF-8/9, FBF-1/2, PUF-3/11/4, and PUF-5/6/7 (Wickens et al., 2002; Stumpf et al., 2008; Hubstenberger et al., 2012; Liu et al., 2012). Among the identified PUF proteins, FBF-1 and FBF-2 that are enriched in germline stem cells support stem cell maintenance (Crittenden et al., 2002; Lamont et al., 2004; Voronina et al., 2012), yet each is functionally distinct. This chapter focuses on the contribution of FBF-1 and FBF-2 to germline stem and progenitor cell function. We then discuss recent advances in uncovering the determinants that regulate FBF biological functions.

C. elegans Germline, a Powerful Model for Stem Cell Studies

Overall Structure of C. elegans Germline

The *C. elegans* germline is a simple but very powerful model system for studying stem cell biology (Figure 1-1A). *C. elegans* can exist as hermaphrodites or males, and in this review, we are focusing on hermaphrodites, although mechanisms regulating germline stem cells are similar in the two sexes. A *C. elegans* adult contains two symmetric U-shaped germlines. Most of the *C. elegans* germline, except for late oocytes, is a syncytium, where individual germ cells have an opening to a central shared cytoplasmic core (Hirsh et al., 1976). Although germ cells have access to continuous cytoplasm, the communication between cells is limited and neighboring germ cells can be seen at distinct stages of cell cycle or differentiation. Similar to the germlines of other organisms, the *C. elegans* germline is maintained by a population of proliferative stem cells in the stem cell niche at its distal end (Figure 1A; Pazdernik and Schedl, 2013). When progenitor cells leave the niche, they enter meiosis followed by differentiation into sperm during larval development and into oocytes in adulthood. Maintenance of stem and progenitor cells in the mitotic zone is critical for *C. elegans* germline development and worm fertility.

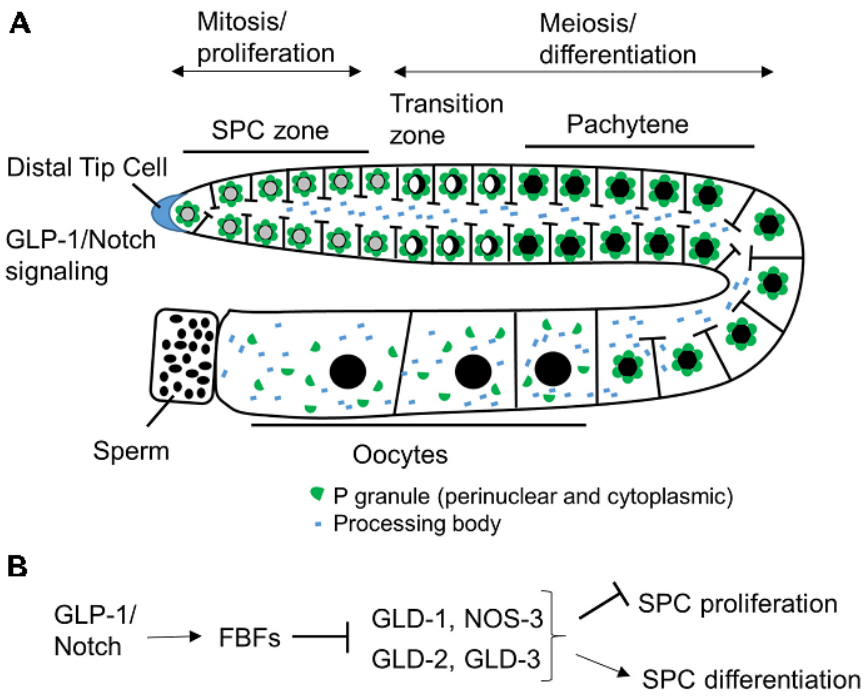

Figure 1-1. Schematic of *C. elegans* hermaphrodite germline and RNA-binding protein network downstream of GLP-1/Notch. (A) *C. elegans* germline development is supported by continuous SPC proliferation promoted by GLP-1/Notch signaling from the DTC (Pazdernik and Schedl, 2013). Progenitors enter meiosis when they reach the transition zone, and later differentiate into sperm and oocytes. Several types of RNA granules reside in germ cells and facilitate germ cell development and embryogenesis. (B) Downstream of GLP-1/Notch, FBFs maintain SPC proliferation by repressing the expression of GLD-1, GLD-2, and GLD-3 that inhibit SPC proliferation and promote differentiation (Kimble and Crittenden, 2007 and references in sections "RNA-Binding Protein Network Downstream of GLP-1/Notch" and "PUF Function in Maintaining Germline SPCs").

Germline Stem and Progenitor Cells

The proliferative zone of the *C. elegans* germline extends about 20 cell diameters from the distal tip, and contains cells in a mitotic cell cycle and cells that have entered meiotic S-phase (Crittenden et al., 2006; Fox et al., 2011; Jaramillo-Lambert et al., 2007). Unlike other stem cell systems with distinct stem cells and transit amplifying cells, the proliferative zone contains

developmentally equivalent cells (Fox and Schedl, 2015). In this review, we collectively refer to the cells that have not entered meiosis as stem and progenitor cells (SPCs). The *C. elegans* germline SPC zone is maintained within a niche formed by a single mesenchymal cell, called the distal tip cell (DTC), which caps the distal end of the germline and extends its cytoplasmic processes proximally (Byrd et al., 2014; Crittenden et al., 2006; Kimble and White, 1981). The DTC preserves the mitotic identity and promotes mitotic division of SPCs through the canonical GLP-1/Notch signaling that is highly conserved in most multi-cellular organisms (Austin and Kimble, 1987). Loss-of-function mutations of GLP-1/Notch signaling components such as the receptor *glp-1,* ligands *lag-2* and *apx-1*, and downstream transcriptional targets *lst-1* and *sygl-1* cause germline stem cells to enter meiosis prematurely, which is similar to the DTC removal (Austin and Kimble, 1987; Henderson et al., 1997; Kershner et al., 2014; Kimble and White, 1981; Nadarajan et al., 2009). By contrast, germ cells of the *glp-1(oz112gf)* gain-of-function mutant with constitutive GLP-1 signaling fail to exit from the mitotic cell cycle leading to tumorous germlines (Berry et al., 1997).

RNA-Binding Protein Network Downstream of GLP-1/Notch

Post-transcriptional control is the prevalent mechanism for regulating gene expression in the *C. elegans* germline (Merritt et al., 2008). Downstream of GLP-1/Notch, germline stem cell development is regulated by a network of posttranscriptional regulators that includes a large number of RBPs, a subset of which is shown in Figure 1-1B. FBF-1 and FBF-2, PUF family RBPs expressed in the distal germline, control stem cell maintenance and sex fate (Crittenden et al., 2002; Zhang et al., 1997). Additionally, four RNA regulators, including three GLD proteins and NOS-3, act in two parallel pathways that inhibit mitosis and promote meiosis (Kimble and Crittenden, 2007). GLD-1 (a KH-motif RBP) and NOS-3 (Nanos protein family member) form a translational repression pathway (Hansen et al., 2004b), while the cytoplasmic poly(A) polymerase formed by the complex of GLD-2 (the poly(A) polymerase enzyme) and GLD-3 (a homolog of Bicaudal-C RBP) constitutes a translational activation pathway (Eckmann et al., 2004).

Cytoplasmic Organization of RNA Regulation

Many RBPs that mediate post-transcriptional regulation of germ cell development are found enriched at cytoplasmic foci called RNA granules. Germ cells have a number of RNA granule

subtypes (Figure 1-1A), including germ granules or P granules in *C. elegans*, processing bodies, and stress granules (Voronina et al., 2011). The processing bodies and stress granules are distributed throughout the cytoplasm in somatic cells as well as in germ cells (Boag et al., 2005; Hubstenberger et al., 2017; Lechler et al., 2017; Noble et al., 2008). By contrast, P granules are perinuclear cytoplasmic RNA granules specific to germ cells and present throughout germline development, excluding mature sperm (Strome and Wood, 1982). All PUF proteins expressed in the *C. elegans* germline are found in RNA granules (Ariz et al., 2009; Haupt et al., 2019b; Noble et al., 2008; Voronina et al., 2012). PUF-5 colocalizes with processing body components (Noble et al., 2008), PUF-8 and FBF-2 localize to P granules (Ariz et al., 2009; Voronina et al., 2012; Wang et al., 2016), and the identities of RNA granules containing FBF-1 or PUF-3 and PUF-11 are currently unknown.

Regulatory Roles of FBF Proteins in *C. elegans* Germline Stem and Progenitor Cells

FBF Function in Maintaining Germline SPCs

Germline stem cells are maintained by promoting proliferation and/or inhibiting cell death and differentiation. FBF-1 and FBF-2 are redundantly required for maintaining germline SPCs in adult hermaphrodites since a *C. elegans* double mutant for both FBFs lose their germline stem cells by 24 hours after the last larval stage (Crittenden et al., 2002). Several FBF targets have been proposed to contribute to FBFs' role in SPC maintenance (Figure 2A). First, FBFs are suggested to repress expression of MPK-1, a homolog of Mitogen-activated protein kinase (MAPK)/ERK, and *mpk-1* mRNA contains two FBF binding elements in its 3'UTR (Lee et al., 2007a). This repression was hypothesized to be important for stem cell maintenance since RNAi-mediated knockdown of *mpk-1* increased the number of mitotic germ cells, while promoting MPK-1 activity by a Ras gain-of-function mutation *let-60(n1046)* decreased the number of mitotic germ cells (Lee et al., 2006). Similarly, MAPK repression is observed to promote self-renewal of embryonic stem cells and skeletal muscle stem cells (Bernet et al., 2014; Burdon et al., 1999). However, in addition to repressing MPK-1, FBFs repress the expression of its negative regulator, MAPK inactivating phosphatase LIP-1 (Lee et al., 2006). Therefore, an *fbf* mutation would derepress both MPK-1 and LIP-1 that inhibits MAPK activity and thus might not result in abnormal activation of MPK-1 in SPCs. Instead, such mutation would result in a sensitized background that might deregulate MPK-

1 following additional genetic lesions. Regulation of MAPK by PUF homologs appears conserved in evolution, and was also documented in human embryonic stem cells as well as in mouse spermatocytes (Chen et al., 2012; Lee et al., 2007a). Second, FBFs promote self-renewal of germline stem cells by repressing expression of CKI-2 (Kalchhauser et al., 2011), a Cyclin-dependent kinase inhibitor that regulates cell cycle entry/exit decisions (Buck et al., 2009). Removing *cki-2* partially rescues the germline stem cell depletion phenotype in *fbf-1 fbf-2* double mutant adult hermaphrodites (Kalchhauser et al., 2011), suggesting that repression of *cki-2* is not the only mechanism by which FBFs promote stem cell proliferation. CIP/KIP family cyclin-dependent kinase inhibitors are conserved targets of PUF proteins as they were found to be regulated by PUFs in mouse embryos and human cells (Kedde et al., 2010; Lin et al., 2019). Interestingly, genes encoding diverse cell cycle regulators, beyond *cki-2* and its homologs, are enriched among target mRNAs pulled down with FBFs as well as PUF proteins from other organisms (Chen et al., 2012; Hafner et al., 2010; Kershner and Kimble, 2010; Porter et al., 2019; Prasad et al., 2016), suggesting a conserved mechanism of PUF-mediated control of cell proliferation. Third, FBFs prevent premature meiotic entry of SPCs by inhibiting expression of target mRNAs that encode differentiation-promoting regulators, such as GLD-1 (Crittenden et al., 2002), GLD-2 (Millonigg et al., 2014), and GLD-3 (Eckmann et al., 2004), as well as structural components of meiotic chromosomes, such as HTP-1,-2 orthologs of human HORMAD1 and 2 (Merritt and Seydoux, 2010).

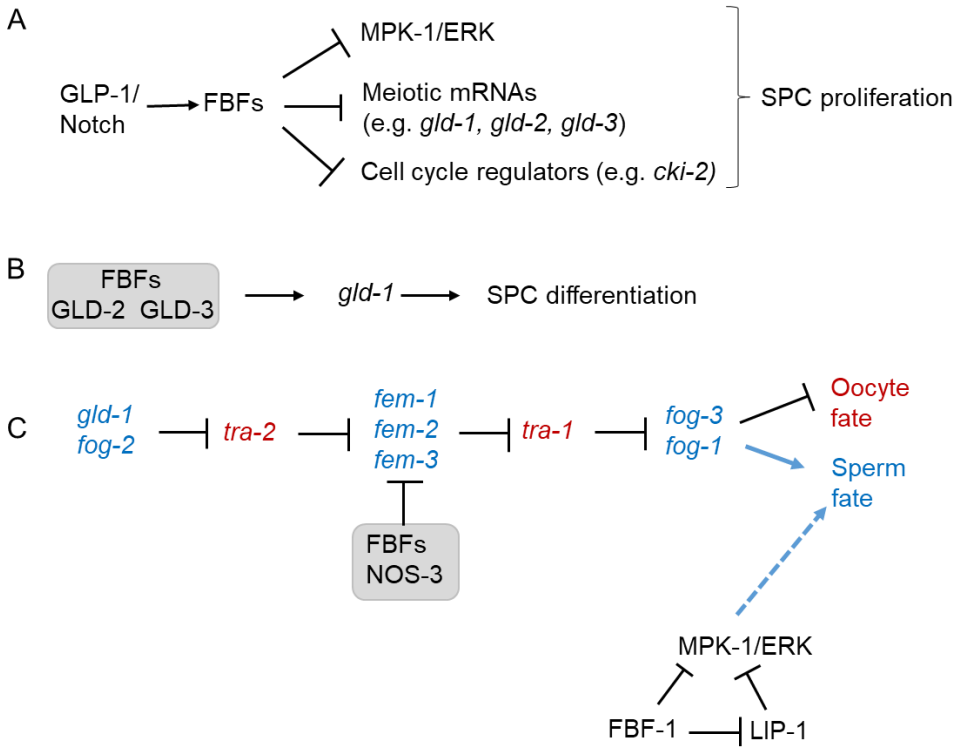

Figure 1-2. The multiple functions of FBFs in *C. elegans* germline SPCs. (A) Downstream of GLP-1/Notch, FBFs promote germline SPC proliferation by repressing cell cycle regulators, meiotic mRNAs, and *mpk-1* MAP kinase (Crittenden et al., 2002; Lee et al., 2007a; Kalchhauser et al., 2011). (B) FBFs act with GLD-2, GLD-3 complex to promote SPC meiosis by activating GLD-1 expression (Suh et al., 2009). (C) FBF proteins control the sperm/oocyte switch by acting with NOS-3 to repress *fem-3* (Kraemer et al., 1999; Arur et al., 2011) as well as by repressing *fog-1* and possibly *fog-3* (Thompson et al., 2005). FBF-1 cooperate with LIP-1 to repress MPK-1 activity in SPCs, dpMPK-1 refers to a diphosphorylated active form of MPK-1 (discussion and references in section "FBF Function in Controlling the Sperm/Oocyte Decision in Germline Mitotic Zone"). dpMPK-1 promotes spermatogenesis, although specific relevant substrates are yet unknown.

FBF Function in Inhibiting Mitotic Cell Fate of SPCs and Promoting Differentiation

In addition to facilitating stem cell maintenance, both FBFs were unexpectedly found to limit stem cell numbers by promoting stem cell exit from mitosis and differentiation (Figure 1-2B). Genetic evidence suggests that FBFs act to promote meiotic entry of SPCs through the GLD-2, GLD-3 genetic pathway (Crittenden et al., 2002). GLD-1, NOS-3 and GLD-2, GLD-3 are the two

main pathways that redundantly promote SPC meiotic entry (Figure 1B; Kimble and Crittenden, 2007). In the absence of *gld-1*, FBFs are no longer required to sustain germline proliferation and the *gld-1; fbf-1 fbf-2* mutant worms have tumorous germline with all mitotic cells (Crittenden et al., 2002). This tumorous germline phenotype is similar to the tumors observed in *gld-1; gld-2* and *gld-1; gld-3* mutants (Eckmann et al., 2004; Kadyk and Kimble, 1998), suggesting a possibility that FBF proteins function through the GLD-2, GLD-3 genetic pathway to promote meiotic entry. Direct interaction of FBF with GLD-3 that might underlie this function is discussed further in section "Protein Cofactors That Change PUF Regulatory Outcome".

The fact that PUF proteins appear to regulate both proliferation and differentiation is enigmatic and has promoted several interpretations. For example, functional annotation of mRNAs co-isolated with FBFs suggests that they associate with and repress mRNAs required for both differentiation as well as cell cycle progression of germ cells (Porter et al., 2019; Prasad et al., 2016). One intriguing interpretation is that this allows FBFs to simultaneously control the rate of both SPC proliferation and differentiation, thus maintaining the balance between these two cell fates. In order to maintain stem cell numbers over time, their self-renewal needs to be matched with differentiation (Morrison and Kimble, 2006). In *C. elegans*, SPC homeostasis is controlled at a population level, where some progenitor cells are lost through differentiation, while other cells proliferate, with both outcomes observed at the same frequency (Kimble and Crittenden, 2007). Although *C. elegans* SPCs proliferate continuously, the rate of SPC proliferation changes during development and is responsive to environmental conditions and nutrition (Hubbard et al., 2013). Simultaneous control of SPC proliferation and differentiation by FBFs might work to match the output of the stem cell compartment to the proliferative demands of the germline, while keeping the two fates in a balance.

FBF Function in Controlling the Sperm/Oocyte Decision in Germline Mitotic Zone

The mechanism underlying sperm/oocyte decision has been a long-standing question in all animals (Casper and Van Doren, 2006; Kimble and Page, 2007). In *C. elegans* hermaphrodites, germlines first produce sperm and then oocytes, but it is still not clear when, where, and how the

sperm/oocyte switch is executed. As recently reviewed (Zanetti and Puoti, 2013), the germline sex determination is executed through an elaborate pathway involving more than 30 regulators for sperm or oocyte specification, part of which is shown in Figure 1-2C. These regulators, including GLD-1, TRA-1 (GLI transcription factor homolog; Hodgkin, 1987), and FOG-1 (feminization of the germline, a member of cytoplasmic polyadenylation element binding protein family; Jin et al., 2001b) are expressed in the proximal mitotic region and transition zone, suggesting that the commitment of germline sperm/oocyte fate might occur in distal germline. Studies of sex determination in a temperature-sensitive *fog-1* mutant suggested that germ cells might become committed to the sperm or oocyte fate when they enter meiosis (Barton and Kimble, 1990). FBF-1, and FBF-2 contribute to the control of the sperm/oocyte decision by regulating expression of sex-determination regulators (Figure 1-2C).

FBF-1 and FBF-2 are redundantly required for controlling the sperm/oocyte switch. Nematodes mutant for individual *fbf* genes produce both sperm and oocytes, but the *fbf* double mutants fail to switch from spermatogenesis to oogenesis and only produce sperm (Zhang et al., 1997). The two FBF paralogs promote oogenesis by repressing several target mRNAs including *fem-3, fog-1*, and possibly *fog-3* that are positive regulators for sperm fate decision (Thompson et al., 2005; Zhang et al., 1997). Additionally, Nanos homolog NOS-3 physically interacts with FBF proteins and participates in the FBF-mediated sperm/oocyte switch through forming a regulatory complex that represses the translation of *fem-3* mRNA (Arur et al., 2011; Kraemer et al., 1999). The binding between NOS-3 and FBF-1 is disrupted by MPK-1/ERK-dependent phosphorylation of NOS-3 to limit formation of the functional complex to the distal germline (Arur et al., 2011). Lastly, functional splicing machinery promotes efficient sperm/oocyte switch (Kerins et al., 2010), and a combination of *fbf* single mutants and splicing factor knockdown results in enhanced germline masculinization, suggesting that the splicing machinery facilitates FBF function in sex determination (Novak et al., 2015).

One of the many functions of MAPK/ERK signaling pathway in *C. elegans* is to promote the sperm fate (Lee et al., 2007b). Hyperactivation of MPK-1 and excessive spermatogenesis were observed in *puf-8; lip-1* as well as in *fbf-1; lip-1* genetic backgrounds (Morgan et al., 2010; Sorokin et al., 2014). In these genetic backgrounds, spermatogenesis was dependent on MPK-1 activity and

repressed by a small molecule MEK inhibitor U0126 (Morgan et al., 2010; Sorokin et al., 2014). Activation of MPK-1 in *fbf-1; lip-1* genetic background likely results from the loss of FBF-mediated repression of *mpk-1* translation and the loss of LIP-1-mediated post-translational inhibition of MPK-1(Lee et al., 2007a).

Mechanisms mediating FBF functions

As reviewed in the previous section, in *C. elegans* germline stem cells, activities of FBF proteins promote many aspects of healthy stem cell function. The highly conserved RNA-binding domain of FBF proteins recognizes the same stereotypical consensus binding sites in target mRNAs (Zhang et al., 1997) and share most of the target RNAs (Porter et al., 2019; Prasad et al., 2016). Yet, individual FBF proteins have distinct regulatory functions (Voronina et al., 2012). Here we will survey the recent insights into the factors mediating FBF function.

Protein Cofactors That Change RNA Target Preference

While determination of *in vivo* FBF targets confirmed FBF preferential association with mRNAs containing canonical FBF-binding element identified *in vitro*, many of the identified targets did not contain the canonical motif, suggesting that FBF binding specificity may be altered *in vivo* (Porter et al., 2019; Prasad et al., 2016). Biochemical and structural studies of PUFs in complex with their partner proteins revealed that several PUF interacting partners can affect the RNA-binding affinity and specificity of PUF proteins (Figure 1-3A, B). Crystal structure of Nanos-Pumilio-RNA complex from *Drosophila* suggested that Nanos embraces Pumilio and RNA, contributes to sequence-specific contacts, and increases Pumilio affinity for *hunchback* mRNA (Malik et al., 2019; Weidmann et al., 2016). By contrast, association of Pumilio with *mothers against dpp (mad)* mRNA requires Bam and Bgcn proteins, but not Nanos (Malik et al., 2019). In *C. elegans*, both FBF proteins physically interact with CPB-1, a cytoplasmic polyadenylation element binding protein (Luitjens et al., 2000; Menichelli et al., 2013). The assay investigating binding of FBF-2 PUF domain to target mRNA in the presence of a 40-amino-acid fragment of CPB-1 outside of the RNA-binding domain demonstrated that association with CPB-1 fragment alters FBF's preference for specific RNA sequences (Campbell et al., 2012; Menichelli et al., 2013). Additional FBF interaction partners include novel proteins SYGL-1 and LST-1 that are required for FBF-dependent target mRNA repression in germline SPCs (Brenner and Schedl, 2016; Haupt et al.,

2019a; Kershner and Kimble, 2010; Shin et al., 2017). Using SEQRS *(in vitro* selection, high-throughput sequencing of RNA, and sequence specificity landscapes), analysis of RNA-binding preference of FBF-2 PUF domain bound to a 150-amino-acid LST-1 fragment containing one of FBF-binding sites revealed a distinct RNA-binding specificity of the FBF-2/LST-1 complex (Qiu et al., 2019). Crystal structure of FBF-2 in complex with a 24-amino-acid fragment of LST-1 and an 8-nucleotide RNA oligo isolated by *in vitro* selection showed that FBF-2 PUF domain changes its RNA-binding mode to 1:1 association of PUM repeats R4-R5 with GA in positions four and five (Qiu et al., 2019). However, the structural basis for the changes in the RNA-binding specificity is not entirely clear since association with LST-1 peptide appeared to weaken FBF-2 affinity for all tested target sequences (Qiu et al., 2019). Further studies are necessary to understand whether association with full-length LST-1 has similar effects on FBF-2 binding to its targets.

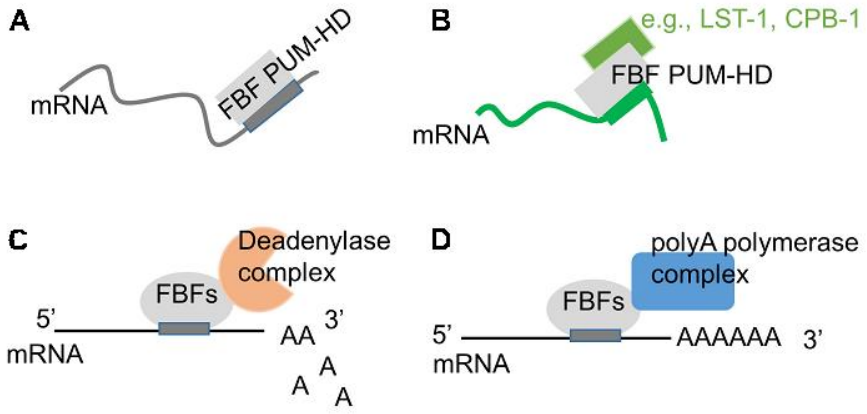

Figure 1-3. Modification of FBF biological activity though interactions with protein partners. (A) On its own, FBF PUF domain binds to target mRNAs containing a canonical 9-nt motif (Wang et al., 2009; Bhat et al., 2019; Qiu et al., 2019). (B) FBF PUF domain's RNA-binding specificity can be influenced by interactions with protein partners such as CPB-1 (Menichelli et al., 2013) and LST-1 (Qiu et al., 2019). (C) FBFs can repress target mRNAs by recruiting deadenylase complex (Goldstrohm et al., 2006; Suh et al., 2009). (D) FBFs can promote mRNA polyadenylation by interacting with the poly(A) polymerase complex (Eckmann et al., 2002; Suh et al., 2009).

Protein Cofactors That Change PUF Regulatory Outcome

PUF proteins lack enzymatic activity and often mediate their regulatory influence by recruiting specific cofactors to their target mRNAs (Cho et al., 2006; Cho et al., 2005; Eckmann et al., 2002; Friend et al., 2012; Goldstrohm et al., 2006; Kadyrova et al., 2007; Sonoda and Wharton, 1999; Sonoda and Wharton, 2001; Suh et al., 2009). PUF proteins typically reduce expression of their targets by repressing translation or promoting RNA decay (Cao et al., 2010; Crittenden et al., 2002; Goldstrohm et al., 2006; Olivas and Parker, 2000; Weidmann and Goldstrohm, 2012; Wreden et al., 1997). This repressive function of PUF proteins in *C. elegans* and other species can be mediated by CCR4-NOT deadenylase that promotes RNA deadenylation and decay (Figure 1-3C), and both FBFs bind deadenylase enzyme CCF-1 (Goldstrohm et al., 2006; Suh et al., 2009). One alternative repressive mechanism suggested for FBFs relies on PUF domain interaction with Argonautes resulting in attenuated translational elongation (Friend et al., 2012).

In several cases, PUF proteins appear to activate translation: FBFs are suggested to promote GLD-1 expression in spermatogenic germline as well as translation of EGL-4 in neurons, while PUF-8 facilitates translation of FARL-11 in germline SPCs (Kaye et al., 2009; Maheshwari et al., 2016; Suh et al., 2009). A search for cofactors of FBFs uncovered an interaction with poly(A) polymerase complex identifying one potential mechanism for translational activation (Figure 3D; Eckmann et al., 2002; Kimble and Crittenden, 2007). FBFs interact with the GLD-3 subunit of GLD-3/GLD-2 cytoplasmic poly(A) polymerase complex (Eckmann et al., 2002). FBFs also interact with the GLD-2 subunit in the RNA-independent manner, and this interaction is facilitated by formation of a larger complex including GLD-3 (Suh et al., 2009). Interaction with GLD-3 does not affect FBFs binding to their target mRNA, and is instead hypothesized to switch the regulatory outcome from repression to activation (Wu et al., 2013).

Distinct FBF Localization

FBF-1 and FBF-2 are nearly identical in primary sequence, share most of the target mRNAs (Prasad et al., 2016; Porter et al., 2019), and function redundantly in maintaining germline SPCs. Nevertheless, they differentially affect germline SPC zone size as *fbf-2* mutant maintains a larger SPC zone than the *fbf-1* mutant does (Lamont et al., 2004). In addition, FBF homologs have different effects on their target mRNAs: FBF-1 promotes the clearance of target mRNAs required

for meiosis out of the mitotic region, whereas FBF-2 sequesters target mRNAs while preventing their translation (Voronina et al., 2012). These differences correlate with FBFs' localization to distinct RNA granules. FBF-2 localizes to P granules and requires P granule integrity for its activity, while FBF-1 localizes to perinuclear RNA granules adjacent to P granules and its activity does not require P granule integrity (Voronina et al., 2012).

Conclusion and hypothesis

Pumilio and FBF family RBPs have evolved as essential post-transcriptional regulators of stem cell development in eukaryotes. PUF-mediated RNA regulation is achieved through recognizing target mRNAs and subsequently changing their rates of degradation or translation. The *C. elegans* germline is a powerful model for studying PUF protein function in stem cells. FBF-1 and FBF-2 expressed in *C. elegans* germline mitotic region are required for many aspects of germline SPCs development, including SPC proliferation and differentiation. Studies in *C. elegans* resulted in considerable advances in understanding the mechanisms regulating diverse biological activities of FBFs as shown in Figure 1-3.

FBF-1 and FBF-2 are very similar in primary sequence and share most of the target mRNAs, and yet they have different localization and function in germline SPCs. The next challenge to this field is to uncover the mechanisms allowing differential activities of FBF homologs in germline SPCs. In this study, **we hypothesize that FBFs' distinct localization and their differential regulation of target mRNAs and SPC development are likely influenced by their cooperation with distinct cellular cofactors**. Since FBF proteins that are highly conserved in eukaryotes, elucidating their regulatory mechanisms will advance our understanding of the role of translational repressors in controlling stem cell proliferation and differentiation in other organisms, including humans.

Chapter 2. Splicing Machinery Facilitates Post-Transcriptional Regulation by FBFs and Other RNA-Binding Proteins in *Caenorhabditis elegans* Germline

(This chapter is a modified version of the manuscript published in G3, 2015. doi: 10.1534/g3.115.019315.)

Abstract

Genetic interaction screens are an important approach for understanding complex regulatory networks governing development. We used a genetic interaction screen to identify cofactors of FBF-1 and FBF-2, RNA-binding proteins that regulate germline stem cell proliferation in *Caenorhabditis elegans*. We found that components of splicing machinery contribute to FBF activity as splicing factor knockdowns enhance sterility of *fbf-1* and *fbf-2* single mutants. This sterility phenocopied multiple aspects of loss of *fbf* function, suggesting that splicing factors contribute to stem cell maintenance. However, previous reports indicate that splicing factors instead promote the opposite cell fate, namely, differentiation. We explain this discrepancy by proposing that splicing factors facilitate overall RNA regulation in the germline. Indeed, we find that loss of splicing factors produces synthetic phenotypes with a mutation in another RNA regulator, FOG-1, but not with a mutation in a gene unrelated to posttranscriptional regulation (*dhc-1*). We conclude that inefficient pre-mRNA splicing may interfere with multiple posttranscriptional regulatory events, which has to be considered when interpreting results of genetic interaction screens.

Introduction

Whole-genome synthetic interaction screens are used widely to identify functional partners of genes of interest. Large-scale analyses performed in *Caenorhabditis elegans* suggest that the majority of genes fail to produce a phenotype when singly depleted (Kamath and Ahringer, 2003), partially because of genetic redundancy. Synthetic phenotypes produced by simultaneous depletion of two genes and not observed in either single mutant often are interpreted as an indication of functional connections between genes. Synthetic interaction screens are a valuable

tool to probe the complex regulatory networks. Here, we use synthetic interaction screen to identify factors contributing to regulation of the network that maintains the balance between stem cell proliferation and differentiation in the germline.

Caenorhabditis elegans germ cells undergo a stereotypical developmental program that ends in the production of mature gametes prepared for fertilization (Pazdernik and Schedl, 2013). The germline functions as an assembly line, where stem cell proliferation and self-renewal occurs at the distal region in the stem cell niche supported by the activation of GLP-1/Notch signaling pathway (Kimble and Crittenden, 2007). Meiotic differentiation is triggered as the germ cells are displaced from the niche (reviewed in Kershner et al., 2014). As germ cells move proximally, they transit through the stages of meiotic prophase and ultimately form fully differentiated gametes (sperm or oocytes). In a *C. elegans* hermaphrodite, germ cells of late larva develop along the male pathway and form sperm, and germ cells of the adult develop along the female pathway, forming oocytes. The balance between stem cell self-renewal and differentiation must be carefully maintained to support tissue development and maintenance. Regulation of stem cell proliferation and differentiation is characterized by multiple redundancies, feedback and feed-forward modules, and is also tightly integrated with regulation of germline sex determination.

In *C. elegans* germline, posttranscriptional mechanisms play a major role in the regulatory network determining the extent of germline proliferation (Hansen and Schedl, 2013). For example, the PUF domain RNA-binding proteins FBF-1 and FBF-2 (collectively referred to as FBFs) maintain germline stem cell fate and prevent meiotic differentiation (Crittenden et al., 2002; Lamont et al., 2004; Zhang et al., 1997). FBFs repress differentiation-associated mRNAs, which include genes promoting differentiation/meiotic entry, genes supporting meiotic processes, and genes associated with spermatogenesis (Crittenden et al., 2002; Merritt and Seydoux, 2010; Thompson et al., 2005). In addition to the FBFs, several splicing factors contribute to the regulation of the balance of proliferation and differentiation (Belfiore et al., 2004; Kasturi et al., 2010; Mantina et al., 2009; Wang et al., 2012; Zanetti et al., 2011) . The data to date suggest that an overall decrease in spliceosomal activity may induce overproliferation of germline, although the mechanism of splicing factor regulatory contribution remains unknown.

Germ cell differentiation into sperm or oocytes depends on the germline sex determination pathway. The developmental switch of *C. elegans* germline from spermatogenesis to oogenesis also is under posttranscriptional regulation that determines the number of sperm produced before the hermaphrodite switches to oogenesis (Crittenden et al., 2002; Francis et al., 1995; Zanetti and Puoti, 2013). This decision depends on the relative abundance of proteins promoting male fate (such as FOG-1, FOG-3, and FEM-3) and the proteins promoting female fate (such as TRA-2 and TRA-3) (reviewed in Zanetti and Puoti 2013). In the L3/L4 larval stages, when *C. elegans* hermaphrodites produce sperm, proteins promoting male fate, including FOG-1, are expressed, whereas the female fate-associated *tra-2* is translationally repressed. In the adult hermaphrodite, germ cells switch from spermatogenesis to oogenesis in response to the translation of the female fate mRNA *tra-2* and translational repression of the male fate mRNA *fem-3* (Ahringer and Kimble, 1991). FOG-1 is one of the germline regulatory proteins necessary for sperm development and is an RNA-binding protein of the cytoplasmic polyadenylation element binding protein (CPEB) family (Jin et al., 2001b; Thompson et al., 2005). FOG-1 promotes proliferation and spermatogenesis during male as well as hermaphrodite larval development (Barton and Kimble, 1990; Thompson et al., 2005). *fog-1* is one of the terminal regulators in the germline sex determination cascade, and loss-of-function mutations in *fog-1* cause germline feminization, which is epistatic to a number of masculinizing mutations (reviewed in Zanetti and Puoti 2013).

Several factors coordinately regulate both the germline stem cell proliferation/differentiation switch and the spermatogenesis/oogenesis transition. For example, in addition to promoting stem cell renewal, the FBF proteins also repress protein production from *fem-3* and *fog-1* mRNAs (Thompson et al., 2005; Zhang et al., 1997). Indeed, fbf-1 fbf-2 double mutant animals fail to make oocytes, which results in germline masculinization (Crittenden et al., 2002). *fog-1* mRNA is a direct target of FBFs, its 3-prime untranslated region (3'UTR) contains FBF binding sites that are necessary for silencing FOG-1 protein expression in the mitotic germ cells (Thompson et al., 2005). Similarly, loss-of-function mutations in a number of splicing factors cause masculinization of the germline, possibly through regulation of *fem-3* translation (Graham (Graham and Kimble, 1993) (Belfiore et al., 2004; Kasturi et al., 2010; Kawano et al., 2004; Kerins et al., 2010; Konishi et al.,

2008; Mantina et al., 2009; Puoti and Kimble, 1999; Puoti and Kimble, 2000; Wang et al., 2012; Zanetti et al., 2011).

Splicing of pre-mRNA proceeds through the activity of the spliceosome, which is a large and dynamic protein−RNA complex that assembles on the mRNA in a characteristic step-wise fashion while progressing from recognition of 5' and 3' intron boundaries to eventual intron excision (Lee and Rio, 2015). Efficient splicing is critical to generate a translatable open reading frame, and additionally plays a role in regulating multiple aspects of RNA metabolism including nuclear export, mRNA stability, localization, and translational activity (Hachet and Ephrussi, 2004; Nott et al., 2003; Popp and Maquat, 2014).

In this study, we set out to identify cofactors of FBF-2 by using genetic interaction screening. FBF-1 and FBF-2 are redundant, and although inactivation of a single gene does not produce a phenotype, simultaneous inactivation of both *fbfs* leads to a loss of germline stem cells and sterility. Previously, we reported that FBF-1 and FBF-2 repress their target mRNAs using distinct mechanisms (Voronina et al., 2012), which now allows to identify genes required for FBF-2 function. Knockdown of such genes results in sterility only when *fbf-1* function is compromised but not when *fbf-2* function is compromised. In this study, we find that knockdown of splicing factors disrupted FBF function as well as compromised the function of at least one other RNA-binding protein. We conclude that in addition to their established role in mRNA biogenesis, the splicing factors act more broadly to maintain efficient translational control of germline mRNAs.

Materials and Methods

NEMATODE CULTURE

C. elegans strains (table 2-1) were derived from Bristol N2 and cultured according to standard protocols (Brenner 1974) at 15°, 20°, or 24° as indicated.

Table 2-1 Nematode strains used in the study

Genotype	Transgene Description	Strain	Reference
Transgenes: GFP::H2B::3′UTR			
rrf-1(pk1417) axIs1772 [pCM1.90] I	*pie-1* prom::GFP::H2B::*fog-1* 3′UTR	UMT193	This study
rrf-1(pk1417) axIs1772 [pCM1.90] I; fbf-1(ok91) II	*pie-1* prom::GFP::H2B::*fog-1* 3′UTR	UMT191	This study
rrf-1(pk1417) axIs1772 [pCM1.90] I; fbf-2(q738) II	*pie-1* prom::GFP::H2B::*fog-1* 3′UTR	UMT194	This study
Mutant strains; no transgene			
dhc-1(or195) I	–	EU828	Hamill *et al.* 2002
rrf-1(pk1417) I	–	MAH23	Kumsta and Hansen, 2012
rrf-1(pk1417) I; fbf-1(ok91) II	–	UMT186	This study
rrf-1(pk1417) I; fbf-2(q738) II	–	UMT203	This study
fog-1(q523) rrf-1(pk1417) I	–	UMT220	This study

RNA INTERFERENCE (RNAI)

RNAi was performed by feeding method, RNAi constructs were derived from Source BioScience RNAi library (Kamath and Ahringer, 2003) ; all clones were verified by sequencing. Empty vector pL4440 was used as a negative control throughout the experiments. Three colonies of freshly transformed RNAi plasmids were combined for growth in LB/Carbenicillin media for 4 hr and induced with 10 mM Isopropyl β-D-1-thiogalactopyranoside for 2 hr more at 37°. RNAi plates (NNGM plates containing 75 µg/mL carbenicillin and 0.4 mM Isopropyl β-D-1-thiogalactopyranoside) were seeded with the pelleted cells. RNAi treatments for genetic interactions with *fbf-1*, *fbf-2*, and *fog-1* were performed by feeding the L1 hermaphrodites synchronized by bleaching with bacteria expressing double-stranded RNA for 70 hr at 24° (*fbf-1, fbf-2*) or for 144 hr at 15° (fog-1). RNAi on strains expressing green fluorescent protein (GFP)-tagged histone H2B was performed at 24°.

ASSESSMENT OF STERILITY, MASCULINIZATION, AND REPORTER DEREGULATION

Sterility of the treated worms was scored when no embryos were observed in the uterus at day 1 post L4. Masculinization of germlines was assessed after the treated worms were fixed, and chromatin was stained with 4’, 6-diamidino-2-phenylindole (DAPI); germlines with sperm and no oocytes were scored as masculinized. Regulation of GFP::H2B::fog-1 3’UTR reporter was assessed by obtaining images of all germlines with identical exposure settings (2.8 sec). Epifluorescent images were acquired with an AxioCam MRm camera attached to a Zeiss Axioscop with a 63x Plan-Apochromat NA 1.4 objective using Zen Blue software (Zeiss). When expression of the fluorescent reporter was detected in the distal mitotic region, the germline was scored as “derepressing in stem cells.” To assess reporter overexpression, accumulation of nuclear GFP

reporter was quantified in five transition zone nuclei per each germline and corrected to background using Zen Blue. Brightness values were normalized to the average intensity of the reporter in the *rrf-1* background following control RNAi. Image processing was performed in Adobe Photoshop CS4.

EMBRYONIC LETHALITY ASSESSMENT

RNAi treatments were performed at 15°. Wild-type (N2) or *dhc-1(or195ts)* animals at the fourth larval stage were placed on RNAi feeding plates and left overnight. The next day, the adult worms were transferred into a fresh RNAi plate and incubated for 5 hr before being removed from the plate. After removal of the adult worms, plates were incubated for 48 hr at 15°, and the number of unhatched eggs and larval worms on the plate was scored. Embryos were scored as dead or arrested if they didn't hatch after at least 2 d after being deposited on the plate.

Results

SPLICING FACTOR RNAI RESULTS IN ENHANCED SYNTHETIC STERILITY WITH MUTANTS OF EITHER FBF-1 OR FBF-2

To identify possible FBF-2 cofactors and additional genes involved in regulation of the proliferation/differentiation transition in the germline, we performed an RNAi enhancer screen of 16 candidate genes predicted to contribute to FBF-2–mediated regulation (www.geneorienteer.org; Zhong and Sternberg, 2006) as well as a subset of 34 genes predicted to function in RNA regulation or metabolism and highly expressed during oogenesis (Reinke et al., 2004). The oogenesis-enriched RNA regulators tested in this study are a part of an ongoing large-scale genetic interaction screen. We assayed for enhanced sterility in the *fbf-1* mutant background compared with the control strain. Both strains carried a mutation in *rrf-1* to preferentially direct RNAi to germline tissues (Kumsta and Hansen, 2012; Sijen et al., 2001). Knockdown of three splicing factors, *prp-17, lsm-4*, and *gut-2*, resulted in enhanced sterility when depleted in *rrf-1; fbf-1* mutant worms compared with the *rrf-1* strain (Figure 2-1A and data not shown). All three splicing factors were present in the list of predicted FBF-2 cofactors. *prp-17* and *gut-2* also belong to the complete oogenesis-enriched RNA regulator gene set that was analyzed only partially in this study, but likely also had potential to recover splicing factors. The rest of the

tested clones (47) failed to show enhanced sterility resulting either in completely fertile worms in both genetic backgrounds or in equal percentages of sterile worms across tested genetic backgrounds. These results suggest that multiple components of the spliceosome genetically interact with the *fbf-1* mutant.

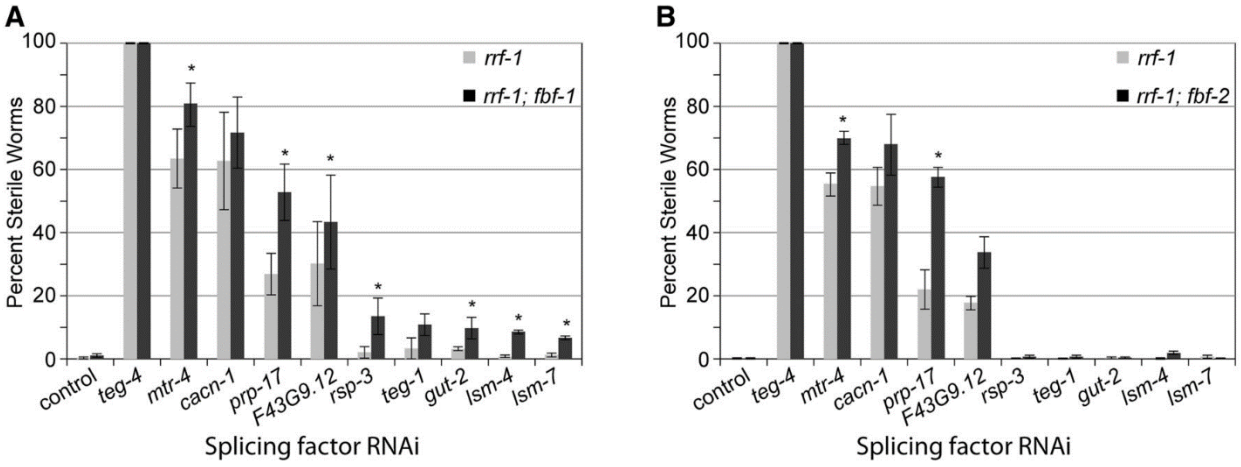

Figure 2-1. Splicing factor RNAi causes enhanced sterility of fbf-1 and fbf-2 mutants. The percentage of sterile hermaphrodites of the *rrf-1, rrf-1; fbf-1* (A) or *rrf-1; fbf-2* (B) genotype subjected to the indicated RNAi treatments. Sterile animals were identified by the absence of embryos in the uterus after 24 hr past the L4 larval stage. Error bars indicate SEM (from three or four experiments). Asterisks mark the treatments that caused significant increase in sterility of the double-mutant animals compared to the rrf-1 mutant (Student's paired t-test; $P < 0.05$).

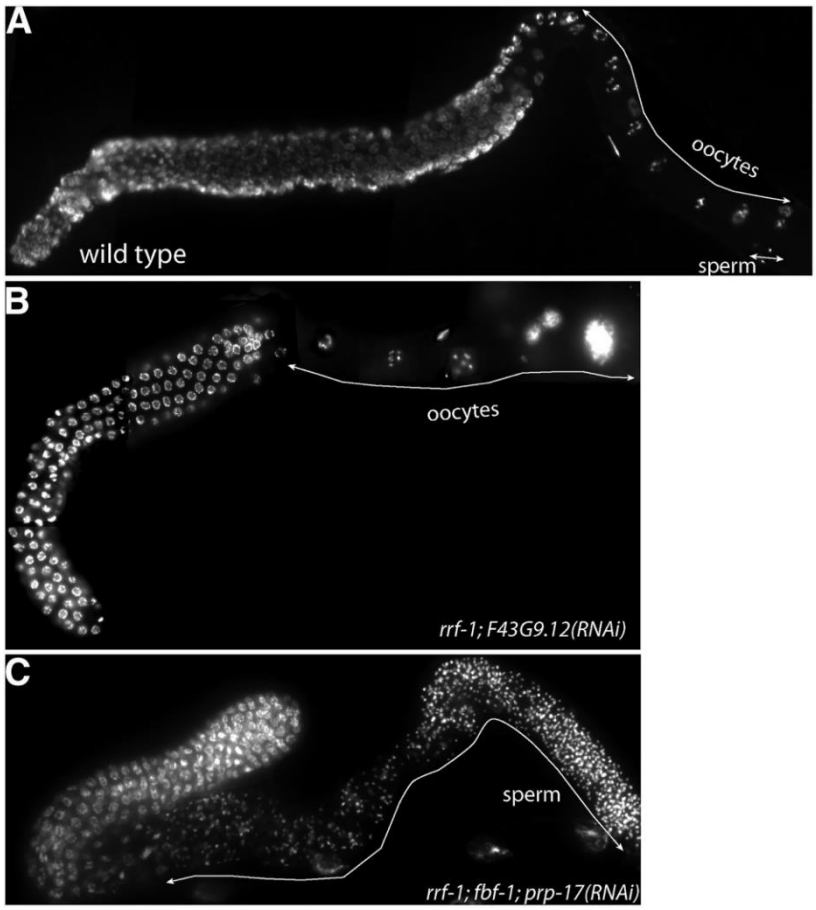

Figure 2-2. Germline masculinization after splicing factor knockdown. Full germlines were dissected and fixed, and chromatin was stained with DAPI. (A) Control treatment, wild-type germline. (B) *rrf-1; F43G9.12(RNAi)*, germline with degenerating endomitotic oocytes. (C) *rrf-1; fbf-1; prp-17(RNAi*), masculinized germline. The control germline contains all stages of germ cell differentiation, including oocytes. By contrast, masculinized germline contains mainly spermatogenic cells.

To test whether other components of the splicing machinery genetically interact with *fbf-1*, we used RNAi to deplete seven additional splicing factors distributed throughout the splicing reaction cycle. We chose the genes suggested in previous reports to function in splicing reaction and focused on those that have previously produced genetic interaction with *glp-1*, a regulator of germline proliferation (Kerins et al., 2010; Mantina et al., 2009). Knockdown of six of these genes resulted in enhanced synthetic sterility in the *rrf-1; fbf-1* mutant (which reached statistical significance in four cases), whereas knockdown of the seventh (teg-4) induced 100% sterility even

in the *rrf-1* strain (Figure 2-1A). Collectively, seven distinct components of the spliceosome significantly interact with *fbf-1* and thus may contribute to FBF-2 function.

We next tested whether the synthetic sterility in the RNAi assays phenocopied that of *fbf-1 fbf-2* double mutants, which fail to transition from spermatogenesis to oogenesis (Crittenden et al., 2002). We determined gamete chromatin morphology in the three treatments (*mtr-4*, F43G9.12, and *prp-17*(RNAi)) that produced high levels of enhanced sterility in the fbf-1 mutant background (Figure 2-1A). Similar to *fbf-1 fbf-2* double mutants, the sterility of *rrf-1; fbf-1* worms after splicing factor depletion was associated with an increased prevalence of masculinized germlines (Figure 2-2C; Table 2-2), in contrast to the fertile germlines containing both oocytes and sperm (Figure 2-2A). The other sterile phenotype was associated with degenerated endomitotic oocytes (Figure 2-2B) and was more prevalent in the *rrf-1* background than in *rrf-1; fbf-1* background. This phenotype is not relevant to sex determination or *fbf* function. These observations suggest that splicing factors may contribute to *fbf-2* activity.

Table 2-2 Germline masculinization in sterile worms after splicing factor knockdown

RNAi	Strain		
	rrf-1 %Mog (*n*)	*rrf-1*; *fbf-1* %Mog (*n*)	*rrf-1*; *fbf-2* %Mog (*n*)
Control day 1	0	0	0
day 3	0	0	0
mtr-4 day 1	43% (23)	97% (33)	80% (45)
day 3	37% (27)	89% (35)	48% (31)
prp-17 day 1	62% (42)	100% (33)	98% (64)
day 3	47% (15)	87% (46)	93% (29)
F43G9.12 day 1	4% (23)	41% (34)	52% (46)
day 3	0% (26)	56% (34)	25% (56)

Germline masculinization was scored after staining of dissected gonads of sterile worms with DAPI if formation of sperm but not oocytes was detected. The animals were fixed and stained on day 1 post-L4 stage (3d) and on day 3 post-L4 stage (5d). In several treatments, percent masculinized germlines decreased on day 3 post-L4, suggesting that some but not all observed masculinization on day 1 post-L4 was attributable to a delay in the switch to oogenesis. Control RNAi treatments did not have sterile worms. (*n*), number of germlines scored.

To test whether splicing factors were selective for *fbf-2* or also contribute to *fbf-1* function, we tested whether the splicing factor RNAi is synthetically sterile with the *fbf-2* mutation. We found that knockdowns of two splicing factors, *mtr-4* and *prp-17*, produced significant synthetic sterility with *fbf-2* (Figure 2-1B). In contrast, knockdowns of five genes producing synthetic sterility with the *fbf-1* mutation (*rsp-3, teg-1, gut-2, lsm-4,* and *lsm-7*) failed to generate synthetic sterility with

fbf-2, indicating either specific cooperation of these splicing factors with FBF-2 or a weaker overall FBF regulation in *fbf-1* mutant leading to a greater sensitivity to synthetic interactions. The synthetic sterility in *fbf-2* background was associated with an increased prevalence of masculinized germlines (Table 2-2). Together, these results suggest that the splicing machinery contributes to function of both FBF-1 and FBF-2, and depletion of splicing factors promotes sterility when either FBF-1 or FBF-2 are absent.

SPLICING FACTOR RNAI AFFECTS FBF TARGET REGULATION

Next, we directly tested whether splicing factor RNAi affects FBF function by observing the effect of splicing factor depletion on an FBF target gene *fog-1* (Thompson et al., 2005). Expression of a transgenic GFP::Histone H2B::fog-1 3'UTR reporter is silenced in the mitotic zones of wild-type, *fbf-1*, and *fbf-2* worms, but it becomes derepressed in the mitotic zones of *fbf-1 fbf-2* double-mutant germlines (Merritt et al., 2008). Upon splicing factor knockdown, 40–80% of sterile *rrf-1; fbf-1* hermaphrodites derepressed *fog-1* 3'UTR reporter in the mitotic region (Figure 2-3, A and B). By contrast, control depletion of the splicing factors in the *rrf-1* background did not result in significant reporter derepression in the mitotic region. These results indicate that depletion of splicing factors compromises FBF-2 activity in *fbf-1* mutant background.

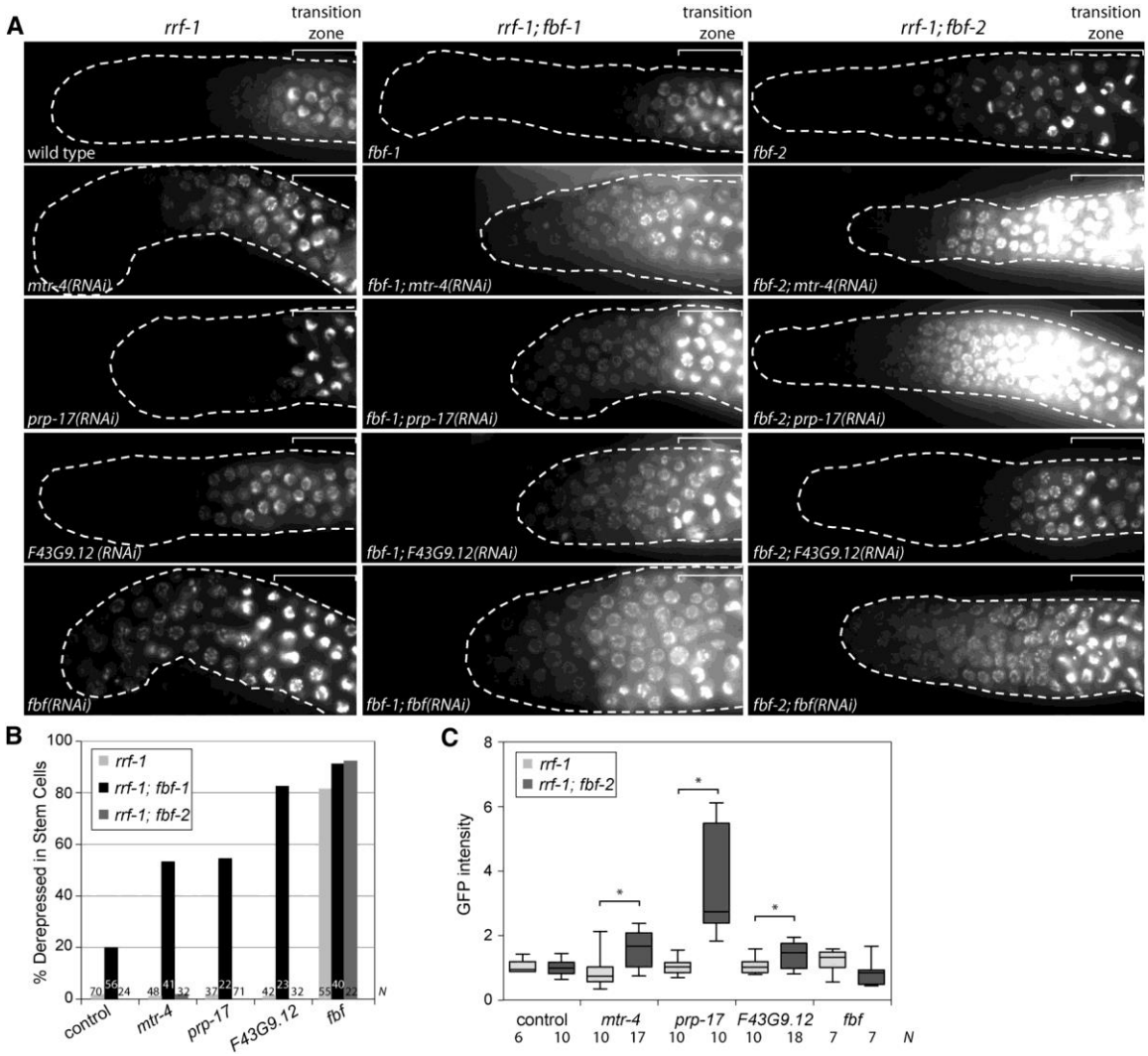

Figure 2-3 Derepression of FBF target genes upon splicing factor RNA interference (RNAi) in sensitized backgrounds. (A) Distal gonads of the indicated genotypes expressing a GFP::Histone H2B fusion under the control of the *fog-1* 3'UTR after RNAi of the indicated splicing factor genes. Gonads are outlined; white brackets indicate the position of the transition zone as recognized by the "crescent-shaped" chromatin. All images were taken with a standard exposure. (B) The percentage of *rrf-1* (light gray), *rrf-1; fbf-1* (black), or *rrf-1; fbf-2* (dark gray) gonads following indicated RNAi with GFP::H2B::fog-1 3'UTR expression extending to the distal end. N, number of germlines scored. (C) Background-corrected GFP intensity in transition zone nuclei (normalized to the average GFP intensity of control RNAi on *rrf-1* strain) plotted for *rrf-1* (light gray) and *rrf-1;fbf-2* (dark gray) gonads after indicated RNAi treatments. Box plot whiskers indicate the minimum and maximum intensity values. N, number of germlines scored. Asterisks mark the treatments that caused significant increase in the reporter intensity of the double-mutant animals compared to the *rrf-1* mutant (Student's t-test; $P < 0.01$). Note that the difference between reporter

fluorescence after F43G9.12(RNAi) in *rrf-1* and *rrf-1;fbf-2* backgrounds is significant, although the absolute value of the increase is small (1.4-fold) and no germlines have fluorescence values twofold higher than the control. GFP, green fluorescent protein.

To determine whether the splicing factors affect FBF-1 activity, we repeated the same experiments in the *fbf-2* mutant background (Figure 2-3, A and B). Although no treatments derepressed the transgenic reporter in the distal-most stem cell region, *prp-17*(RNAi) and *mtr-4*(RNAi) resulted in a dramatic increase of *fog-1* 3'UTR reporter expression in the transition zone where the cells entered meiosis (Figure 2-3A). Transition zone nuclei expressing *fog-1* 3'UTR reporter in the *rrf-1; fbf-2* background had on average 1.6 to 3.5 fold more GFP signal compared to the transition zone nuclei of the control germlines (Figure 2-3C; $P < 0.01$, Student's t-test). Thus, knockdown of splicing factors may limit FBF-1 activity in the *fbf-2* mutant background. These results are consistent with previous findings that splicing factors *mog-1* and *mog-6* repress expression of *fem-3* 3'UTR reporter in somatic cells (Gallegos et al., 1998).

SPLICING FACTOR RNAI ENHANCES FEMINIZATION OF FOG-1(TS) MUTANT

Our results indicate that loss of splicing factors enhances the single *fbf* mutant phenotype and that, like the *fbfs*, splicing factors are required for stem cell maintenance. However, previous studies suggested that a decrease in splicing factor activity instead leads to the opposite phenotype: overproliferation and formation of synthetic germline tumors in combination with a weak gain of function allele of *glp-1* (Kerins et al., 2010; Mantina et al., 2009; Wang et al., 2012). Because of these opposing combinatorial effects, we hypothesize that the role of splicing factors in germline stem cell proliferation and differentiation extends beyond generating specific splice isoforms of the stem cell maintenance regulators. We suggest the splicing factors act more broadly to maintain efficient translational control of germline mRNAs.

To test whether splicing factors are broadly required for RNA regulation, we took advantage of the *fog-1(q253ts)* mutant, which leads to failure of sperm production at the restrictive temperature of 25° but permits spermatogenesis at 15° (Barton and Kimble, 1990; Jin et al., 2001a). The level of FOG-1 expression is tightly controlled and correlates with sperm number produced by the hermaphrodite (Barton and Kimble, 1990; Lamont and Kimble, 2007) ; therefore,

any defect in FOG-1 function would be manifested in decreased or absent sperm production. If the normal function of splicing factors is to act with the *fbfs* to promote oogenesis, splicing factor knockdown would still cause masculinization in the *fog-1(ts)* background at the permissive temperature, where FOG-1(ts) is functional. Alternatively, if splicing factor knockdown disrupts RNA regulation in general rather than selectively affecting *fbf* function, it would produce synthetic feminization of the *fog-1(ts)* mutant at the permissive temperature.

Knockdown of splicing factors at permissive temperature failed to masculinize *rrf-1 fog-1(ts)* strain. By contrast, RNAi of all tested splicing factors in *rrf-1 fog-1* background produced some level of synthetic feminization; this feminization reached statistical significance in three cases (Figure 2-4E). Feminized phenotypes included arrested oocytes characteristic of *fog-1* loss of function (sometimes disorganized) and ovulated unfertilized oocytes, indicating defects in spermatogenesis (Figure 2-4, B–D). In some cases, feminization was incomplete, and small amounts of sperm were produced before a switch to oogenesis detected by the presence of two to three embryos in the adult's uterus followed by ovulated or arrested oocytes. None of these phenotypes was observed in *fog-1(ts)* worms exposed to the control RNAi, in nonmasculinized *rrf-1* mutant worms exposed to splicing factor RNAi, or in previous reports of splicing factor mutants. Because splicing factor knockdown may lead to either synthetic masculinization (*fbf* mutant background) or synthetic feminization (in *fog-1(ts)* background), the function of splicing factors in germline sex determination is not specific to the FBFs or oogenesis. Instead, we conclude that the functional splicing cascade facilitates RNA regulation carried out by multiple regulatory proteins in the germline.

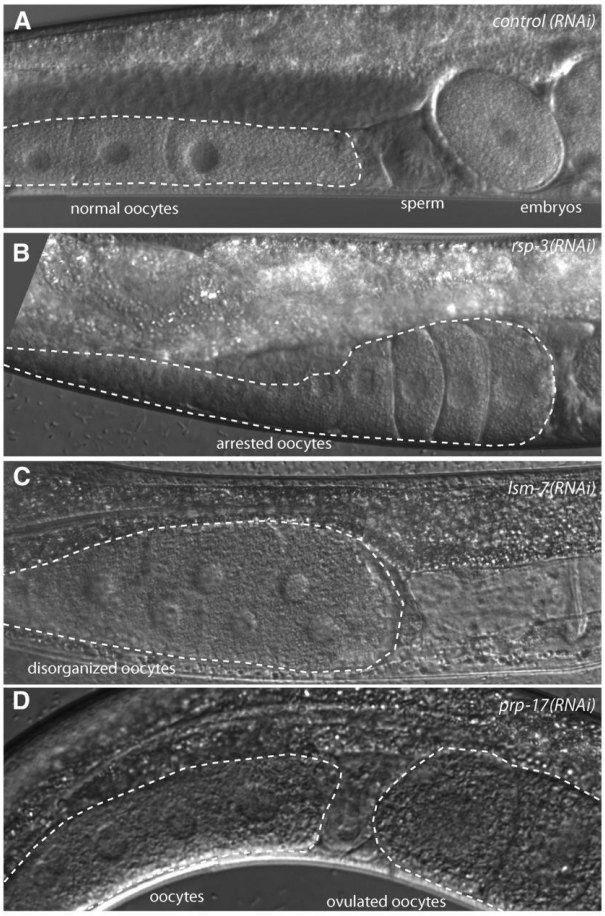

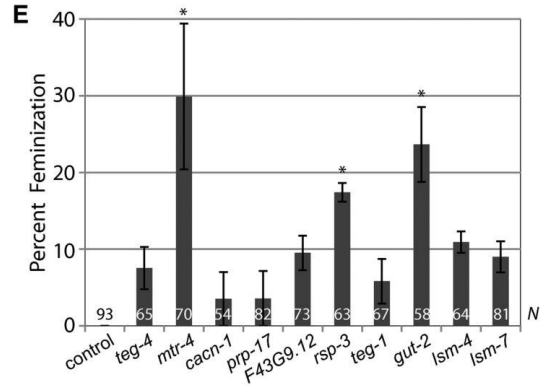

Figure 2-4 Defective spermatogenesis in *fog-1(ts)* mutants treated with splicing factor RNA interference (RNAi). (A) Normal germline, containing both oocytes and sperm. (B−D) A range of phenotypes caused by splicing factor RNAi in *fog-1(ts)* strain at permissive temperature includes arrested, disorganized, or ovulated oocytes. Each panel indicates the corresponding RNAi treatment. (E) The percentage of *fog-1(ts)* hermaphrodites showing spermatogenesis defects following indicated RNAi treatments. Error bars indicate SEM (from three or four experiments). Asterisks mark the treatments that caused significant increase in defective spermatogenesis compared to the control pL4440 RNAi ($P < 0.05$; corrected for multiple comparisons). Control and experimental groups were compared by one-way analysis of variance ($P = 0.0002$), followed by post-test comparison of treatments to control by the Dunnett multiple comparison test. N, number of hermaphrodites scored.

SPLICING RNAI DOES NOT ENHANCE EMBRYONIC LETHALITY OF DHC-1(OR195TS)

One potential consequence of splicing factor knockdown is general deterioration of all cellular functions; in that case, it would be expected to worsen the phenotype of any loss-of-function mutation, especially those that affect cell viability. To test whether a partial loss of function mutation would be nonselectively enhanced by depletion of splicing factors, we tested our panel of splicing factor RNAi in a strain carrying the temperature-sensitive S3200L mutation in the motor subunit of dynein, *dhc-1(or195ts)* (Hamill et al., 2002). This mutation causes embryonic lethality at 25° because of failure of mitotic spindle alignment, chromosome congression defects, and mitotic spindle collapse within 1 min of temperature upshift; thus, the phenotype most likely does not involve changes in posttranslational regulation of gene expression (Schmidt et al., 2005). We expect that if splicing factor depletion causes nonspecific loss of viability and enhances reduction-of-function mutation phenotypes, the embryonic lethality of *dhc-1(ts)* would be enhanced at the permissive temperature. Conversely, if splicing factor depletion primarily affects RNA regulation, the embryonic lethality of *dhc-1(ts)* would be equal either to the lethality of untreated *dhc-1(ts)* or to the lethality of splicing factor-depleted wild-type control.

RNAi knockdowns of *mtr-4, F43G9.12, lsm-4, lsm-7, gut-2,* and *teg-1* resulted in lethality similar to that observed in *dhc-1(ts)* treated with control RNAi. Knockdowns of *cacn-1, prp-17, and rsp-3* showed pronounced embryonic lethality, albeit equal between N2 and *dhc-1(ts)* strains treated with splicing factor RNAi (Figure 2-5). *teg-4(RNAi)* caused small but statistically significant enhancement of embryo lethality in the *dhc-1(ts)* mutant. Because the severity of the lethality caused by combined *teg-4(RNAi)* and *dhc-1(ts)* is close to the sum of the effects of the two perturbations individually, this effect appears additive rather than synthetic. We conclude that in the majority of cases splicing factor knockdowns do not exacerbate a developmental defect unrelated to RNA regulation.

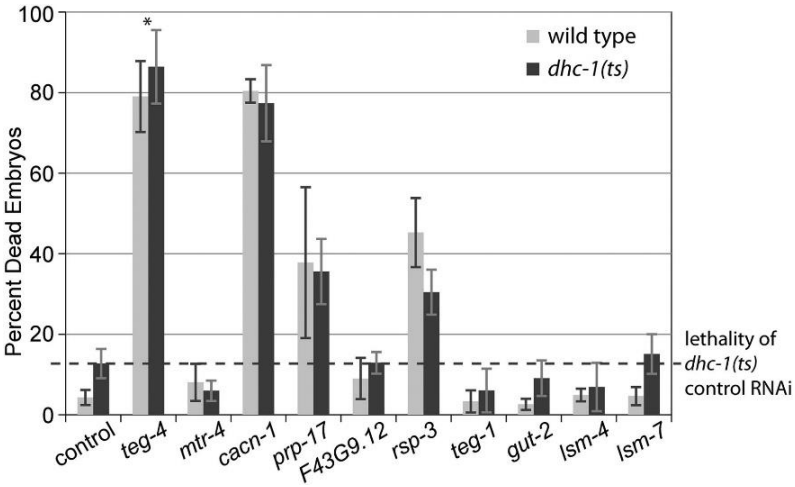

Figure 2-5 Splicing factor RNA interference (RNAi) does not produce synthetic lethality with *dhc-1(ts)* mutant. The percentage of dead embryos produced by N2 (wild type) or *dhc-1(ts)* hermaphrodites treated with indicated RNAi. Error bars indicate SEM (from two to four experiments). Asterisk marks *teg-4(RNAi),* which caused a significant increase in embryonic lethality in *dhc-1(ts)* mutant compared to wild type control (Student's paired t-test; P = 0.007).

Discussion

Here, we demonstrate that reduction in the activity of the splicing pathway in *C. elegans* germline disrupts multiple processes that depend on posttranscriptional control of gene expression. This destabilization of RNA regulation is uncovered by genetic interaction assays that identify splicing factor knockdowns as genetic enhancers of partial loss-of-function mutations in RNA-binding proteins. We suggest that an important function of the splicing pathway is to facilitate RNA regulation in general, which includes regulation by PUF-family translational repressors FBFs. Regulation of germline stem cell balance between proliferation and differentiation as well as spermatogenesis to oogenesis transition is centered at the posttranscriptional level. Our hypothesis explains the observations that reduction of splicing factor function may exacerbate defects that lead to opposite phenotypic outcomes such as masculinization and feminization; or overproliferation and stem cell loss. In our study, the strains that are mutant for RNA-binding proteins don't show sterility, sex determination, or reporter misexpression phenotypes unless splicing factors are knocked down. This suggests that the enhanced phenotypes resulting from a combination of RNA-binding protein mutation with splicing factor knockdown reflect a synthetic interaction rather than an additive effect.

Synthetic interactions observed in this and other studies likely do not result from missplicing of one specific transcript, because splicing factor knockdowns produce opposite synthetic phenotypes depending on the genetic background (tumor vs. loss of stem cells; masculinization vs. feminization). Indeed, so far, no specific missplicing events accounting for overproliferation or masculinization phenotypes of the majority of splicing factor mutants have been identified (Puoti and Kimble, 1999; Belfiore et al. 2004; Kasturi et al. 2010; Zanetti et al. 2011), although general defects in splicing have been suggested (Zanetti et al. 2011). Export of unspliced *tra-2* mRNA and aberrant cytoplasmic splicing resulting in accumulation of a dominant-negative protein is thought to cause masculinization after depletion of exon junction complex components *mag-1* and *Y14* (Shiimori et al., 2013). However, cytoplasmic leakage of unspliced *tra-2* mRNA was not a consequence of a general splicing defect, and was not observed upon depletion of other splicing factors.

Despite the essential contribution of splicing to gene expression, splicing factor knockdowns change gene expression patterns in germline rather than cause tissue degeneration. This is likely due to a partial loss-of-function produced by splicing factor RNAi treatments.

TRANSLATIONAL REPRESSION

The switch from spermatogenesis to oogenesis in the adult depends in part on translational repression of *fem-3* mRNA by FBF proteins (Zhang et al. 1997). Splicing factor genes *mog-1, mog-4,* and *mog-5* were isolated in the screen for mutations that disrupt the sperm to oocyte switch (Graham and Kimble 1993; Graham et al. 1993). A transgenic reporter expressed in the somatic tissues and regulated by fem-3 3'UTR was used previously to assess the role of *mogs* in the translational control of *fem-3* (Gallegos et al. 1998). In wild-type animals, the reporter was expressed only weakly, but in the *mog* mutant background, significant derepression was observed in somatic tissues. The conclusion that mog genes contribute to *fem-3* translational repression in the somatic tissues also was presumed true for the germline, although the mechanism of regulatory input by MOG proteins remained unclear (Gallegos et al. 1998).

We find that disruption of splicing factor genes by RNAi derepresses a germline-expressed *fog-1* transgenic reporter, which is normally silenced by FBF activity in stem cells. We observed two

types of derepression: expression of the reporter throughout distal mitotic region and up-regulation of the reporter expression in meiotic cells (typically along with reporter expression in some but not all mitotic cells). Up-regulation of the *fog-1* reporter in meiotic cells is reminiscent of the regulation of another FBF target, FEM-3. Normally, FEM-3 is expressed in the primary spermatocytes, but several conditions disrupting *fem-3* regulation by the FBFs lead to an expansion of FEM-3 expression to pachytene, but not to the stem cell region (Zanetti et al., 2012). We observed *fog-1* reporter derepression in the backgrounds where one of two *fbf* genes was mutated, but rarely in the wild-type background worms subjected to splicing factor RNAi. We hypothesize that combined residual activity of FBF-1 and FBF-2 upon splicing factor depletion in the wild-type background is sufficient to maintain FBF-mediated target repression in germline stem cells. Why then did the previous study find somatic *fem-3* reporter derepression in splicing factor mutants despite the presence of both FBF-1 and FBF-2 (Gallegos et al. 1998)? Both FBFs are predominantly expressed in the germline, and the baseline somatic activity of these proteins is much lower than the germline activity. This marginal activity of FBFs that represses *fem-3* 3'UTR reporter in somatic tissues is further reduced by mutation in splicing factors causing *fem-3* reporter derepression. By contrast, in germline, the level of FBF protein and activity are greater, so that one of the genes has to be mutated for the splicing factor RNAi to have an effect. Combined, our and previous results suggest that deficient splicing activity leads to disruption of translational control by FBFs.

SPLICING FACTORS AND SEX DETERMINATION

One of the synthetic phenotypes observed upon splicing factor RNAi in the *fbf* mutant background is masculinization of the germline. Germline masculinization was reported for single mutants of several splicing factors, including *prp-17* (Kerins et al. 2010). In addition, we observed synthetic masculinization after *mtr-4*(RNAi) and F43G9.12(RNAi), that were not reported to produce masculinization when depleted singly (Kerins et al. 2010). If splicing machinery were specifically required to work with FBFs (directly or indirectly), splicing factor RNAi would result in masculinization independent of genetic background. Instead, we observed that splicing factor RNAi of *fog-1(ts)* animals at the permissive temperature was associated with weak but significant synthetic feminization of germline indicative of *fog-1* loss of function. We hypothesize that the

temperature-sensitive mutation in the RNA-binding domain of FOG-1 renders it sensitive to the ribonucleoprotein (RNP) assembly defects resulting from inefficient splicing activity. Previous studies of splicing factors in sex determination found that feminizing null mutations in *fog-1, fog-3,* and *fem-3* are epistatic to masculinization of germline observed in splicing factor mutants (Graham and Kimble, 1993; Kerins et al., 2010; Wang et al., 2012). Genetically, it suggests that splicing factors function upstream of the *fog/fem* genes. However, we find that knockdowns of splicing factors instead enhance weak *fog-1* mutation, suggesting that in addition to regulating FOG-1 production, splicing machinery is important for FOG-1 function.

HOW DO SPLICING FACTORS CONTRIBUTE TO GENE REGULATION?

We propose that the splicing process contributes to efficient posttranslational control of mature spliced mRNA. Disruption of the splicing cascade may lead to defects in the assembly of messenger RNPs, which then fail to undergo normal cytoplasmic regulation. Therefore, the effects of mild splicing disruption will be most pronounced in systems heavily reliant on the posttranscriptional control of gene expression, such as *C. elegans* germline, and readily manifest in the sensitized mutant backgrounds. Some splicing factors remain associated with the spliced transcript, such as the exon junction complex, or EJC (Kataoka et al., 2000; Le Hir et al., 2000, reviewed in ; Le Hir and Séraphin, 2008). Although the core of the EJC persists during RNP maturation, peripherally associated components change as the messenger RNP is exported from the nucleus and regulated in the cytoplasm. Splicing-dependent deposition of the EJC plays a profound role in mRNA metabolism, regulating nuclear export, nonsense-mediated decay, efficiency of translation, and RNA localization (Ghosh et al., 2012; Ghosh et al., 2014; Hachet and Ephrussi, 2004; Popp and Maquat, 2014). One possibility is that deposition of EJC or similar complexes is disrupted by the treatments reducing overall splicing efficiency.

SPLICING FACTOR KNOCKDOWN SPECIFICALLY ENHANCES MUTATIONS AFFECTING RNA REGULATION

Our results suggest that down-regulation of splicing pathway enhances the phenotypes caused by defects in RNA regulation but not embryonic lethality resulting from disruption of cytoplasmic dynein. Similarly, a whole-genome synthetic interaction screen for genes contributing to function

of *mel-28* failed to retrieve splicing factors as genetic interactors (Fernandez et al., 2014). MEL-28 is a conserved component of nuclear pores needed for reestablishment of nuclear envelope after cell division and is not expected to contribute to RNA regulation. In the same vein, mutation in splicing factor *teg-4* does not enhance weak *lin-12* mutations interfering with Notch signaling in the anchor cell/vulval precursor cell fate decision, despite showing genetic interactions with pathways regulating the balance between germ cell proliferation and differentiation (Mantina et al., 2009). By contrast, splicing factors were isolated as enhancing the phenotype of *lin-35* Retinoblastoma homolog (Ceron et al., 2007), whose regulatory targets are under extensive posttranscriptional control (Grishok et al., 2008; Grishok and Sharp, 2005). Additionally, splicing factors were isolated in synthetic screens for the enhancers of germline overproliferation phenotype in the sensitized backgrounds of weak *glp-1(gf)* (Kerins et al., 2010; Mantina et al., 2009; Wang et al., 2012). Together, these data suggest that the processes involving RNA regulation are likely to produce genetic interaction with splicing factors.

The broad contribution of splicing to posttranscriptional control needs to be taken into account when interpreting results of large-throughput genetic enhancer screens. We recommend to take genetic screen results identifying splicing factors as enhancers of a particular mutant phenotype as an indication that posttranscriptional gene regulation plays a major role in the process under investigation. However, in absence of other supporting evidence, genetic interaction most likely reflects a broad role for the splicing factors in maintaining efficient RNA regulation rather than specific contribution to the function of the gene mutated to sensitize a strain to genetic interaction.

Acknowledgments

We thank the Caenorhabditis Genetics Center funded by the National Institutes of Health (NIH) for providing some nematode strains used in this work and J. Wang for comments on the manuscript. This work was funded by a grant from the NIH (R01GM109053) to E.V. Work in the Voronina lab is also supported by the Center for Biomolecular Structure and Dynamics NIH CoBRE grant (P20GM103546).

Chapter 3. Dynein light chain DLC-1 promotes localization and function of the PUF protein FBF-2 in germline progenitor cells

(This chapter is a modified version of the manuscript published in Development, 2016. DOI: 10.1242/dev.140921)

Abstract

PUF family translational repressors are conserved developmental regulators, but the molecular function provided by the regions flanking the PUF RNA-binding domain is unknown. In *C. elegans*, the PUF proteins FBF-1 and FBF-2 support germline progenitor maintenance by repressing production of meiotic proteins and use distinct mechanisms to repress their target mRNAs. We identify dynein light chain DLC-1 as an important regulator of FBF-2 function. DLC-1 directly binds to FBF-2 outside of the RNA-binding domain and promotes FBF-2 localization and function. By contrast, DLC-1 does not interact with FBF-1 and does not contribute to FBF-1 activity. Surprisingly, we find that the contribution of DLC-1 to FBF-2 activity is independent of the dynein motor. Our findings suggest that PUF protein localization and activity are mediated by sequences flanking the RNA-binding domain that bind specific molecular partners. Furthermore, these results identify a new role for DLC-1 in post-transcriptional regulation of gene expression.

Introduction

Translational control is essential for numerous processes in development and learning, and it also impacts disease progression (Brinegar and Cooper, 2016). The PUF family of proteins is an important class of RNA-binding regulatory proteins that are conserved in most eukaryotes (Quenault et al., 2011). PUF family regulators promote translational repression and/or degradation of target mRNAs by directly binding conserved elements in the 3' untranslated region (UTR). PUF proteins often assemble with their target mRNAs and other translational regulators into RNA granules, cytoplasmic structures lacking a membrane boundary. For example, rat PUM2 and human PUM1 are found at stress granules, the sites of storage of translationally repressed mRNAs (Morris {Morris, 2008, Ribonomic analysis of human Pum1 reveals cis-trans

conservation across species despite evolution of diverse mRNA target sets}et al., 2008; Vessey et al., 2006).

To repress target mRNAs, PUF proteins are assembled in protein complexes with other co-regulator proteins (Miller and Olivas, 2011). The composition of PUF repressive complexes and the molecular mechanisms resulting in translational repression vary among organisms, tissue types and mRNA targets. Additionally, several negative regulators of PUF activity have been documented, including a kinase that inhibits PUF activity by phosphorylation, as well as proteins that inhibit PUF protein-mRNA interactions (Miller and Olivas, 2011). Most known regulatory interactions involve the conserved PUF RNA-binding domain, despite the fact that the regions flanking the RNA-binding domain are required for full PUF activity (Muraro et al., 2008; Weidmann and Goldstrohm, 2012). There are no reports of PUF protein interactors that promote PUF subcellular localization or binding to the target mRNA.

In the germline of adult *Caenorhabditis elegans*, germ cells are arranged in a stereotypic progression, with stem cells located at the distal mitotic region and differentiating cells in a more proximal position (Pazdernik and Schedl, 2013). Cells displaced by division from the stem cell niche switch from proliferation to differentiation and enter meiosis, eventually forming differentiated gametes at the proximal end of the germline. *C. elegans* hermaphrodites produce sperm during late larval development and switch to oogenesis upon reaching adulthood. The balance between stem cell proliferation and differentiation supports stem cell maintenance and continued gamete production. Germline stem cell proliferation is regulated at the level of post-transcriptional control of gene expression (Kimble and Seidel, 2013). The regulatory network governing stem cell proliferation is closely integrated with the control of the switch from spermatogenesis to oogenesis (reviewed by Hansen and Schedl, 2013).

C. elegans germline stem cell maintenance depends on the activity of two conserved PUF family proteins, FBF-1 and FBF-2 (Zhang et al., 1997). In the absence of both FBF-1 and FBF-2, all cells in the mitotic zone precociously enter meiosis after the L4 stage of development when maintained at 20 °C (Crittenden et al., 2002), but are maintained in a mitotic state if grown at 25 °C (Merritt and Seydoux, 2010). FBF-1 and FBF-2 recognize the same motif present in the 3’ UTR of their

target mRNAs in vitro and form complexes with largely the same mRNAs in vivo (Bernstein et al., 2005; Merritt and Seydoux, 2010; Prasad et al., 2016). Despite high similarity between FBF-1 and FBF-2 (89% identity at the amino acid level) and apparent redundancy in their control of the switch from spermatogenesis to oogenesis, single *fbf-1* and *fbf-2* mutants have distinct phenotypes, suggesting that these genes play unique roles (Lamont et al., 2004). By examining the effects of single mutants on target mRNAs, it has been shown that FBF-1 inhibits accumulation of the target mRNAs in the mitotic zone and FBF-2 primarily represses mRNA translation (Voronina et al., 2012). In addition, only FBF-2 localizes to the germ cell-specific subtype of RNA granules called P granules, and this localization is required for the function of FBF-2 (Voronina et al., 2012). By contrast, FBF-1 does not localize to P granules and functions independently of these structures. The basis for these functional differences is not understood, but could involve interactions with distinct protein partners.

In this study, we report the identification of DLC-1 as a prominent regulator of FBF-2 localization and function. DLC-1 homologs (known as LC8 family proteins) were first described as subunits of the cytoplasmic dynein motor complex that traffics organelles, proteins and RNAs towards microtubule minus ends (reviewed by Vale, 2003; Medioni et al., 2012; Roberts et al., 2013). More recently, LC8 proteins have emerged as 'hub' proteins that support assembly of protein complexes beyond the dynein motor (Rapali et al., 2011b). Direct DLC-1–FBF-2 interaction promotes FBF-2 localization to P granules and also promotes FBF-2 function. The DLC-1–FBF-2 complex functions in a dynein motor-independent manner. DLC-1 binds FBF-2 outside of the RNA-binding domain, and does not interact with FBF-1. Our work suggests that the regions flanking the FBF-2 RNA-binding PUF domain regulate FBF-2 localization through a specific molecular interaction. In addition, our results identify DLC-1 as a new player in post-transcriptional control of gene expression in development.

Materials and Methods

NEMATODE CULTURE AND GENETICS

C. elegans strains were derived from Bristol N2 and cultured as per standard protocols (Brenner, 1974) at 20°C or 24°C (if containing a transgene). FX14547 *dlc-1(tm3153)*/hT2 III was obtained

from the National Bio-Resource Project (Japan), outcrossed to wild type, and rebalanced with a GFP-marked qC1 balancer to generate UMT222. *dlc-1(tm3153)* results in a maternal-effect embryonic lethal phenotype. Homozygous *dlc-1(tm3153)* mutants produce both sperm and oocytes; however, oocytes in diakinesis have unpaired chromosomes similar to the *dlc-1(RNAi)* phenotype (Dorsett and Schedl, 2009; Figure 3-1D) and result in dead embryos upon fertilization.

GENERATION OF TRANSGENIC AND GENETICALLY MODIFIED ANIMALS

All transgene constructs were generated by Gateway cloning (Thermo Fisher Scientific); additional information is in the supplementary Materials and Methods. Transgene insertion into universal Mos1 insertion sites was confirmed by PCR spanning homology region. The CRISPR/Cas9 co-conversion genome-editing approach (Arribere et al., 2014, Paix et al., 2014) was used to generate a 26-amino acid C-terminal deletion in endogenous *fbf-2*; mutants were identified by PCR genotyping screening and verified by restriction enzyme digest and Sanger sequencing. Two mutant lines generated by CRISPR/Cas9 approach were outcrossed six times with wild type before analysis.

IMMUNOLOCALIZATION AND MICROSCOPY

Adult hermaphrodites were washed in M9 and germlines were dissected on poly-L-lysine treated slides, covered with a coverslip to ensure attachment to slide surface, and flash-frozen on aluminum blocks chilled on dry ice. The samples were fixed for 1 min in 100% methanol (−20°C) followed by 5 min in 2% electron microscopy-grade paraformaldehyde in 100 mM K2HPO4 pH 7.2 at room temperature. The samples were blocked for at least 30 min in PBS/0.1% bovine serum albumin (BSA)/0.1% Tween 20. All primary antibody incubations were overnight at 4°C; all secondary antibody incubations were for 2 h at room temperature.

IMAGING

Epifluorescence images were acquired with a Leica DFC3000G camera attached to a Leica DM5500B microscope with a 40× PL FLUOTAR NA1.3 objective using LAS-X software (Leica). Confocal images were obtained on Olympus FluoView FV1000 confocal mounted on an inverted IX81 microscope. Image processing was performed in Adobe Photoshop CS4.

IMMUNOBLOTTING

To determine the effect of *dlc-1(RNAi)* on FBF-2 levels, synchronized cultures of GFP::FBF-2(wt) were exposed to either *dlc-1* or control RNAi. Lysates were separated on 7.5% SDS-PAGE gels (Bio-Rad), and proteins were transferred to Immobilon-P PVDF membrane (EMD Millipore). After blocking in TBS/0.1% Tween 20/5% non-fat dry milk, the blots were probed with antibodies diluted in blocking solution. Antibodies are described in supplementary Materials and Methods. Blots were developed using Luminata Crescendo Western HRP substrate (EMD Millipore) and recorded on ChemiDoc MP Imaging System (Bio-Rad).

IMMUNOPRECIPITATION

Immunoprecipitation was performed as previously published (Voronina and Seydoux, 2010). The amount of proteins pulled down with and without RNase A treatment was compared by spectral counting label-free quantification (Bantscheff et al., 2007). See supplementary Materials and Methods for further details.

RNAI

RNAi clones were either obtained from the Source BioScience RNAi library (Kamath and Ahringer, 2003) or generated by PCR amplification and cloning of genomic sequences into the pL4440 vector. Empty vector pL4440 was used as a control throughout the experiments. All plasmids were verified by sequencing and transformed into HT115(DE3) Escherichia coli. Three colonies of freshly transformed RNAi plasmids were combined for growth in LB/75 μg/ml carbenicillin media for 4 h, and induced with 10 mM isopropyl β-D-1-thiogalactopyranoside (IPTG) for 2 h at 37°C. RNAi plates (NNGM plates containing 75 μg/ml carbenicillin and 0.4 mM IPTG) were seeded with the pelleted cells. RNAi treatments were performed by feeding the L1 hermaphrodites synchronized by bleaching with bacteria expressing double-stranded RNA for 3 days at 24°C. Sterility of the treated worms was scored when no embryos were observed in the uterus 1 day post L4. Masculinization of germlines was assessed after the treated worms were fixed and chromatin was stained with DAPI. Regulation of the GFP::H2B::fog-1 3'UTR reporter after RNAi was assessed by imaging dissected germlines (Novak et al., 2015).

GST PULLDOWN ASSAY

For GST pulldown, cleared cell extracts of 6x-His-FBF proteins were added directly to GST-DLC-1 bound glutathione-Sepharose beads in 2 mM Tris pH 7.5, 500 mM NaCl, 10 mM beta-mercaptoethanol, 1 mg/ml BSA, 0.1% Triton X-100 and 1× protease inhibitor cocktail (Roche). Binding reactions were incubated at 15°C for 3 h and washed for four times with 10 mM Tris pH 7.5, 150 mM NaCl, 0.1% NP-40 and 1 mg/ml BSA. For elution, beads were heated to 80°C in sodium dodecyl sulfate sample buffer and 10 mM dithiothreitol. See supplementary Materials and Methods for details of recombinant protein production.

FLUORESCENCE POLARIZATION ASSAY

Fluorescein-labeled RNA oligonucleotide [5'-(Flc)UCAUGUGCCAUAC-3'; FBEa13; Qiu et al., 2012] was synthesized by Sigma-Aldrich. Polarization at each protein concentration was measured after incubation at room temperature for 40 min using a Biotek Synergy 2 plate reader, and dissociation constants were determined by GraphPad Prism. See supplementary Materials and Methods for further details, including recombinant protein production.

Results

IDENTIFICATION OF FBF-2-CONTAINING COMPLEXES

To identify novel protein co-factors important for FBF-mediated regulation in germline stem cells of *C. elegans*, we affinity purified FBF-2 protein complexes. We used anti-GFP antibodies to immunoprecipitate GFP::FBF-2 fusion protein expressed as a rescuing transgene in nematodes mutant for the endogenous *fbf-2* gene (data not shown). To test whether any FBF-2 ribonucleoprotein complex components associate with FBF-2 in an RNA-dependent manner, we immunoprecipitated GFP::FBF-2 in the presence of RNase A (data not shown), and analyzed both RNA-dependent and RNA-independent interactors. Proteins co-purifying with FBF-2 were identified by mass spectrometry. Among the proteins co-purified with FBF-2, many are RNA-binding proteins or splicing factors (Table 3-1). Other co-purifying proteins likely represent contaminants resulting from very high expression levels (for example, VIT-6/vitellogenin and UNC-54/myosin; data not shown). Four of the identified proteins were previously isolated with

glutathione S-transferase (GST)-tagged FBF-2 from C. elegans lysates by GST pulldown (Friend et al., 2012). Proteins identified in negative controls (immunoprecipitations of GFP alone) or as abundant contaminants were excluded from consideration, leaving a smaller list of FBF-2-associated proteins; however, this approach does not guarantee that all contaminants were excluded (Mellacheruvu et al., 2013). Using this approach, we generated a list of candidate FBF-2 co-regulators for follow-up analysis (data not shown).

Table 3-1 Proteins that co-purify with FBF-2 and are implicated in RNA regulation, cell signaling or intracellular trafficking

Protein	Coverage (%)*	RNase sensitive?	Comment
FBF-2	42	No	Immunoprecipitation target
DLC-1	26	No	Dynein light chain
GLD-1	23	Yes	KH-domain RNA-binding protein
PAR-5	15	No	14-3-3 domain protein
CGH-1	12	Yes	DEAD-box helicase
DAZ-1	10	No	RNA-binding protein
RACK-1	9	Yes	Stress granule component
RSP-3	7	Yes	R/S rich, splicing factor
GLH-3	3	No	DEAD-box helicase, P granule component
CACN-1	3	Yes	Cactin, splicing factor

*Calculated by dividing the number of amino acids in all peptides identified by mass spectrometry by the total number of amino acids in the entire protein sequence.

A GENETIC SCREEN IDENTIFIES DLC-1 AS A POTENTIAL CO-REGULATOR OF FBF-2

We next performed a genetic screen to identify potential FBF-2 co-regulators inactivation of which causes synthetic enhancement of sterility in an *fbf-1* loss-of-function [abbreviated as *fbf-1(lf)*] background, compared with the wild-type and *fbf-2(lf)* backgrounds. Knockdown of the genes selectively required for FBF-2 function is expected to cause enhanced sterility when *fbf-1* is compromised, but not when FBF-1 is available to compensate for a disruption of FBF-2 activity. The knockdown experiments were performed in strains mutant for *rrf-1* to preferentially direct the effects of RNAi to the germline and avoid the indirect effects of depleting gene function in the somatic cells (Sijen et al., 2001; Kumsta and Hansen, 2012). These experiments focused on

FBF-2 ribonucleoprotein (RNP) components with function related to RNA regulation, but included a number of other proteins identified in the co-immunoprecipitations. Out of knockdowns of 21 candidates, two, *dlc-1(RNAi)* and *rsp-3(RNAi),* reproducibly showed increased sterility in the *fbf-1(lf)* background, but not in either wild-type or *fbf-2(lf)* backgrounds (data not shown). This study focuses on the investigation of the synthetic phenotype with the LC8-type dynein light chain *dlc-1*. Analysis of synthetic phenotypes with *rsp-3* was described elsewhere (Novak et al., 2015).

DLC-1 CONTRIBUTION TO FBF-2 FUNCTION IS INDEPENDENT OF THE DYNEIN MOTOR

DLC-1 was first described as an LC8-type subunit of the dynein motor complex (Pfister et al., 1982); however, extensive dynein-independent functions of DLC-1 have also been identified (Herzig et al., 2000; Rapali et al., 2011b). To investigate whether other components of the dynein motor complex contribute to FBF-2 activity, we tested for their genetic interaction with *fbf-1(lf).* All 23 annotated *C. elegans* subunits of dynein and dynactin (dynein activity regulator and cargo adapter) complexes were depleted in *fbf-1(lf)* background and assayed for sterility (Figure 3-1A). We find that only a single additional knockdown, dynein intermediate chain *dyci-1(RNAi)*, showed significantly increased sterility in the *fbf-1(lf)* background ($P<0.05$, paired Student's t-test). Additionally, we found that RNAi of one of the dynein motor subunits, DHC-1, caused equally high sterility across the tested backgrounds (Figure 3-1A, B). Knockdown of *dlc-1* is expected to disrupt both dynein-dependent and dynein-independent cellular functions; however, knockdowns of the other dynein complex subunits affect the motor function without disrupting motor-independent functions of DLC-1. The lack of genetic interactions between *fbf-1(lf)* and the majority of dynein motor subunits suggest that DLC-1 might promote the function of FBF-2 independently of the dynein motor.

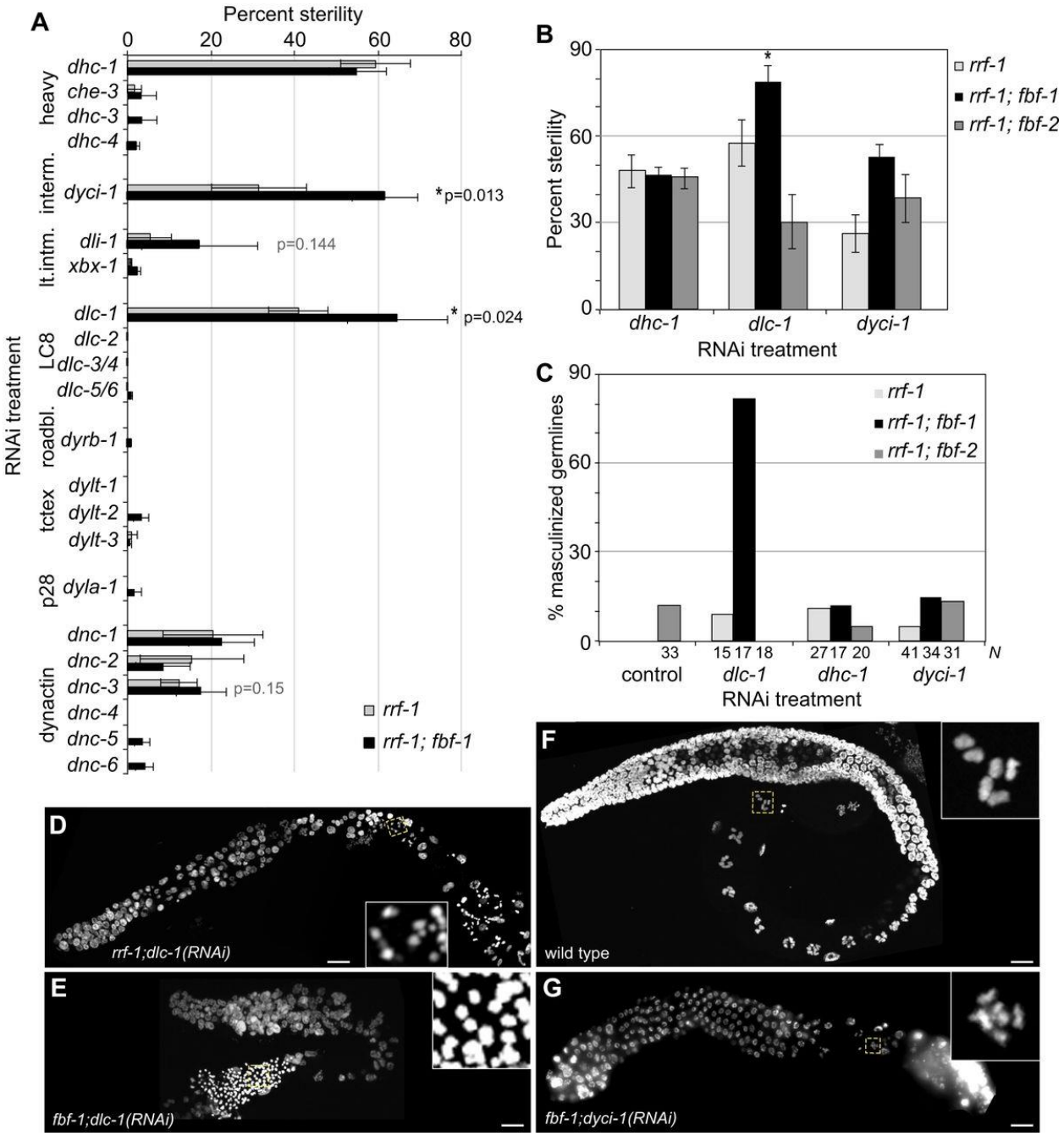

Figure 3-1 DLC-1 is required for FBF-2 function independent of the dynein motor complex. (A) The percentage of sterile hermaphrodites in the *rrf-1* and *rrf-1; fbf-1* genetic backgrounds following RNAi treatments targeting various subunits of the dynein motor as indicated on the y-axis. Data are represented as mean ± s.e.m. from three or four experiments scoring 25-60 worms per treatment. If a knockdown appeared to cause enhanced sterility in the *rrf-1; fbf-1* background, the differences between strains'

response to that RNAi were evaluated for statistical significance by Student's paired t-test; P values are shown next to the treatment pairs, and significant differences are indicated by asterisks. (B) The percentage sterility in the *rrf-1, rrf-1; fbf-1* and *rrf-1; fbf-2* genetic backgrounds after the indicated RNAi treatments. Plotted are mean ± s.e.m. from three or four experiments as in A. Asterisks mark the significant differences between genetic backgrounds in sterility caused by RNAi (P<0.05; corrected for multiple comparisons). The effects of each RNAi treatment on different strains were compared by one-way ANOVA [P<0.001 for *dlc-1*(RNAi); P>0.1 for both *dhc-1* and *dyci-1*(RNAi)], followed by post-test comparison by Tukey's multiple comparison test. (C-F) Germline masculinization was observed after *dlc-1* knockdown. (C) Masculinization was scored after staining dissected gonads of sterile worms with DAPI 1 day post-L4 stage if formation of sperm but not oocytes was observed. The percentage of masculinized germlines is plotted for the *rrf-1, rrf-1; fbf-1* and *rrf-1; fbf-2* genetic backgrounds after the indicated RNAi treatments. Treatment of *rrf-1* and *rrf-1; fbf-1* mutants with control RNAi did not produce sterile worms. n, number of germlines scored (shown below the bars). (D) *rrf-1; dlc-1*(RNAi), germline with small oocytes. (E) *fbf-1; dlc-1*(RNAi), masculinized germline. (F) Control treatment, wild-type germline. (G) *fbf-1; dyci-1*(RNAi), germline with degenerating endomitotic oocytes. Insets in D, F and G are magnified views of DAPI-stained oocyte chromatin. Inset in E shows magnified view of sperm chromatin. Regions enlarged in the insets are marked in panels D, F,G by dashed boxes. Scale bars: 10 µm.

We further tested whether FBF-2 function was affected in the genetic backgrounds with reduced *dhc-1* and *dlc-1* function using a hypomorphic temperature-sensitive (ts) mutation *dhc-1(or195)* and a deletion loss-of-function (lf) allele *dlc-1(tm3153)* (Hamill et al., 2002; this paper). We find that 78% of *fbf-1(lf); dlc-1(lf)* double mutants are sterile. This is a specific synthetic phenotype as 98% of *dlc-1(lf)* single mutants and *fbf-2(lf); dlc-1(lf)* double mutants are fertile and produce dead embryos (Table 3-2). By contrast, the *dhc-1(ts); fbf-1(lf)* double mutants grow to fertile adults when cultured from L1 larvae at the permissive temperature, and display similar penetrance of sterile adults and dead embryos at the restrictive temperature (Table 3-2). We conclude that *dlc-1*, but not *dhc-1*, shows significant genetic interaction with *fbf-1*, which is consistent with DLC-1 contributing to FBF-2 function.

Table 3-2 Synthetic sterility of *fbf-1; dlc-1* mutants

Genotype and temperature	Sterile (%)*	*n*
dlc-1(tm3153) 20°C	2±2	156
fbf-1(ok91); dlc-1(tm3153) 20°C	78±12	231
fbf-2(q738); dlc-1(tm3153) 20°C	1±2	180
dhc-1(or195); fbf-1(ok91) 15°C	4±1‡	181
dhc-1(or195) 15°C	5±1‡	158
dhc-1(or195); fbf-1(ok91) 20°C	3±2	245
dhc-1(or195) 20°C	2±0.4	185
dhc-1(or195); fbf-1(ok91) 24°C	10±1	210
dhc-1(or195) 24°C	8±2	153

*Sterile animals were identified by the absence of embryos in the uterus >24 h past the L4 larval stage, unless otherwise noted. Mean±s.d. shown. *n*, number of animals scored.
‡Animals grown at 15°C were analyzed 2 days post L4.

We next tested whether sterility observed after knockdown of three dynein subunits (*dlc-1, dhc-1* and *dyci-1*) resulted from the same defect as in *fbf-1 fbf-2* double mutants, which fail to initiate oogenesis following initial spermatogenesis, resulting in masculinized germlines (Crittenden et al., 2002). By identifying chromatin morphology characteristic of spermatogenesis or oogenesis, we find that sterility of *rrf-1; fbf-1* worms following *dlc-1*(RNAi) was associated with a significant degree of masculinization (Figure 3-1C,E). By contrast, *dlc-1(RNAi)* in other genetic backgrounds and control RNAi in all backgrounds still allowed oocyte formation (Figure 3-1C,D,F). Furthermore, we observed that masculinization was the cause of sterility observed in *fbf-1; dlc-1* double mutant animals (Table 3-3). Knockdowns of the other dynein components *dhc-1* and *dyci-1* in *rrf-1, rrf-1; fbf-1* and *rrf-1; fbf-2* backgrounds did not cause significant masculinization. The sterility in *dhc-1* and *dyci-1*(RNAi)-treated animals results from formation of small oocytes that became endomitotic (Figure 3-1 C,G). These results indicate that FBF-2 requires *dlc-1* and not *dhc-1* or *dyci-1* for function, and that FBF-1 does not require either of these.

Table 3-3 Masculinization of *fbf-1; dlc-1* mutant germlines

Genotype	Masculinized (%)	*n*
dlc-1(tm3153)	0	27
fbf-1(ok91); dlc-1(tm3153)	89	28
fbf-2(q738); dlc-1(tm3153)	4	23

Animals were grown at 20°C, fixed and stained for gamete identification >24 h post L4 stage. *n*, number of animals scored.

Taken together, these results indicate that DLC-1 has a specific role in FBF-2 regulatory activity. As DLC-1 is the only subunit of the dynein motor that is required for FBF-2 function promoting oogenesis, we hypothesize that DLC-1 cooperation with FBF-2 is independent of the role of DLC-1 in the dynein motor complex. In the following experiments, we focus on testing the contribution of *dlc-1* to FBF-2-mediated regulation and include dynein motor subunit *dhc-1* knockdown to further substantiate the conclusion that the dynein motor does not affect FBF-2 function.

DLC-1 IS REQUIRED FOR FBF-2-MEDIATED RNA REGULATION

FBFs act as translational repressors by binding the 3'UTRs of their target mRNAs (Kimble and Seidel, 2013). We tested whether knockdown of *dlc-1* affected regulation of FBF target genes repressed in the mitotic region. *fog-1* is an FBF target that contains FBF regulatory sites in its 3'UTR (Thompson et al., 2005). A transgenic reporter, GFP::H2B::fog-1 3'UTR, recapitulates repression of *fog-1* in the distal cells and becomes derepressed in a *fbf-1 fbf-2* double mutant background (Merritt et al., 2008). Upon *dlc-1*(RNAi), we observed derepression of the reporter in 54% of gonads of *fbf-1(lf)* mutant background, but not in the control genetic backgrounds (Figure 3-2A,C). By contrast, *dhc-1*(RNAi) did not produce significant derepression in any genetic background, consistent with a dynein motor-independent role for DLC-1 in promoting FBF-2 function.

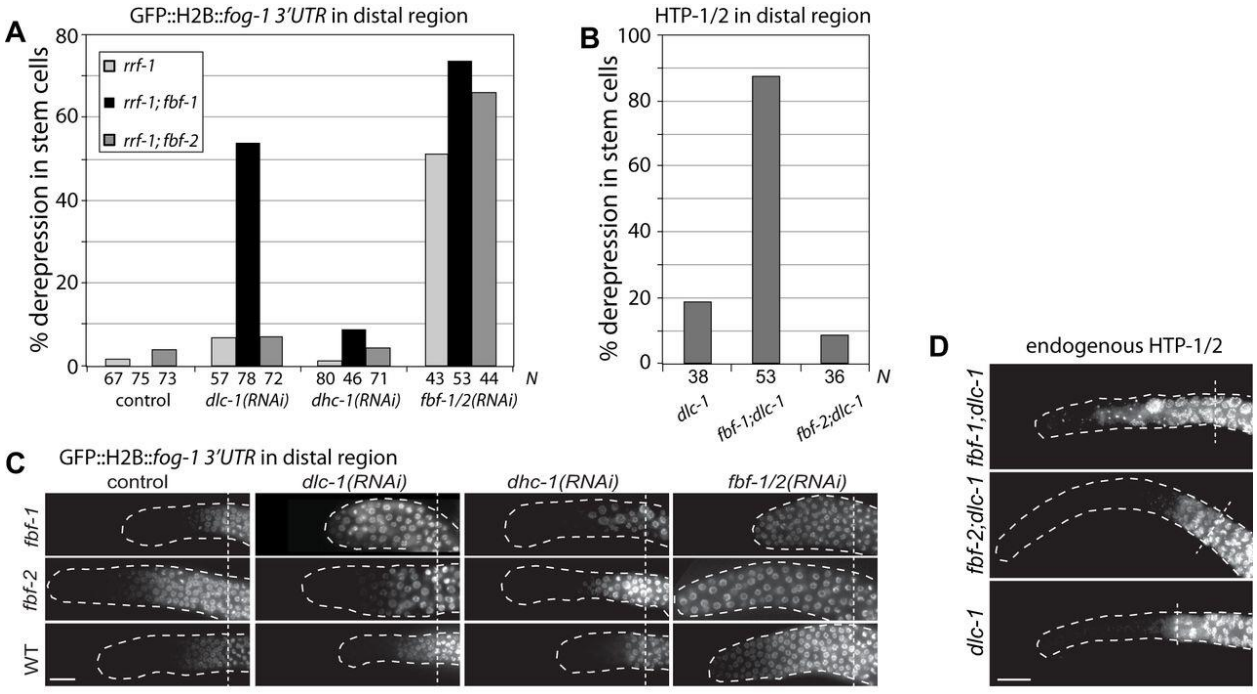

Figure 3-2 Knockdown of *dlc-1* affects FBF-2 regulatory function. (A) The percentage of *rrf-1* (light gray), *rrf-1; fbf-1* (black) or *rrf-1; fbf-2* (dark gray) gonads following the indicated RNAi with GFP::H2B::fog-1 3'UTR expression extending to the distal end. n, number of germlines scored (shown below the bars). (B) The percentage of *dlc-1, fbf-1; dlc-1* and *fbf-2; dlc-1* gonads showing HTP-1/2 staining extending to the distal end. n, number of germlines scored (shown below the bars). (C) Distal gonads of the indicated genotypes expressing a GFP::Histone H2B fusion under the control of the *fog-1* 3'UTR after the indicated RNAi treatments. Gonads are outlined; vertical dashed lines indicate the beginning of the transition zone as recognized by the 'crescent-shaped' chromatin. All images were taken with a standard exposure. (D) Distal gonads of the indicated genotypes following *dlc-1*(RNAi) immunostained for the synaptonemal complex proteins HTP-1 and HTP-2 (the antibody recognizes both proteins; Martinez-Perez et al., 2008). Gonads are outlined; vertical dashed lines indicate the beginning of transition zone. Scale bars: 10 µm.

HTP-1 and HTP-2 are two highly homologous HORMA domain meiotic proteins that are silenced by the FBFs in the mitotic region (Merritt and Seydoux, 2010). We observed ectopic expression of endogenous HTP-1 and HTP-2 in 87% of *dlc-1; fbf-1* hermaphrodites compared with 18% and 8% derepression in *dlc-1* and *dlc-1; fbf-2*, respectively (Figure 3-2B,D). We conclude that *dlc-1;*

fbf-1 mutants display the same range of defects as observed in *fbf-1 fbf-2* mutants, consistent with conclusion that *dlc-1* is required for *fbf-2* activity.

DLC-1 PROMOTES FBF-2 LOCALIZATION TO P GRANULES

In the distal mitotic cells, FBF-2 is localized to perinuclear foci overlapping with P granules, and this localization is required for FBF-2 activity (Voronina et al., 2012). Because DLC-1 is required for FBF-2 regulatory activity, we tested whether DLC-1 played a role in FBF-2 localization to P granules. Using RNAi, we found that DLC-1 knockdown prevents FBF-2 localization to P granules in both wild-type and *fbf-1(lf)* backgrounds (Figure 3-3A, first and second rows). By contrast, FBF-1 still localizes to perinuclear foci adjacent to but rarely overlapping with P granules (Figure 3-3B). We found that FBF-2 protein levels are not affected by *dlc-1*(RNAi) (Figure 3-3C). We conclude that DLC-1 is required to localize FBF-2 to P granules.

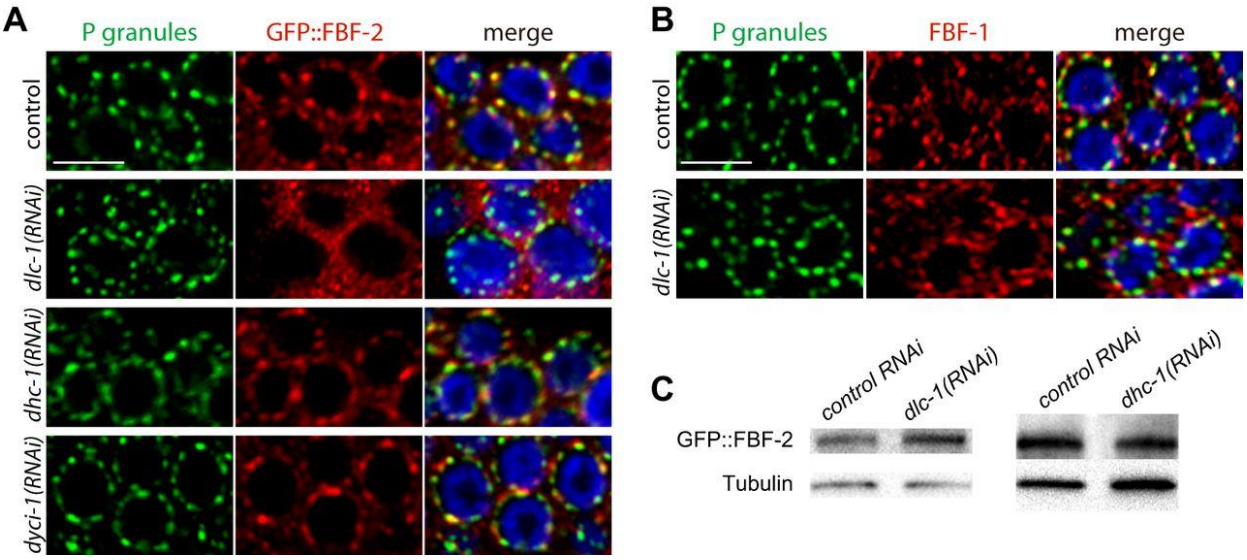

Figure 3-3 DLC-1 is required for FBF-2 localization. (A, B) Confocal images of the mitotic zone of gonads following the indicated RNAi treatments double immunostained for the P granule component PGL-1 (green) and FBF-2 or FBF-1 (red). DNA is in blue. Scale bars: 5 µm. (C) Western blot of whole worm lysates following the indicated RNAi treatments. GFP::FBF-2 protein abundance does not decrease in the *dlc-1*(RNAi) or *dhc-1*(RNAi) backgrounds. Tubulin is used as a loading control.

We next tested whether depletion of the dynein motor subunit DHC-1 or dynein intermediate chain DYCI-1 would affect FBF-2 protein localization. We found that following *dhc-1*(RNAi) or *dyci-1*(RNAi), FBF-2 still localized to perinuclear P granules (Figure 3-3A, third and fourth rows). The levels of FBF-2 protein were not affected by *dhc-1*(RNAi) (Figure 3-3C). The effectiveness of *dhc-1*(RNAi) was verified by western blotting for endogenous DHC-1 (data not shown). We conclude that FBF-2 localization to P granules does not depend on *dhc-1* or *dyci-1*.

DLC-1 IS BROADLY DISTRIBUTED IN THE CYTOPLASM AND OVERLAPS WITH P GRANULES

If DLC-1 is involved with dynein motor-independent activities, the localization of DLC-1 is expected to be different from that of DHC-1. To compare the distribution of DLC-1 and DHC-1 proteins in the germline, we generated a single-copy FLAG-tagged transgene of DLC-1, which rescues *dlc-1(lf),* and co-stained FLAG::DLC-1 with either endogenous DHC-1 (Gönczy et al., 1999) or the GFP::DHC-1 transgene (Gassmann et al., 2008). Both approaches yielded similar results. DHC-1 was observed, as previously reported, in perinuclear patches in the transition zone (Sato et al., 2009) and at the nuclear envelope in pachytene (Figure 3-4A). By contrast, DLC-1 showed a broad diffuse distribution across the germline, overlapping with DHC-1, but without detectable enrichment at the sites of DHC-1 accumulation (Figure 3-4 A-C). We conclude that the differential localization of DLC-1 and DHC-1 supports the proposed motor-independent functions of DLC-1.

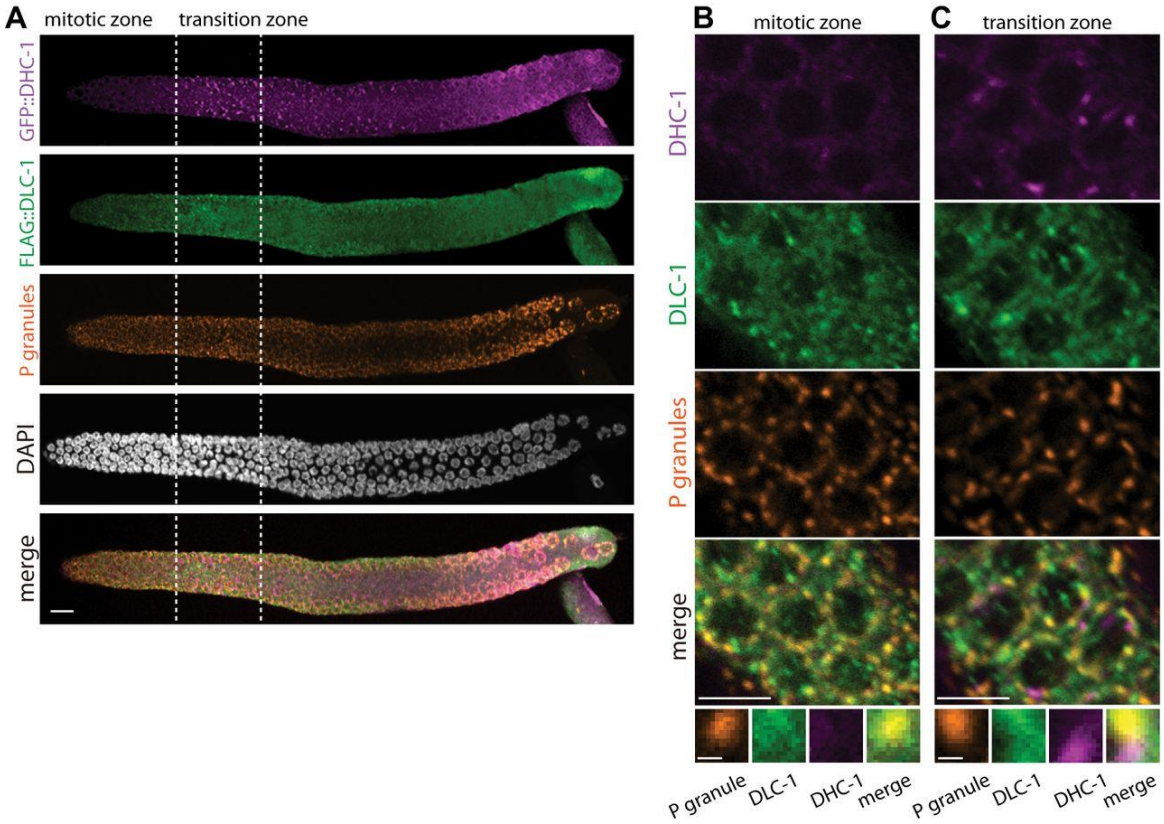

Figure 3-4. DLC-1 overlaps both P granules and DHC-1 patches. (A) Expression of GFP::DHC-1 and FLAG::DLC-1 in a wild-type germ line. (B) In mitotic cells, FLAG::DLC-1 is broadly distributed and overlaps with P granules. A cropped image of a single P granule is shown below. (C) In meiotic cells (transition zone), FLAG::DLC-1 overlaps with both P granules and GFP::DHC-1 patches. GFP::DHC-1 patches do not colocalize with P granules. A cropped image of a P granule adjacent to a GFP::DHC-1 patch is shown below. Scale bars: 10 µm (A); 5 µm (B,C, top panels); 0.5 µm (B,C, bottom cropped images).

If DLC-1 is bound to FBF-2, a fraction of DLC-1 might be observed in P granules. Indeed, we find that FLAG::DLC-1 is present within P granules in both the mitotic region and the transition zone (Figure 3-4B,C, insets). DLC-1 was not particularly enriched in P granules compared with overall cytoplasmic background. Additionally, we observed foci of DLC-1 that did not coincide with either P granules or DHC-1 patches. As DLC-1 overlaps with both P granules and DHC-1 patches, we conclude that DLC-1 might support function of both protein complexes.

To test whether DLC-1 localization to P granules depends on FBF-2 or dynein motor components, we documented DLC-1 localization following RNAi-mediated knockdown of FBFs, DHC-1 or DYCI-1. We find that DLC-1 overlaps P granules in all conditions tested, suggesting that DLC-1

localization to P granules is not affected by the dynein motor or the presence of FBF-2 (data not shown).

DLC-1 BINDS FBF-2 IN VITRO

To test whether the interaction between DLC-1 and FBF-2 is direct, we performed GST pulldown assays with recombinant GST-tagged DLC-1 and His-tagged FBF-2 and FBF-1. We found that His-tagged FBF-2, but not His-tagged FBF-1, binds GST-DLC-1 in vitro (Figure 3-5A). FBF-1 and FBF-2 are highly similar, and their differences are focused in four 'variable regions', three of which map outside of the RNA-binding domain (Figure 3-5B). We hypothesized that the interaction between FBF-2 and DLC-1 depends on the sequences in variable regions (VRs). To test which variable region(s) are important for FBF-2 binding to DLC-1, we created chimeric FBF-1 proteins, referred to as SWAP constructs that contained a single FBF-2 variable region each (Figure 3-5B). VR1, VR2 and VR4 of FBF-2 were each found to be sufficient to mediate interaction with DLC-1 when transferred to FBF-1 (Figure 5C). LC8-type dynein light chains interact with linear peptide sequences of their direct targets that possess a relatively weak (D/S)KX(T/V/I)Q(T/V)(D/E) sequence motif; however, some interacting targets significantly deviate from this motif (Rapali et al., 2011a; Bodor et al., 2014). FBF-2 does not contain this sequence motif in the VRs mediating the interaction with DLC-1. We thus focused on the amino acids that differ between FBF-1 and FBF-2 in VR1 and VR2, and mutated them individually to identify the residues that contribute to the interaction between FBF-2 and DLC-1 (data not shown). Binding of FBF-2(VR1) to DLC-1 can be disrupted by a single mutation, P28A, and binding of FBF-2(VR2) to DLC-1 can be disrupted by either deleting Y139 and G140, or by mutating S136 and K137 to either asparagines (to imitate FBF-1) or alanines (data not shown). FBF-2(VR4) maps to the C-terminal tail, which is completely different from that of FBF-1. C-terminal truncation of VR4 by removing 26 amino acids completely prevents VR4 from binding DLC-1 (data not shown). Combining these substitutions in VR1 and VR2 with the VR4 truncation in the context of the wild-type FBF-2 generated an FBF-2 mutant that was no longer able to bind DLC-1 in vitro (Figure 3-5C). For simplicity, we refer to this mutant as FBF-2vrm.

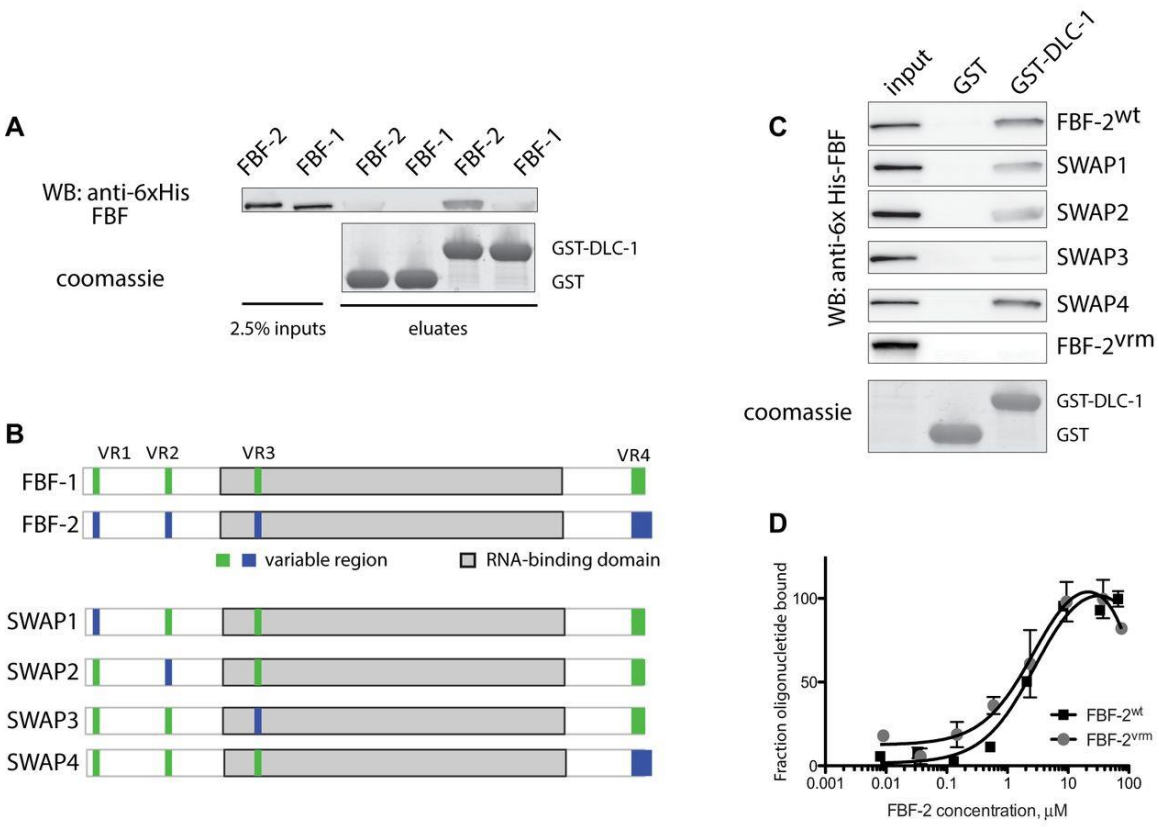

Figure 3-5 FBF-2 binds DLC-1 in vitro. (A) GST-DLC-1 (Coomassie) was assayed for binding to full-length 6×-His-FBF-2 or 6×-His-FBF-1 (detected by western blotting). (B) Schematics of FBF-1 and FBF-2 proteins; variable regions 1-4 and RNA-binding domain are indicated. SWAP chimeric proteins were generated by transferring individual variable regions from FBF-2 to FBF-1. (C) Identification of the FBF-2 variable regions responsible for the interaction with DLC-1 using GST-pulldown analysis analogous to panel A. SWAP chimeric proteins are indicated on the right of the blots. FBF-2vrm contains mutations in variable regions 1, 2 and 4 in the background of wild-type FBF-2 (P28A, S136A, K137A, deleted YG139-140, deleted amino acids 607-632). (D) FBF-2vrm binds to the labeled oligonucleotide with the same affinity as the wild-type protein (Kd of 2.99 µM and 2.91 µM, respectively; P=0.964). Mean±s.e.m. is shown.

We next tested whether the RNA-binding activity of FBF-2 was affected by the mutations that prevent the interaction with DLC-1. FBF-2 binding to RNA oligonucleotides with its recognition motif has been well characterized in vitro (Crittenden et al., 2002; Qiu et al., 2012). Typically, the FBF-2 RNA-binding domain is expressed and assayed in isolation, but as mutations in FBF-2vrm are all outside of the RNA-binding domain, we expressed full-length FBF-2wt and FBF-2vrm to

characterize their binding to a fluorescently labeled target RNA oligonucleotide in vitro. Using fluorescence polarization, we found that FBF-2wt and FBF-2vrm bind to their target oligonucleotide with similar affinities (Kd of 2.99 µM and 2.91 µM, respectively; Figure 3-5D) that are not significantly different from one another (P=0.964). We conclude that mutations preventing FBF-2 interaction with DLC-1 do not lead to general protein misfolding and do not affect FBF-2vrm RNA binding in vitro.

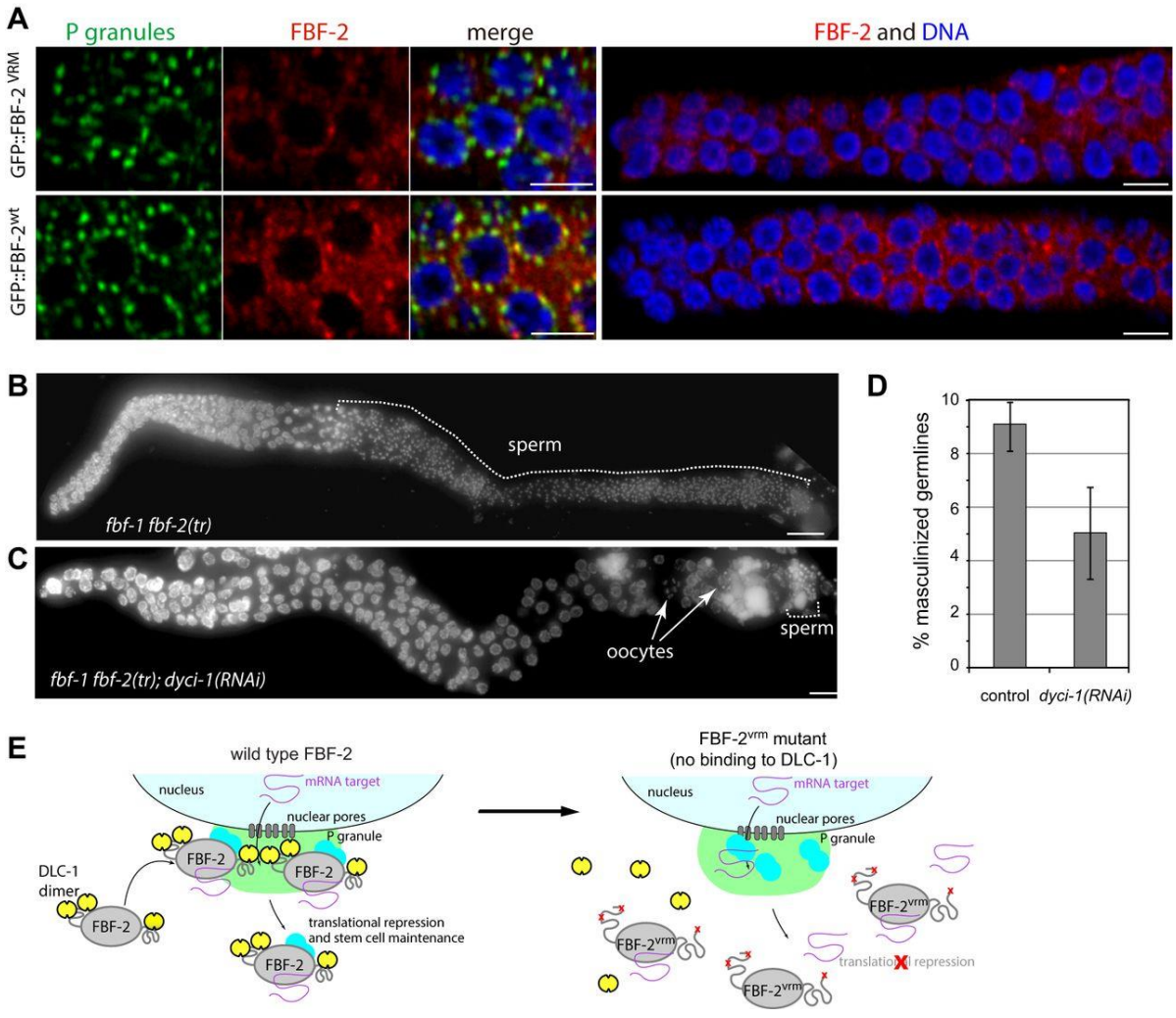

Figure 3-6 Interaction with DLC-1 is required for the localization and function of FBF-2 in vivo. (A) Left panels: confocal images of GFP::FBF-2vrm and GFP::FBF-2wt expression in distal germ cells double immunostained with the antibodies to the P granule component PGL-1 (green) and to GFP (red). Right panels: lower-magnification confocal images of GFP::FBF-2vrm and GFP::FBF-2wt expression in the distal

end of the germline immunostained for GFP (red); gonads are outlined. DNA is in blue. (B,C) Full gonads of sterile *fbf-1(lf) fbf-2(tr)* mutants following control or *dyci-1*(RNAi) treatment stained with DAPI to reveal chromatin morphology. (B) Control germlines: excess sperm (dotted bracket) and no oogenesis. (C) *dyci-1*(RNAi): small oocytes that become endomitotic. (D) Quantification of germline masculinization of *fbf-1(lf) fbf-2(tr)* mutants following control or *dyci-1*(RNAi). The average percentage of masculinization is significantly reduced in the *dyci-1*(RNAi) treatment compared with control ($P<0.01$ by Student's t-test). Mean±s.d. is shown. (E) Working model of DLC-1 supporting FBF-2 activity. Wild-type FBF-2 binds to DLC-1 via variable regions 1, 2 and 4. This binding promotes FBF-2 localization to P granules. Mutations in FBF-2 that preclude its association with DLC-1 interfere with FBF-2 localization to P granules and function. Scale bars: 5 μm (A); 10 μm (B,C).

BINDING OF DLC-1 IS REQUIRED FOR FBF-2 LOCALIZATION TO PERINUCLEAR FOCI IN VIVO

To determine the effect of DLC-1 binding on FBF-2 localization in vivo, we generated a transgene expressing GFP::FBF-2vrm and compared its localization in the germline with that of the wild-type GFP::FBF-2. As previously reported, wild-type GFP::FBF-2 localized to P granules in the distal cells (Figure 3-6A). By contrast, GFP::FBF-2vrm, which lacks the ability to interact with DLC-1, loses its enrichment in perinuclear P granules (Figure 3-6A) and localizes to cytoplasmic aggregates similar to wild-type GFP::FBF-2 in the absence of DLC-1 (Figure 3-3A). We conclude that a direct interaction with DLC-1 is necessary for FBF-2 localization to perinuclear P granules.

DIRECT INTERACTION WITH DLC-1 PROMOTES FBF-2 FUNCTION

P granule localization contributes to FBF-2 function (Voronina et al., 2012). Thus, we predict that FBF-2vrm will show decreased ability to complement the genetic loss of fbf-2. As expected, a complementation assay showed that the GFP::FBF-2vrm transgene exhibits a partial loss of function, and rescues the sterile *fbf-1 fbf-2* double mutant to fertility in 81% of the progeny. By contrast, wild-type GFP::FBF-2 rescues sterility of fbf-1 fbf-2 double mutant in 97% of progeny (Table 3-4).

Table 3-4 Transgenic rescue of *fbf-1 fbf-2* phenotypes and phenotype of *fbf-2(tr)* mutant in an *fbf-1* loss-of-function background

	Sterile (%)	*n*
fbf-1(lf) fbf-2(lf)+transgene		
No transgene	100	61
gfp::fbf-2(wt)	3	90
gfp::fbf-2(vrm)	19	803
Genotype		
fbf-1(lf)	0	419
fbf-1(lf) fbf-2(tr) line 1	12	313
fbf-1(lf) fbf-2(tr) line 2	10	232

Sterility was scored under dissecting microscope by the absence of embryos in the uterus >24 h past the L4 larval stage at 24°C. *n*, number of animals scored.

To test whether the DLC-1-binding regions are important in the context of the endogenous protein, we truncated 26 C-terminal amino acids from the endogenous *fbf-2* using CRISPR/Cas9. This mutation, designated *fbf-2(tr)*, removed one of the three DLC-1-binding sites and was generated in the *fbf-1* mutant background to allow functional analysis of the truncated FBF-2 without compensation by *fbf-1* function. We find that *fbf-1(lf) fbf-2(tr)* strains produce on average 11% sterile progeny when cultured at 24°C, suggesting that the truncated FBF-2 protein is not fully functional (Table 3-4). Chromatin staining of the sterile *fbf-1(lf) fbf-2(tr)* hermaphrodites indicates that sterility is due to a failure to initiate oogenesis during development, consistent with disruption of FBF function in the germline (Figure 3-6B). Multiple DLC-1 binding sites might serve to increase overall affinity of FBF-2 for DLC-1 in a manner similar to other proteins with multiple LC8-binding motifs (Nyarko et al., 2013). We conclude that removing one of three DLC-1 binding sites affects FBF-2 activity in vivo.

DYNEIN MOTOR-RELATED DLC-1 FUNCTION COMPETES WITH FBF-2-RELATED FUNCTION

All data thus far indicate that DLC-1 functions with FBF-2 independently of its function with the dynein motor. To test further whether these functions are separable, we sought to determine whether the dynein motor and FBF-2 might compete for DLC-1 and thus antagonize each other. If true, release of DLC-1 from the dynein motor would be expected to result in enhanced motor-independent function of DLC-1. We took advantage of the partial loss of function of the *fbf-2(tr)*

mutant, in which interaction of FBF-2(tr) with DLC-1 is weakened. If DLC-1 functions in a motor-independent manner, additional DLC-1 released from the dynein motor would promote more efficient FBF-2–DLC-1 complex formation and thus rescue FBF-2(tr) function and oocyte formation. By contrast, if FBF-2 requires dynein motor function, disruption of the motor by *dyci-1*(RNAi) should further compromise FBF-2(tr) function and enhance germline masculinization.

We released DLC-1 from the motor complex by knockdown of dynein intermediate chain dyci-1. Knockdown of dyci-1 resulted in a significant decrease of germline masculinization compared with the control (Figure 3-6 C,D). This rescue of oocyte formation upon disruption of the motor complex, as opposed to enhancement of masculinization, is consistent with DLC-1 functioning with FBF-2 independently of the dynein motor.

Discussion

This study supports three main conclusions that advance our understanding of PUF protein activity regulation. First, we reveal that the regions flanking the PUF RNA-binding domain regulate FBF-2 localization and activity through a specific interaction. Direct association of FBF-2 with DLC-1 is required for FBF-2 concentration in perinuclear P granules and promotes FBF-2 function (Figure 3-6E). Second, by identifying and characterizing the first selective interacting partner of FBF-2 (versus FBF-1) we are able to improve our understanding of the basis for the observed differences between FBF-1/FBF-2 localization and regulatory activity. Third, our data show that the function of DLC-1 in promoting FBF-2 activity is independent of the role of DLC-1 in the dynein motor complex. Although dynein-independent functions of DLC-1/LC8 proteins have been noted before, this study is the first report describing dynein-independent role of DLC-1/LC8 in post-transcriptional control of gene expression.

ASSOCIATION WITH DLC-1 IS REQUIRED FOR FBF-2 LOCALIZATION

PUF proteins are conserved regulators of gene expression in development. Their core RNA-binding domain is required but not sufficient for translational repression (Deng et al., 2008; Muraro et al., 2008; Weidmann and Goldstrohm, 2012). Drosophila Pumilio and mammalian Pum2 have glutamine/asparagine-rich domains that might impact their association with RNA granules, but the mechanism of localization and its relevance to PUF activity are unclear (Vessey

et al., 2006; Salazar et al., 2010). Our work identifies DLC-1 as the first molecular partner recruited through binding sites outside of the FBF-2 RNA-binding domain. Interaction with DLC-1 plays a crucial role in FBF-2 localization to perinuclear foci associated with P granules. DLC-1 does not appear to influence the stability of FBF-2 as DLC-1 knockdown does not affect FBF-2 protein levels.

How does association with DLC-1 change the spatial distribution of its binding partner? One possibility is that DLC-1 recruits FBF-2 to P granules by interacting with other P granule components. However, immunostaining indicates that DLC-1 overlaps with P granules, but is not enriched in P granules compared with the rest of the cytoplasm, suggesting that it is unlikely to target FBF-2 to P granules. An alternative is that DLC-1 forms a complex with FBF-2 in the cytoplasm, which then facilitates stabilization of the disordered regions of FBF-2, forming a scaffold for interaction with other protein partners to mediate recruitment to P granules. DLC-1 is expressed throughout the *C. elegans* germline (Dorsett and Schedl, 2009 and Figure 3-4), with a broader distribution than the motor DHC-1, and is available to form a complex with FBF-2 in germline progenitor cells.

DLC-1 IS AN INTERACTOR SPECIFIC FOR FBF-2

FBF-1 and FBF-2 are similar and partially redundant translational repressors important for *C. elegans* stem cell maintenance. Despite their sequence similarity and association with similar mRNA targets, FBF-1 and FBF-2 show distinct localization patterns in germ cells (Lamont et al., 2004; Voronina et al., 2012). Additionally, single mutants of *fbf-1* and *fbf-2* have opposite effects on the size of the mitotic region of the germline and distinct effects on their shared target mRNAs (Lamont et al., 2004; Voronina et al., 2012). These differences might be due to FBF-1 and FBF-2 interacting with distinct protein partners, and in this study we identify DLC-1 as the first interacting partner specific for FBF-2 over FBF-1. FBF-1 does not interact with DLC-1, and the localization and activity of FBF-1 are not affected by the presence of DLC-1. It is possible that FBF-1 assembles with its own specific binding partner(s) to facilitate its respective localization and function.

LC8 proteins associate with their partners through symmetrical binding sites formed at the two edges of the LC8 dimer interface and are able to interact with a diverse set of partner peptides

(Barbar, 2008; Rapali et al., 2011b). LC8 binding motifs are short linear peptides, often found in intrinsically disordered segments. All three DLC-1-interacting motifs in FBF-2 are located outside of the well-structured RNA-binding domain and are predicted by the PrDOS algorithm to be disordered (Ishida and Kinoshita, 2007) at a 2% false-positive rate. The N-terminal DLC-1 binding sites are not well conserved in nematode FBF homologs. However, C-terminal extension found in FBF-2, but not FBF-1, is also present in the FBF-1/2 homologs from Caenorhabditis japonica and briggsae, suggesting that the interaction with DLC-1 might be conserved. Because none of these regions matches to a consensus DLC-1/LC8-binding site, it would be informative improve our understanding of the structural basis of the FBF-2–DLC-1 association in the future.

DLC-1 PROMOTES FBF-2 ACTIVITY INDEPENDENT OF THE DYNEIN MOTOR

Cytoplasmic motors contribute to post-transcriptional regulation of gene expression. For example, the dynein motor complex is required for asymmetric RNP localization during Drosophila oogenesis and early embryogenesis (Wilkie and Davis, 2001; Bullock and Ish-Horowicz, 2001; Duncan and Warrior, 2002). Our results argue that DLC-1 contributes to FBF-2 function through a dynein motor-independent mechanism. The strongest evidence leading to this conclusion is that releasing DLC-1 from the dynein motor complex alleviates the phenotype of the truncated FBF-2(tr) lacking one of DLC-1 interaction sites. We hypothesize that DLC-1 promotes FBF-2 function by binding to FBF-2 and changing FBF-2 folding or assembly with other proteins.

DLC-1 AS AN ALLOSTERIC REGULATOR OF PROTEIN FUNCTION

LC8 proteins are highly conserved through evolution and contribute to a variety of biological processes (reviewed by Barbar, 2008). LC8 proteins function as regulatory hubs that promote assembly of protein complexes by interacting with short linear motifs of their binding partners (Rapali et al., 2011b). Structurally, binding of LC8 facilitates folding of its partners and increases their alpha-helical content (Nyarko et al., 2004; Bodor et al., 2014). The stabilized alpha-helices could then provide a binding interface for assembly of LC8 partners into larger protein complexes

or otherwise allosterically modify their function. Further research is needed to elucidate whether FBF-2 association with DLC-1 changes FBF-2 structure or integration in a larger protein complex.

DLC-1 IN RNA REGULATION

Is the dynein-independent contribution of DLC-1/LC8 to localization and function of RNA-binding proteins conserved? Similar to *C. elegans* FBF-2, the Drosophila RNA-binding protein Egalitarian (Egl), which is important for asymmetric RNP localization, binds the LC8 dynein light chain Dlc, and this association is required for Egl function (Navarro et al., 2004). Interestingly, a mutation in Egl that disrupts its binding to Dlc does not affect Egl association with the dynein motor adapter BicD. This Egl mutant might be tethered to the dynein motor yet non-functional (Navarro et al., 2004). Similar to FBF-2, the Egl mutant that is unable to bind Dlc can still associate with its RNA target in vitro (Dienstbier et al., 2009).

We propose that DLC-1/LC8 interactions with RNA-binding proteins might impact their regulatory output in a motor-independent fashion, analogous to what we observed for FBF-2. Our work adds post-transcriptional regulation of gene expression to the long list of LC8 functions. This finding opens new directions for further inquiry, such as what other RNA-binding proteins and mRNAs are found in association with DLC-1/LC8 and how association with DLC-1/LC8 affects regulatory activity of its partners.

Acknowledgements

We thank A. Dernburg and P. Gonczy for sharing antibodies; N. Day, M. Maley, E. Osterli and C. A. Pereira for assistance; G. Seydoux and A. Paix for protocols and reagents for co-CRISPR; E. Griffin, E. Gustafson and J. Wang for discussion. Several strains were provided by CGC funded by the NIH (P40 OD010440), and *dlc-1(tm3153)/hT2* was provided by National BioResource Project (Japan). The K76 antibody was obtained from the Developmental Studies Hybridoma Bank (NICHD, The University of Iowa, Iowa City, IA, USA). We thank the University of Montana Molecular Histology and Fluorescence Imaging Core supported by P20RR017670 award from the NCRR.

Chapter 4. Antagonistic control of *C. elegans* germline stem cell proliferation and differentiation by PUF proteins FBF-1 and FBF-2

(This chapter is a manuscript in revision.)

Abstract

Stem cells support tissue maintenance, but the mechanisms that balance the rate of stem cell self-renewal with differentiation at a population level remain uncharacterized. We find that two PUF family RNA-binding proteins FBF-1 and FBF-2 have opposite effects on *C. elegans* germline stem cell dynamics: FBF-1 restricts the rate of meiotic entry, while FBF-2 promotes both cell division and meiotic entry rates. Antagonistic effects of FBFs are mediated by their distinct activities towards the shared set of target mRNAs, where FBF-1 destabilizes target transcripts and FBF-2 promotes their accumulation. FBF-1-mediated post-transcriptional control requires the activity of CCR4-NOT deadenylase, while FBF-2 is deadenylase-independent. These regulatory differences depend on protein sequences outside of the conserved PUF family RNA-binding domain. We propose that the combined FBF-1 and FBF-2 activities balance stem cell division rate with meiotic entry.

Introduction

Adult tissue maintenance relies on the activity of stem cells that self-renew and produce differentiating progeny (Morrison and Kimble, 2006). It is essential that self-renewal be balanced with differentiation to preserve the size of the stem cell pool over time. One simple model achieving this balance is an asymmetric division that always produces a single stem cell daughter and a daughter destined to differentiate (Chen et al., 2016). Alternatively, tissue homeostasis can be controlled at a population level (Simons and Clevers, 2011), where some stem cells are lost through differentiation while others proliferate, with both outcomes occurring with the same frequency. Such population-level control of stem cell activity is observed in the *C. elegans* germline (Kimble and Crittenden, 2007). However, the mechanisms of population-level balance of stem cell proliferation and differentiation in the adult tissues are largely unclear.

The *C. elegans* hermaphrodite germline is a robust system to explore the mechanisms coordinating stem cell proliferation and differentiation. It is maintained by a stem cell niche that supports about 200-250 mitotically-dividing stem and progenitor cells at the distal end of the gonad (collectively called SPCs, **Figure 4-1A, Cii**). A single somatic distal tip cell serves as a stem cell niche and activates the GLP-1/Notch signaling necessary for SPC pool maintenance (Austin and Kimble, 1987), which in turn supports germline development (Hansen and Schedl, 2013). As germline stem cells move proximally away from the niche, they differentiate by entering meiotic prophase and eventually generate gametes near the proximal gonad end. Mitotic divisions of SPCs are not oriented and there doesn't appear to be a correlation between the position of cell divisions distributed throughout the SPC zone and the position of cells undergoing meiotic entry at the proximal end of the zone (Crittenden et al., 2006; Fox et al., 2011; Jaramillo-Lambert et al., 2007; Maciejowski et al., 2006).

Analysis of *C. elegans* germline stem cell maintenance identified a number of genes affecting SPC self-renewal and differentiation (Hansen and Schedl, 2013).Genes essential for self-renewal include GLP-1/Notch and two highly similar Pumilio and FBF (PUF) family RNA-binding proteins called FBF-1 and FBF-2 (Austin and Kimble, 1987; Crittenden et al., 2002; Zhang et al., 1997). Genetic studies of stem cell maintenance led to a model where a balance of mitosis- and meiosis-promoting activities maintains tissue homeostasis (Hubbard and Schedl, 2019), but the regulatory mechanism coordinating proliferative SPC activity with meiotic entry remained elusive.

Importantly, SPC cell cycle is distinct from that of most somatic stem cells. One characteristic feature of *C. elegans* germline SPC cell cycle is a very short G1 phase (Fox et al., 2011; Furuta et al., 2018), reminiscent of the short G1 phase observed in embryonic stem cells (ESCs, (Becker et al., 2006; Kareta et al., 2015; White and Dalton, 2005). Mouse and human ESCs maintain robust cell division rates supported by cell cycle with a short G1 phase while the length of S and G2 phases is similar to that observed in differentiated mouse somatic cells (Becker et al., 2006; Chao et al., 2019; Kareta et al., 2015; Stead et al., 2002). Despite the abbreviated G1 phase, ESCs maintain S and G2 checkpoints (Chuykin et al., 2008; Stead et al., 2002; White and Dalton, 2005). Similarly, *C. elegans* SPCs retain G2 checkpoints despite the shortened G1 phase (Butuči et al.,

2015; Garcia-Muse and Boulton, 2005; Lawrence et al., 2015; Moser et al., 2009). This may be due to a constant proliferative demand that both SPCs and ESCs are subject to. By contrast, this type of modified cell cycle is not observed in the adult stem cell populations that support regenerative response upon injury, such as adult mammalian bulge stem cells (hair follicle stem cells; (Cotsarelis et al., 1990) or satellite cells (muscle stem cells; (Schultz, 1974; Schultz, 1985; Snow, 1977) that remain in G0 or quiescent phase for the most of the adult life and only reenter cell cycle upon injury. Similarly, adult epidermal stem cells maintaining tissue homeostasis regulate their cell cycle by controlling G1/S transition (Mesa et al., 2018).

Unlike somatic cells' G1 phase that is triggered and marked by increased amounts of cyclins E and D (Aleem et al., 2005; Guevara et al., 1999), the germ cells and ESCs characterized by a shortened G1 phase maintain a constitutive robust expression of G1/S regulators Cyclin E and CDK2 (Fox et al., 2011; Furuta et al., 2018; White and Dalton, 2005). Despite continuous proliferation of *C. elegans* SPCs, the SPC mitotic rate changes during development and in different mutant backgrounds (Kocsisova et al., 2019; Michaelson et al., 2010; Roy et al., 2016) and it is unknown how SPC division and meiotic entry rates might be altered while maintaining cell cycle with an abbreviated G1 phase. Here, we report the mechanism through which PUF family RNA binding proteins FBF-1 and FBF-2 simultaneously change the rates of SPC cell cycle progression and meiotic entry.

PUF proteins are expressed in germ cells of many animals and are conserved regulators of stem cells (Salvetti et al., 2005; Wickens et al., 2002). *C. elegans* PUF proteins expressed in germline SPCs, FBF-1 and FBF-2, share the majority of their target mRNAs (Porter et al., 2019; Prasad et al., 2016) and are redundantly required for SPC maintenance (Crittenden et al., 2002; Zhang et al., 1997). Despite 89% identity between FBF-1 and FBF-2 protein sequences, several reports suggest that FBF-1 and FBF-2 localize to distinct cytoplasmic RNA granules and have unique effects on the germline SPC pool (Lamont et al., 2004; Voronina et al., 2012). Specifically, FBF-1 and FBF-2 each support distinct numbers of SPCs (Lamont et al., 2004). Furthermore, FBF-1 inhibits accumulation of target mRNAs in SPCs, while FBF-2 primarily represses translation of the target mRNAs (Voronina et al., 2012). Some differences between FBF-1 and FBF-2 function might be explained by their association with distinct protein cofactors, as we previously found that a

small protein DLC-1 is a cofactor specific to FBF-2 that promotes FBF-2 localization and function (Wang et al., 2016). Despite the fact that several repressive mechanisms have been documented for PUF family proteins (Quenault et al., 2011), it is relatively understudied how the differences between PUF homologs are specified. Here we sought to take advantage of the distinct SPC numbers maintained by individual FBF proteins to understand how they regulate the dynamics of SPCs cell cycle and meiotic entry and probe the functional differences between FBFs.

Elaborating on the general contribution of PUF proteins to stem cell maintenance, we describe here that FBF-1 and FBF-2 have opposing effects on the rates of germline SPCs cell cycle and meiotic entry. We discovered that FBFs regulate core cell cycle machinery transcripts along with transcripts required for differentiation to coordinately change the steady-state amounts of both transcript classes. We show that FBF-1 decreases steady-state levels of target mRNAs and requires CCR4-NOT deadenylation machinery. By contrast, FBF-2 functions independently of CCR4-NOT and promotes accumulation of target mRNAs. These distinct functions of FBFs are determined by the protein regions outside of the conserved PUF homology domain. The dual regulation of SPC cell division and differentiation by FBFs effectively allows the stem cells to match cell division rate with meiotic entry.

Materials and Methods

C. ELEGANS CULTURE AND STRAINS

All *C. elegans* hermaphrodite strains (Supplemental Table S1) used in this study were cultured on NNGM plates seeded with OP50 as per standard protocols (Brenner, 1974). All GFP tagged transgenic animals were cultured at 24°C to avoid GFP silencing. Temperature sensitive allele *glp-1(ar202)* is a gain-of-function (gf) mutant and is referred to as *glp-1(gf)* in this study. *glp-1(gf)* is fertile at 15°C, but sterile at 25°C because germ cells fail to enter meiosis and produce tumorous germlines. *glp-1(gf)* was crossed with each single *fbf* loss-of-function (lf) mutant, *fbf-1(ok91)* and *fbf-2(q738),* to generate *fbf-1(lf); glp-1(gf)* and *fbf-2(lf)/mIn1; glp-1(gf).* Double mutant strains and *glp-1(gf)* single mutant were maintained at 15°C. Propagation of *fbf-2(lf); glp-1(gf)* for large-scale sample collection is detailed in Supplemental Materials and Methods. Synchronized L1

larvae of *glp-1(gf)* strains were cultured at 25°C until early adulthood. RNA was extracted from tumorous worms and was subsequently used for qPCR and poly(A) tail length analysis.

GENERATION OF TRANSGENIC ANIMALS

All transgene constructs were generated by Gateway cloning (Thermo Fisher Scientific). GFP::FBF-1 and GFP::FBF-2 constructs were generated with the *gld-1* promoter, patcGFP containing introns (Frøkjær-Jensen et al., 2016), *fbf-1* or *fbf-2* genomic coding and 3'UTR sequences in pCG150 (Frøkjaer-Jensen et al., 2008). GFP::FBF-2(vrm) was generated with *gld-1* promoter, patcGFP, *fbf-2* genomic coding sequences with variable regions 1, 2, and 4 mutated (P28A, S136A, K137A, Δ139-140, Δ607-632; Wang et al., 2016), and *fbf-2* 3'UTR in pCG150. GFP::FBF-1(FBF-2vr4) and GFP::FBF-1(FBF-2vr3) constructs were generated with *gld-1* promoter, patcGFP, *fbf-1* genomic coding sequences with swapped variable regions 4 or 3 from *fbf-2*, and *fbf-1* 3'UTR sequences in pCG150. 3xFLAG::CCF-1 construct contains *gld-1* promoter, *ccf-1* genomic coding and 3' UTR sequences in pCFJ150. 3xFLAG::CYB-2.1wt and 3xFLAG::CYB-2.1fbm constructs contain *gld-1* promoter, *cyb-2.1* genomic coding and 3' UTR sequences with either wild type (wt, 5' **UGU**xxxAU 3') or mutated (fbm, 5' **ACA**xxxAU 3') FBF binding sites in pCFJ150.

A single-copy insertion of each GFP-tagged FBF transgene and CYB-2.1 transgenes was generated by homologous recombination into universal *Mos1* insertion site on chromosome III after Cas9-induced double-stranded break (Dickinson et al., 2013; Wang et al., 2016). Similarly, single-copy insertion of 3xFLAG-tagged CCF-1 was generated by targeting universal *Mos1* insertion site on chromosome II. Transgene insertion into universal *Mos1* insertion sites was confirmed by PCR.

GERMLINE SPC ZONE MEASUREMENT

C. elegans were synchronized by bleaching, and hatched L1 larvae were plated on NNGM plates with OP50 bacteria or RNAi culture, cultured at specified temperatures and harvested at varying time points depending on the experiment. L1 larvae of *fbf-2(lf); cyb-2.1fbm*, *fbf-2(lf); cyb-2.1wt* and *fbf-2(lf)* were grown at 15°C for 5 days until adult stage. For the time course of SPC zone dynamics, L1 larvae of *fbf-1(lf), fbf-2(lf)* and the wild type (N2) were cultured at 24°C and dissected at 46 hour (early adults that have initiated oogenesis), 52 hour (adults) and 63 hour (older adults) time points. In all other SPC zone quantification assays, L1 larvae of all worm strains were cultured at 24°C and dissected for staining at 52 hour time point. Gonads were dissected

and stained for mitotic marker REC-8 (Hansen et al., 2004a), and the length of SPC zone in each germline was measured by counting the number of germ cell rows positive for REC-8 staining before transition zone, ending with the last row fully occupied by REC-8-positive cells. Measuring the extent of progenitor zone by counting the number of cell rows positive for mitotic marker REC-8 provides a reliable estimate of progenitor cell numbers and correlates with progenitor cell numbers in the key genotypes including wild type, *fbf-1(lf)*, and *fbf-2(lf)* (R2=0.779; data not shown).

DETERMINATION OF G2-PHASE LENGTH AND MEIOTIC ENTRY RATE

G2-phase length analysis and determination of meiotic entry rates were performed by feeding *C. elegans* 5-ethynyl-2'-deoxyuridine (EdU)-containing bacteria as previously described (Crittenden et al., 2006; Fox et al., 2011; Kocsisova et al., 2018), see Supplemental Methods for details. Germline images were captured as z-stacks spanning the thickness of each germline using a Leica DM5500B microscope. For each replicate time point 7-14 germlines were scored and the data represent 3 or 5 biological replicates. Nuclei were manually counted using the Cell Counter plug-in in Fiji (Schindelin et al., 2012) and the Marks-to-Cells R script (Seidel and Kimble, 2015) was used to remove multiply-counted nuclei.

Percent differences in median G2-phase length or differentiation rate were calculated as for mitotic index above.

LARVAL GERM CELL PROLIFERATION RATE

Germ cell proliferation assays were performed using strains where germ cells were identified by expression of PGL-1::GFP. The nematodes were synchronized by bleaching and hatched L1s were fed on OP50 NNGM plates. The *pgl-1::gfp*, *fbf-1(ok91)*; *pgl-1::gfp* and *fbf-2(q738)*; *pgl-1::gfp* strains were grown at 24°C. At 17 and 21-hour time points after the start of feeding samples were taken to image germ cell accumulation in L2 larvae. The data represents 4 biological replicates, and 15-21 germlines of each strain were scored per time point in each replicate. To analyze CYB-2.1 effect on larval germ cell proliferation, the *fbf-2(q738)*; *pgl-1::gfp*, *fbf-2(q738)*; *cyb-2.1(wt)*; *pgl-1::gfp*, and *fbf-2(q738)*; *cyb-2.1(fbm)*; *pgl-1::gfp* strains were grown at 15^{o}C. At 41 and 46-hour time points after the start of feeding germ cells were imaged in L2 larvae, and the data represents 5 biological replicates with 13-20 germlines scored per time point in each replicate.

The number of germ cells were scored in each germline by counting cells containing P granules. The doubling rate of larval germ cells was estimated by exponential fits performed independently for each biological replicate.

RNAI TREATMENT

The following RNAi constructs were used: *ccr-4, let-711* (Kamath and Ahringer, 2003), *ccf-1* (*cenix:341-c12*; (Sönnichsen et al., 2005) and *cyb-2.1* (genomic CDS) in pL4440 (Timmons and Fire, 1998). Empty vector pL4440 was used as a control in all RNAi experiments. All RNAi constructs were verified by sequencing. RNAi plates were prepared as previously described (Wang et al., 2016) and synchronously hatched L1 larvae were plated directly on RNAi plates, except for *let-711* and *ccf-1(RNAi)*, where L1 larvae were initially grown on OP50 plates and transferred to RNAi plates at the L2/L3 stage. For CCR4-NOT knockdown, worms were grown at 24^{o}C for 52 hours before analysis; for *cyb-2.1* knockdown, worms were grown at 15^{o}C for 120 hours before analysis. The effect of *cyb-2.1(RNAi)* was confirmed by western blot of 3xFLAG::CYB-2.1. The effectiveness of CCR4-NOT RNAi treatments was assessed by scoring sterility (data not shown) or embryonic lethality (data not shown) in the F1 progeny of the fed animals.

RNA EXTRACTION AND PAT-PCR

glp-1(gf) and *fbf-1(lf); glp-1(gf) C. elegans* were synchronized using bleach, hatched L1s were cultured at 25°C and worms were harvested after 52 hours. See notes on the culture of *fbf-2(lf); glp-1(gf)* strain in Supplemental Methods. A subset of animals from each batch were dissected and germlines were stained with DAPI, anti-REC-8, and anti-phospho-histone H3 to assess abnormal proliferation. Although the documented phenotype of *glp-1(ar202)* at 25^{o}C is ectopic germline proliferation in the proximal region, we have often observed formation of full germline tumors in all three genotypes in our culture conditions. The RNA samples were prepared from the cultures with >77% full germline tumors. Worm pellets were washed 2 times with 1x M9 to remove OP50 bacteria, weighed, flash-frozen using dry ice/ethanol slurry and stored at -80°C. Worm pellets of each strain were collected in triplicate and the qPCR data represent 3 biological replicates. Total RNA was isolated from the worm pellets using Trizol (Invitrogen) and Monarch Total RNA miniprep kit (NEB). RNA concentration was measured using Nanodrop (Thermo Fisher Scientific) or Qubit Fluorometric quantitation (Invitrogen). PAT-PCR for the FBF target *cyb-2.1* and

control *tbb-2* was performed using a Poly(A) Tail-Length Assay Kit (Thermo Fisher Scientific). Briefly, G/I tailing, reverse transcription, PCR amplification and detection were performed following the kit protocol. Each G/I tailing reaction used 1 ug total RNA. During PCR amplification, 1 ul of diluted RT sample was used in each PCR reaction and a two-step PCR program was used: 94°C for 2 min, (94°C for 10 sec, 60°C for 1min 30sec) x 35 cycles, 72°C for 5 min. PCR products were assessed using 6% polyacrylamide gel (made with 29:1 Acrylamide/Bis Solution, Bio-Rad) electrophoresis. PCR products were visualized with SYBR Gold stain (Invitrogen) and recorded using ChemiDoc MP Imaging System (Bio-Rad). Poly(A) tail lengths were compared using densitometry analysis in ImageJ.

IMMUNOLOCALIZATION AND IMAGE ANALYSIS

For all immunostaining experiments, *C. elegans* hermaphrodites were dissected and fixed as previously described (Wang et al., 2016). All primary antibody incubations were overnight at 4°C and all secondary antibody incubations were for 1.5 h at room temperature. For colocalization analysis of endogenous FBF-1 and 3xFLAG::CCF-1, dissected gonads of *flag::ccf-1* were stained with anti-FBF-1 (Rabbit) and anti-FLAG primary antibodies (Mouse). For colocalization analysis of GFP::FBFs and 3xFLAG::CCF-1, dissected gonads of *3xflag::ccf-1; gfp::fbf-2* and *3xflag::ccf-1; gfp::fbf-1* were stained with rabbit anti-GFP and mouse anti-FLAG primary antibodies. Secondary antibodies were Goat anti-Mouse or Goat anti-Rabbit. Germline images were acquired using Zeiss 880 confocal microscope. Localization of FBF granules relative to CCF-1 granules were analyzed in a single confocal section per germline with 4-6 germ cells in SPC zone by Pearson's correlation coefficient analysis using the JACoP plugin of ImageJ. For each worm strain, 4-8 independent germline images were analyzed and Pearson's correlation coefficient values were averaged.

PROXIMITY LIGATION ASSAY (PLA)

PLA was performed on dissected *C. elegans* gonads following a modified Duolink® PLA Protocol as described (Day et al., 2020). Fixation was as previously described (Wang et al., 2016). Blocking step included incubation in 1xPBS/0.1% Triton-X-100/0.1% BSA for 2x 15 min at room temperature, in 10% normal goat serum for 1 hr at room temperature, and in Duolink blocking buffer for 1 hr at 37°C. Primary anti-GFP and anti-FLAG antibodies were diluted in Duolink diluent. After overnight incubation with primary antibodies at 4°C, 1:5 dilutions of PLUS and MINUS

Duolink® PLA Probes were added to each slide and incubated at 37°C for 1 hr. Next, slides were incubated at 37°C for ligation (for 30 min) and amplification (for 100 min) steps and finally mounted with Duolink Mounting medium with DAPI. Images were acquired using Zeiss 880 confocal microscope. The ImageJ "Analyze Particles" plugin was used to quantify PLA foci in germline images.

FBF TARGET REPORTER REGULATION ASSAY

Reporter transgene with GFP fused to Histone H2B and the 3' untranslated region (UTR) of *htp-2* (Merritt et al., 2008; Merritt and Seydoux, 2010) was crossed into *rrf-1(lf), rrf-1(lf)/hT2; fbf-1(lf)* and *rrf-1(lf); fbf-2(lf)* genetic backgrounds. RNAi targeting *let-711* and *ccf-1* were conducted on these reporter strains as described above. The effectiveness of RNAi treatments was assessed by scoring F1 embryo lethality. RNAi treated worms were dissected and fluorescent germline images were acquired on a Leica DFC300G camera attached to a Leica DM5500B microscope with a standard exposure. Percentage of germlines that exhibited target reporter derepression in the SPC zone was scored for each strain.

IMMUNOBLOTTING

Synchronous cultures of *C. elegans* were collected at the adult stage by washing in 1xM9 and centrifugation and worm pellets were lysed by sonication. Proteins from worm lysates were separated using SDS-PAGE gel electrophoresis and transferred to a 0.45 µm PVDF membrane (EMD Millipore) as previously described (Ellenbecker et al., 2019). Blots were developed using Luminata Crescendo Western HRP substrate (EMD Millipore) and visualized using ChemiDoc MP Imaging System (Bio-Rad).

Results

FBF-1 AND FBF-2 DIFFERENTIALLY MODULATE CELL DIVISION AND MEIOTIC ENTRY OF *C. ELEGANS* GERMLINE SPCS

During tissue maintenance, stem cells adjust their proliferative activity and differentiation rate through diverse regulatory mechanisms, including RNA-binding protein mediated post-transcriptional regulation. We hypothesized that two paralogous RNA-binding proteins FBF-1 and FBF-2 differentially regulate germline stem cell mitotic rate and meiotic entry in *C. elegans*,

resulting in distinct effects on the size of stem and progenitor cell (SPC) zone. We first determined how the extent of SPC zone was affected by loss-of-function mutations of each *fbf*. SPCs were marked by staining for a nucleoplasmic marker REC-8 (**Figure 4-1A and C**) (Hansen et al., 2004a), and the extent of SPC zone was measured by counting the number of cell rows positive for REC-8 staining in each germline. Consistent with a previous report (Lamont et al., 2004), we observed that the SPC zone of *fbf-1(ok91, loss-of-function mutation, lf)* (~15 germ cell diameters, gcd; **Figure 4-1Ci**) is smaller than that of the wild type (~20 gcd, **Figure 4-1Cii**), whereas the SPC zone of *fbf-2(q738, loss-of-function mutation, lf)* (~25 gcd, **Figure 4-1Ciii**) is larger than that of the wild type (**Figures 4-1B and C**). The differences in the length of SPC zone between *fbf* single mutants and the wild type are consistently observed in animals from the late L4 to the second day of adulthood (data not shown).

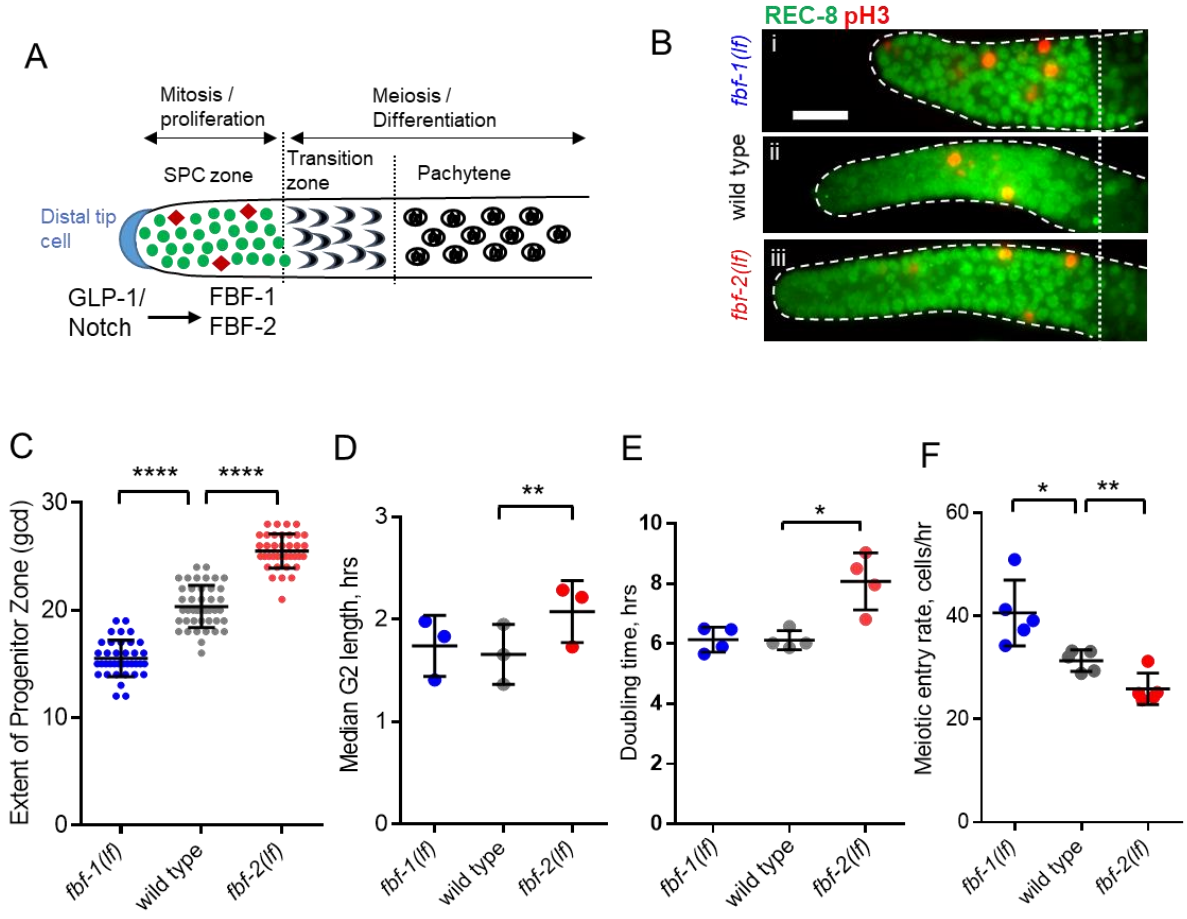

Figure 4-1. FBF-1 and FBF-2 differentially regulate the extent of germline stem and progenitor cell (SPC) zone. (A) Schematic of the distal germline of *C. elegans* adult hermaphrodite. In this and following images, germlines are oriented with their distal ends to the left. GLP-1/Notch signaling from the distal tip cell (blue) supports germline SPC proliferation. Progenitors enter meiosis when they reach the transition zone. FBF-1 and FBF-2, downstream of GLP-1/Notch, are required for SPC maintenance. Green circles, stem and progenitor cells; red diamonds, mitotically dividing cells. (B) Distal germlines dissected from adult wild type, *fbf-1(lf)*, and *fbf-2(lf)* hermaphrodites and stained with anti-REC-8 (green) and anti-phospho-Histone H3 (pH3; red) to visualize the SPC zone and mitotic cells in M-phase. Germlines are outlined with the dashed lines and the vertical dotted line marks the beginning of transition zone as recognized by the 'crescent-shaped' chromatin and loss of REC-8. Scale bar: 10 µm. (C) SPC zone lengths of the wild type, *fbf-1(lf)* and *fbf-2(lf)* germlines were measured by counting germ cell diameters (gcd) spanning SPC zone. Genetic background is indicated on the X-axis and the extent of SPC zone on the Y-axis. Differences in SPC zone lengths were evaluated by one-way ANOVA with Dunnett's post-test. Data were collected from 3 independent experiments. (D) Median SPC G2-phase length in different genetic backgrounds, as indicated on the X-axis. Difference in median G2 length was evaluated by one-way ANOVA with Dunnett's post-test. G2 length was estimated in 3 independent experiments. (E) Larval germ cell doubling time in different genetic backgrounds (as indicated on the X-axis). Plotted values are individual data points and arithmetical means ± SD. Difference in germ cell doubling time was evaluated by one-way ANOVA with Dunnett's post-test. (F) Meiotic entry rate of germline progenitors in different genetic backgrounds indicated on the X-axis. Differences in meiotic entry rate between each *fbf* and the wild type were evaluated by one-way ANOVA with T-test with Bonferroni correction post-test. Meiotic entry rates were estimated in 5 independent experiments. (C-F) All experiments were performed at 24°C. Plotted values are individual data points and arithmetical means ± SD. Asterisks mark statistically-significant differences (****, $P<0.0001$; ***, $P<0.001$; **, $P<0.01$; *, $P<0.05$).

To test whether the differences in the lengths of germline SPC zone between *fbf* mutants and the wild type result from changes in the rate of cell division, we compared cell cycle parameters in each genetic background. We started with measuring the M-phase index (the percentage of SPC zone cells in M phase) following immunostaining for the SPC marker REC-8 and the M-phase marker phospho-histone H3 (pH3, **Figure 4-1B**). We found that the mitotic index of *fbf-1(lf)* was significantly higher than that of the wild type (by 54%). By contrast, the mitotic index of *fbf-2(lf)*

was significantly lower than that of the wild type (by 42%). These results suggested that loss of FBF-2 might reduce SPC proliferation. We also considered the possibility that the loss of FBF-1 might accelerate progression of SPCs through cell cycle. However, as described below, this hypothesis was rejected. Since *C. elegans* stem cells have an abbreviated G1 and an extended G2 phases (Fox and others 2011), we tested whether the G2-phase duration is affected differentially by loss of function mutation of each *fbf.* Using phospho-histone H3 immunostaining and 5-ethynyl-2'-deoxyuridine (EdU) pulse we estimated a median G2 length by determining when 50% of pH3 positive cells become EdU-positive. We found that the median G2 length of *fbf-2(lf)* is significantly greater than that of the wild type, suggesting that loss of FBF-2 results in slower progression through the G2-phase of the cell cycle (by 25%; **Figure 4-1D**). By contrast, the median G2 length of *fbf-1(lf)* is not significantly different from that of the wild type (**Figure 4-1D**). We conclude that FBF-2 accelerates SPC cell cycle by facilitating the G2-phase progression.

Since mutation of *fbf-1* did not affect the length of G2 phase, we tested whether percentage of SPCs in S phase is affected by this mutation. We determined percent SPCs labeled by EdU during a 30-minute pulse (Fox et al., 2011) and found a minor increase in S-phase index in *fbf-1(lf)* compared to the wild type (data not shown). These results refute the interpretation that *fbf-1(lf)* mutation causes faster cell cycle progression.

To directly estimate the rate of germ cell division in wild type and *fbf* mutants, we assayed germ cell proliferation during larval development before the onset of meiotic differentiation. In *C. elegans*, two primordial germ cells in L1 larvae proliferate to produce germline stem cell pools of 20-30 cells in L2 larval stage within 20 hours (Hansen et al., 2004a; Hirsh et al., 1976; Pepper et al., 2003b). We found that *fbf-1(lf)* did not affect the rate of germ cell division, while *fbf-2(lf)* dramatically reduced germ cell accumulation. Exponential fits revealed that *fbf-2(lf)* significantly increased SPC doubling time from 6.1 h to 8.1 h (**Figure 4-1E**). By contrast, there was no significant difference in germ cell proliferation rate between *fbf-1(lf)* and the wild type. We conclude that the cell division rate is decreased in *fbf-2(lf)* and unaffected in *fbf-1(lf)*.

Despite the same SPC cell division rate, the SPC zone of *fbf-1(lf)* is smaller than that of the wild type, suggesting a possibility that *fbf-1(lf)* might result in faster meiotic entry. Conversely,

compared to the wild type, *fbf-2(lf)* maintains a relatively larger SPC population but with slower proliferation, suggesting that the rate of meiotic entry in *fbf-2(lf)* might be slower than in the wild type. To test these possibilities, we determined the rate of meiotic entry in each genetic background. Animals were continuously EdU labeled and stained for EdU and REC-8 at three time points. The number of germ cells negative for REC-8 but positive for EdU were scored at each time point and the rate of meiotic entry was estimated from the slope of plotted regression line. We found that *fbf-1(lf)* results in a significantly increased rate of meiotic entry compared to the wild type (by 31%; **Figure 4-1F**), whereas *fbf-2(lf)* results in a significantly reduced rate of meiotic entry (by 18%; **Figure 4-1F**). We conclude that FBF-2 stimulates meiotic entry while FBF-1 inhibits meiotic entry.

To additionally test whether *fbf-2* promotes meiotic entry, we tested whether *fbf-2(lf)* enhances the overproliferative phenotype of the weak *glp-1* gain-of-function allele, *glp-1(ar202)*. We find that *fbf-2(lf)* is a strong enhancer of *glp-1(gf)* since 97% *fbf-2(lf); glp-1(gf)* animals have tumorous germlines with 24% germlines showing complete tumors, even at the permissive temperature of 15°C (Table 4-1).

Table 4-1 *fbf-2(lf)* enhances the overproliferation phenotype of *glp-1(gf)* at 15°C

Genotype	Normal germline, %	Tum, %	Pro, %	*N*
fbf-2(q738lf)	100	0	0	*many*
fbf-1(ok91lf)	100	0	0	*many*
glp-1(ar202gf)	100	0	0	231
fbf-2(lf); glp-1(gf)	3	24	74	104
fbf-1(lf); glp-1(gf)	99	0	1	414

All animals were maintained at 15°C. For each genotype, after scoring sterility as the lack of embryos in the uterus, germlines of sterile animals were dissected and stained with DAPI, anti-REC-8 antibodies,

and anti-phospho-histone H3 antibodies for evaluation of overproliferation. All animals were analyzed at 1 day after L4 stage. Tum, a complete tumorous germline. Pro, proximal overproliferation phenotype.

In summary, mutations in *fbf-1* and *fbf-2* differentially influence both SPC cell cycle and meiotic entry rate, suggesting FBF proteins have antagonistic effects on SPC proliferation and differentiation. FBF-1 promotes a more quiescent stem cell state characterized by a slower rate of meiotic entry, while FBF-2 promotes a more activated stem cell state characterized by faster rates of both cell cycle and meiotic entry. Although FBF-1 and FBF-2 share the majority of target mRNAs and bind to the same motif in the 3'UTRs (Porter et al., 2019; Prasad et al., 2016), they have different effects on their targets: FBF-1 promotes target mRNA clearance in the stem cell region, whereas FBF-2 sequesters target mRNAs (Voronina et al., 2012). We hypothesized that FBF effects on germline SPC proliferation and differentiation might be explained by their differential regulation of target mRNAs associated with cell cycle progression and meiotic entry in germline SPCs.

PUF-MEDIATED REPRESSION OF CYCLIN B LIMITS ACCUMULATION OF GERMLINE SPCS

Cyclin B/Cdk1 kinase, also known as M-phase promoting factor, triggers G2/M transition in most eukaryotes (Lindqvist et al., 2009). Four cyclin B family genes provide overlapping as well as specific mitotic functions in *C. elegans* (van der Voet et al., 2009). We hypothesized that the slower G2-phase and lower M-phase index of *fbf-2(lf)* SPCs results from translational repression and reduced steady-state levels of four cyclin B family transcripts mediated by the remaining germline-expressed PUF-family proteins. We addressed this hypothesis in two ways. First, we tested whether mutation of FBF binding elements (FBEs) in the 3'UTR of *cyb-2.1* mRNA would result in translational derepression of *cyb-2.1*. Second, we assessed whether derepression of *cyb-2.1* in *fbf-2(lf)* would lead to accumulation of more SPCs by uncoupling PUF-mediated regulation of cell division and meiotic entry.

FBFs repress their target mRNAs by binding to the FBF-binding elements (FBEs; UGUxxxAU) in the 3'UTRs (Bernstein et al., 2005; Crittenden et al., 2002; Merritt and Seydoux, 2010). Four mRNAs encoding Cyclin B family members co-purify with FBF proteins and three of them contain predicted FBEs in their 3'UTRs (Porter et al., 2019; Prasad et al., 2016). Since *cyb-2.1* mRNA is consistently isolated in complex with FBFs and contains more canonical FBE sites in its 3'UTR than the other cyclin B transcripts, we chose to analyze the translational regulation of *cyb-2.1*. If FBFs repress translation of *cyb-2.1* by binding to FBEs, mutation of FBEs would cause derepression of CYB-2.1 protein. To test this prediction, we established a transgenic animal *3xflag::cyb-2.1(fbm)*, expressing 3xFLAG::CYB-2.1 under the control of 3'UTR with mutated FBEs (ACAxxxAU); as a control, a transgenic animal expressing 3x*flag::cyb-2.1(wt)* with wild type FBEs was also established (**Figure 4-2A**). Quantification of transgene transcript levels by qPCR suggested that steady-state transcript levels of *3xflag::cyb-2.1(fbm)* were ~4-fold greater than those of *3xflag::cyb-2.1(wt)*, suggesting that FBEs affect transcript stability (**Figure 4-2B**). By immunoblotting, we found that the expression of 3xFLAG::CYB-2.1 protein was increased ~1.4 fold in *3xflag::cyb-2.1(fbm)* animals compared to *3xflag::cyb-2.1(wt)*, suggesting that the presence of FBEs leads to lower protein production from *cyb-2.1* mRNA (**Figure 4-2C**). The abundance of cyclin family proteins is subject to extensive post-translational control (Langenfeld et al., 1997; Peters, 2002), which likely accounts for a larger difference observed at the level of transcript. *C. elegans* SPCs express five PUF-family proteins that cluster into three groups based on sequence similarity: FBF-1/-2, PUF-8, and PUF-3/-11 (Ariz et al., 2009; Crittenden et al., 2002; Haupt et al., 2019b; Lamont et al., 2004; Stumpf et al., 2008). Each of the three PUF groups has a distinct RNA-binding specificity (Bernstein et al., 2005; Koh et al., 2009; Opperman et al., 2005), so it is likely that FBEs in *cyb-2.1* 3'UTR are predominantly recognized and regulated by FBFs. However, we cannot exclude the possibility that FBEs in the *cyb-2.1* 3'UTR mediate association with PUFs other than FBF-1/-2. We conclude that *cyb-2.1* expression in SPCs is downregulated by PUF proteins recruited to the FBEs.

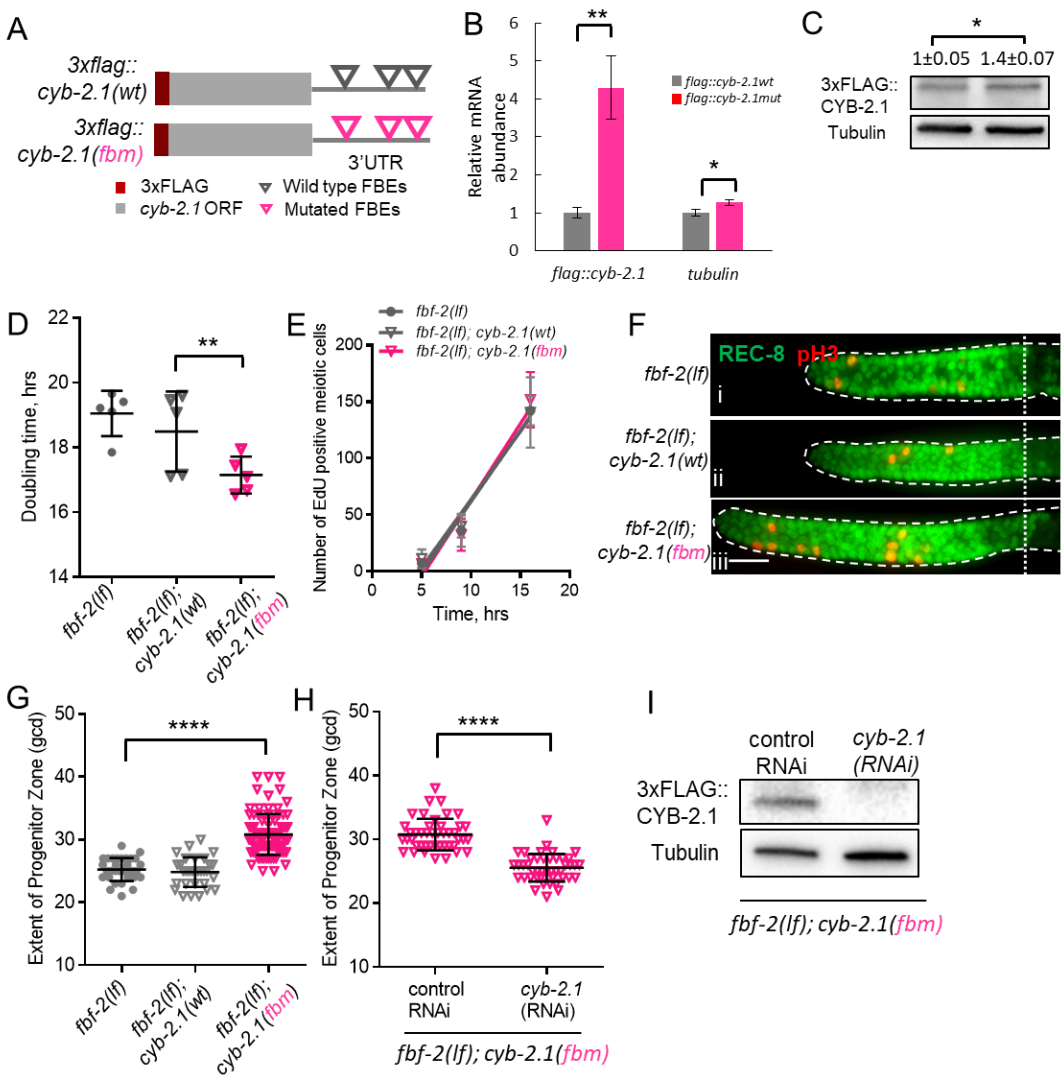

Figure 4-2. FBF-mediated repression of cyclin B limits accumulation of germline progenitor cells. (A) Schematic representation of transgenes encoding 3xFLAG-tagged CYB-2.1(wt) with wild type FBF binding elements (FBEs, UGUxxxAU) in 3'UTR and 3xFLAG-tagged CYB-2.1(fbm) with FBF binding elements mutated (ACAxxxAU). (B) qRT-PCR of *3xflag::cyb-2.1* transcript in *3xflag::cyb-2.1(wt)* and *3xflag::cyb-2.1(fbm)* worms using actin (*act-1*) as a normalization control. (C) Immunoblot analysis of 3xFLAG::CYB-2.1 protein levels in *3xflag::cyb-2.1(wt)* and *3xflag::cyb-2.1(fbm)* worms using α-tubulin as a loading control. (D) Larval germ cell doubling time in different genetic backgrounds (as indicated on the X-axis). Plotted values are individual data points and arithmetical means ± SD. Difference in germ cell doubling time was evaluated by one-way ANOVA with Dunnett's post-test. (E) Meiotic entry rate of progenitors in different genetic backgrounds. Time course of accumulating EdU-labeled, REC-8 negative germ cells in

different genetic backgrounds in one biological replicate (the data is representative of two biological replicates). X-axis displays time points when animals were dissected for staining for EdU and REC-8. Y-axis indicates the number of EdU-positive cells that are negative for REC-8. Plotted values are arithmetical means ± SD. (F) Distal germlines dissected from the *fbf-2(lf), fbf-2(lf); cyb-2.1(fbm)* and *fbf-2(lf); cyb-2.1(wt)* animals and stained with anti-REC-8 (green) and anti-pH3 (red). Germlines are outlined with dashed lines and the vertical dotted line marks the beginning of transition zone. Scale bar: 10 μm. (G) The extent of SPC zone in the *fbf-2(lf), fbf-2(lf); cyb-2.1(fbm)* and *fbf-2(lf); cyb-2.1(wt)* genetic backgrounds. Plotted values are individual data points and arithmetical means ± SD. Differences in SPC zone lengths were evaluated by one-way ANOVA with Dunnett's post-test; asterisks mark statistically-significant difference ($P<0.0001$). Data was collected from 3 independent experiments and 57~110 independent germlines were scored for each genotype. (H) The extent of SPC zone in the *fbf-2(lf); cyb-2.1(fbm)* after *cyb-2.1(RNAi)* compared to the empty vector RNAi control. Plotted values are individual data points and arithmetical means ± SD. Differences in SPC zone lengths were evaluated by T-test; asterisks mark statistically-significant difference ($P<0.0001$). Data was collected from 2 independent experiments and 44 independent germlines were scored for each condition. (I) Immunoblot analysis of 3xFLAG::CYB-2.1 protein levels in *3xflag::cyb-2.1fbm* after *cyb-2.1(RNAi)* compared to the empty vector RNAi control. Tubulin was used as a loading control. (B-I) All experiments were performed at 15°C.

Loss of function mutation in *fbf-2* is associated with slower SPC cell division in conjunction with a slower SPC meiotic entry rate. We hypothesized that both these phenotypes might be mediated by reduced translation of key FBF target mRNAs that are required for cell cycle progression or meiotic entry respectively. We aimed to disrupt the coordinate repression of cell cycle and differentiation-related transcripts in *fbf-2(lf)* by introducing *3xflag::cyb-2.1(fbm)* transgene that produces increased levels of corresponding mRNA and protein. *fbf-2(lf)* with its slow cell cycle rate provides a sensitized background for testing the effects of cyclin B deregulation on cell cycle dynamics since it is not clear whether SPC cell cycle rate could be accelerated beyond that of the wild type. We hypothesized that the slower SPC cell cycle in *fbf-2(lf)* is caused by PUF-mediated destabilization and repression of cyclin B-family mRNAs. If any cyclin B-family gene can promote SPC proliferation, disrupting translational repression of a single cyclin B-family transcript in *fbf-2(lf)* would rescue the slow cell cycle phenotype and accelerate SPC cell division. To test this

hypothesis, we estimated the doubling time of larval germ cells after crossing the *3xflag::cyb-2.1fbm* and *3xflag::cyb-2.1wt* transgenes into *fbf-2(lf)* genetic background. We found that the SPC doubling time of *fbf-2(lf); 3xflag::cyb-2.1fbm* was significantly shorter than that of *fbf-2(lf)* (17 h vs 19 h; **Figure 4-2D**). By contrast, there was no significant difference in the doubling time between *fbf-2(lf); 3xflag::cyb-2.1wt* and *fbf-2(lf)* (**Figure 4-2D**). We expected that overexpression of 3xFLAG::CYB-2.1 in *fbf-2(lf)* genetic background would not affect SPC meiotic entry rate. Determination of SPC meiotic entry rate revealed that there was no significant difference in meiotic entry rate among *fbf-2(lf)*, *fbf-2(lf); cyb-2.1wt*, and *fbf-2(lf); cyb-2.1(fbm)* (**Figure 4-2E**).

Accelerated SPC cell cycle without a change in SPC meiotic entry rate would be expected to result in accumulation of SPCs and an increase of SPC zone length. To test this prediction, we measured the extent of SPC zone of *fbf-2(lf); 3xflag::cyb-2.1fbm* and *fbf-2(lf); 3xflag::cyb-2.1wt*. We found that the SPC zone of *fbf-2(lf)*; *3xflag::cyb-2.1fbm* (~32 gcd, **Figure 4-2Fiii**) is significantly larger than that of the *fbf-2(lf)* (~26 gcd, **Figure 4-2Fi, G**, $P < 0.0001$). By contrast, there is no significant difference in the length of SPC zone between the *fbf-2(lf)*; *3xflag::cyb-2.1wt* and *fbf-2(lf)* (**Figure 4-2Fii, G**). To test whether the expansion of SPC zone in *fbf-2(lf)*; *3xflag::cyb-2.1fbm* results from overexpression of *cyb-2.1*, we measured the extent of SPC zone following knockdown of *cyb-2.1* by RNAi. We found that the SPC zone of *fbf-2(lf); 3xflag::cyb-2.1fbm* after *cyb-2.1(RNAi)* became significantly shorter (~ 26 gcd) compared to the control RNAi (~31 gcd; **Figure 4-2H**). Depletion of CYB-2.1 was confirmed by immunoblot for FLAG::CYB-2.1 after RNAi of *cyb-2.1* compared to the control (**Figure 4-2I**).

We conclude that disrupting PUF-mediated regulation of CYB-2.1 has uncoupled cell cycle dynamics from the rate of meiotic entry in the *fbf-2(lf)* background. These results further suggest that meiotic entry rate and cell cycle progression can be regulated through distinct subsets of FBF targets rather than meiotic entry rate being a direct consequence of how fast SPCs are generated by cell divisions.

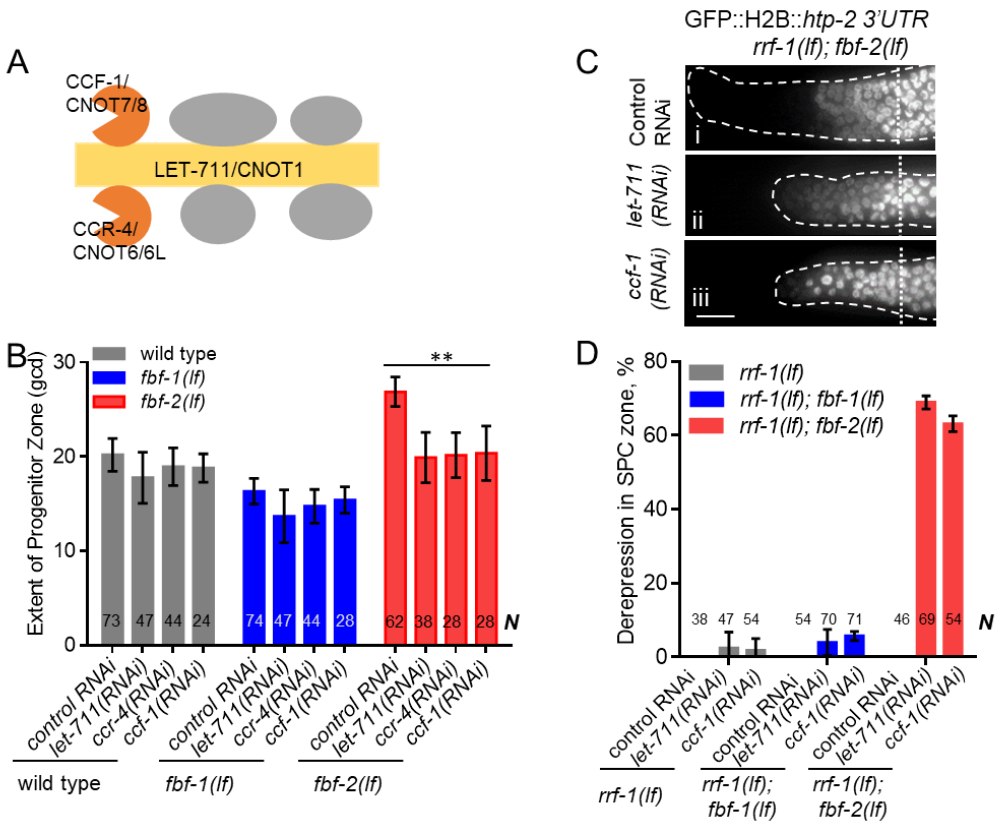

Figure 4-3. CCR4-NOT deadenylase complex promotes FBF-1 function in germline SPCs. (A) Schematic of CCR4-NOT deadenylase complex in humans and *C. elegans*. (B) The extent of SPC zone after knocking down CCR4-NOT subunits in the wild type, *fbf-1(lf)* and *fbf-2(lf)* genetic backgrounds. Genetic backgrounds and RNAi treatments are indicated on the X-axis and the average size of SPC zone ± SD is plotted on the Y-axis. Differences between CCR4-NOT RNAi and the empty vector RNAi control were evaluated by one-way ANOVA. Asterisks mark the group with significant changes in SPC zone length after CCR4-NOT knockdown, $P<0.01$. Data was collected from 3 independent experiments. N, the number of hermaphrodite germlines scored in each RNAi treatment. (C) Distal germlines of *rrf-1(lf); fbf-2(lf)* expressing a GFP::Histone H2B fusion under the control of the *htp-2* 3'UTR after the indicated RNAi treatments. Germlines are outlined with dashed lines and vertical dotted lines indicate the beginning of the transition zone. All images were taken with a standard exposure. Scale bar: 10 μm. (D) Percentage of germlines showing expression of GFP::H2B fusion extended to the distal end in the indicated genetic backgrounds and knockdown conditions. Plotted values are arithmetical means ± SD. Data was collected from 3 independent experiments. *N*, the number of germlines scored. Efficiencies of RNAi treatments were confirmed by sterility or embryonic lethality. (B-D) All experiments were performed at 24°C.

FBF-1 FUNCTION REQUIRES CCR4-NOT DEADENYLASE COMPLEX

One mechanism of PUF-dependent destabilization of target mRNAs is through recruitment of CCR4-NOT deadenylase that shortens poly(A) tails of the targets (Quenault et al., 2011). CCR4-NOT deadenylase is a complex that includes three core subunits: two catalytic subunits CCR-4/CNOT6/6L and CCF-1/CNOT-7/8 and one scaffold subunit LET-711/CNOT1, which are highly conserved in *C. elegans* and humans (**Figure 4-3A**; (Nousch et al., 2013). Although multiple PUF family proteins, including FBF homologs in *C. elegans*, interact with a catalytic subunit of CCR4-NOT *in vitro,* the contribution of CCR4-NOT to PUF-mediated repression *in vivo* is still controversial (Suh et al., 2009; Weidmann et al., 2014). We hypothesized that the enlarged germline SPC zone in *fbf-2(lf)* mutant results from FBF-1-mediated destabilization and translational repression of target mRNAs required for meiotic entry achieved through the activity of CCR4-NOT deadenylase. If so, knockdown of CCR4-NOT in *fbf-2(lf)* genetic background would lead to derepression of target mRNAs in SPCs and a decrease of the length of SPC zone.

First, we measured the extent of SPC zone after RNAi-mediated knockdown of core CCR4-NOT subunits, and found that CCR4-NOT RNAi dramatically shortened the SPC zone in *fbf-2(lf)* compared to the control RNAi (P<0.01; **Figure 4-3B**). By contrast, the lengths of SPC zones in the wild type and *fbf-1(lf)* animals were not significantly affected by CCR4-NOT knockdown (**Figure 4-3B**). We note that the observed effects of CCR4-NOT knockdown are milder than those reported by a recent publication (Nousch et al., 2019); the cause for these differences is unclear. Our findings suggest that CCR4-NOT is required for FBF-1-mediated regulation of germline SPC zone length, but does not significantly contribute to FBF-2 function.

Next, we tested whether CCR4-NOT knockdown disrupts FBF-1-mediated translational repression in SPCs. One FBF target mRNA associated with meiotic entry is *htp-2*, a HORMA domain meiotic protein (Merritt and Seydoux, 2010). Translational regulation of a transgenic reporter encoding GFP::Histone H2B fusion under the control of *htp-2* 3'UTR recapitulates FBF-mediated repression in germline SPCs, where GFP::H2B::*htp-2 3'UTR* production is inhibited in the wild type and both *fbf-1* and *fbf-2* single mutant gonads, but is strongly derepressed in *fbf-1 fbf-2* double mutant gonads (Merritt and Seydoux, 2010). If CCR4-NOT is required for *fbf-1* activity, then *fbf-2(lf)* after

CCR4-NOT subunit RNAi should show the same phenotype as *fbf-1(lf) fbf-2(lf)*, or derepression of the reporter. We performed CCR4-NOT RNAi in the *rrf-1(lf)* background to preferentially direct the RNAi effects to the germline and avoid any effects on the somatic cells (Kumsta and Hansen, 2012; Sijen et al., 2001) and observed derepression of the reporter in SPCs of 63-69% germlines of *rrf-1(lf); fbf-2(lf)* genetic background (**Figure 4-3C, D**). By contrast, derepression of the reporter was observed only in 3-5% of *rrf-1(lf)* and *rrf-1(lf); fbf-1(lf)* genetic backgrounds (**Figure 4-3D**). These data suggest that the CCR4-NOT deadenylase complex is necessary for FBF-1-mediated repression of target mRNAs in germline SPCs, but is dispensable for FBF-2 regulatory function. *fbf-1 fbf-2* double mutant hermaphrodites are sterile (Crittenden et al., 2002). We observed significantly increased sterility upon CCR4-NOT knockdown in *rrf-1(lf); fbf-2(lf)* compared to the *rrf-1(lf)* and *rrf-1(lf); fbf-1(lf)* (data not shown). Like *fbf-1 fbf-2* double mutants, the majority of *rrf-1(lf); fbf-2(lf)* sterile germlines following CCR4-NOT knockdown failed to initiate oogenesis resulting in germline masculinization (data not shown). These observations suggest that CCR4-NOT is required for *fbf-1* activity.

CCR4-NOT knockdown might disrupt FBF-1 regulatory function or FBF-1 protein expression and localization. To distinguish between these possibilities, we determined the abundance of endogenous FBF-1 after *ccf-1(RNAi)* by immunoblotting using tubulin as a loading control. We found that FBF-1 protein abundance is not decreased after CCF-1 knockdown compared to the control (data not shown). Immunostaining for the endogenous FBF-1 showed that in control germlines FBF-1 localized in foci adjacent to perinuclear P granules (data not shown) as previously reported (Voronina et al., 2012). Upon CCF-1 knockdown, FBF-1 foci were still observed next to P granules (data not shown). Therefore, we conclude that CCR4-NOT is not required for FBF-1 expression and localization, and CCR4-NOT knockdown specifically disrupts FBF-1 function.

In summary, we conclude that CCR4-NOT is required for FBF-1, but not FBF-2-mediated regulation of target mRNA and germline SPC zone length. We further predicted that FBF-1 localizes together with CCR4-NOT to the same RNA-protein complex in SPCs.

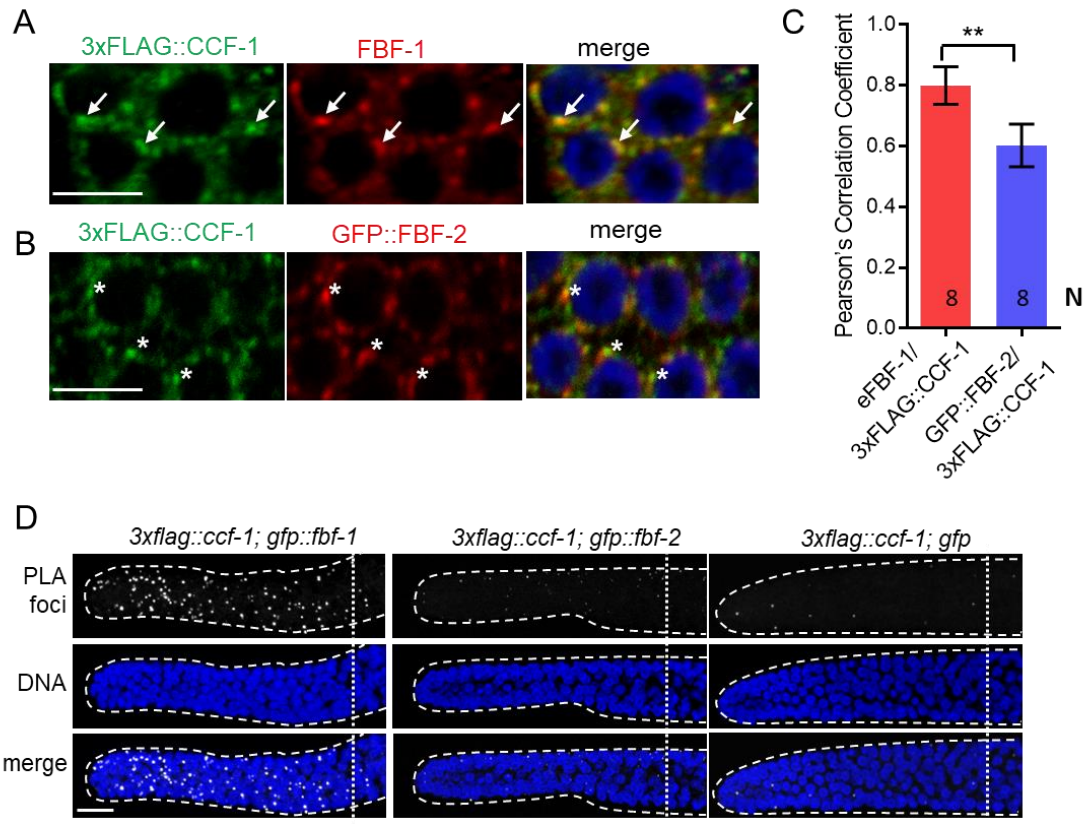

Figure 4-4. FBF-1 colocalizes with CCR4-NOT complex in germline SPCs. (A-B) Confocal images of SPCs co-immunostained for endogenous FBF-1 (A) or GFP-tagged FBF-2 (B, red) and 3xFLAG-tagged CCF-1 (green). DNA staining is in blue (DAPI). Arrows indicate complete overlap of FBF-1 and CCF-1 granules. Asterisks denote FBF-2 granules localizing close but not overlapping with CCF-1 granules. Scale bars in A and B: 5 µm. (C) Pearson's correlation analysis quantifying the colocalization between FBF and CCF-1 granules in co-stained germline images. Plotted values are arithmetical means ± SD. *N*, the number of analyzed germline images (single confocal sections through the middle of germline SPC nuclei including 5-8 germ cells). Statistical analysis was performed by Student's t-test, asterisks mark statistically significant difference, $P<0.01$. (D) Confocal images of the distal germline SPC zones with PLA foci (grayscale) and DNA staining (blue). Germlines are outlined with dashed lines and vertical dotted lines indicate the beginning of the transition zone. Genotypes are indicated on top of each image group. Scale bar: 10 µm. (A-D) All experiments were performed at 24°C.

FBF-1 COLOCALIZES WITH CCR4-NOT IN GERMLINE SPCS

Using co-immunostaining of endogenous FBF-1 or GFP::FBF-1 and 3xFLAG::CCF-1 followed by Pearson's correlation coefficient analysis based on Costes' automatic threshold (Costes et al., 2004), we found that both endogenous FBF-1 and GFP::FBF-1 foci colocalize with 3xFLAG::CCF-1 foci in SPC cytoplasm (**Figure 4-4A, C**). By contrast, the colocalization between GFP::FBF-2 and 3xFLAG::CCF-1 is significantly less robust (**Figure 4-4B, C**). As an alternative metric of colocalization, we used proximity ligation assay (PLA) that can detect protein-protein interactions *in situ* at the distances <40 nm (Fredriksson et al., 2002). PLA was performed in *3xflag::ccf-1; gfp::fbf-1*, *3xflag::ccf-1; gfp::fbf-2*, and *3xflag::ccf-1; gfp* animals using the same antibodies and conditions for all three protein pairs. We observed significantly more dense PLA signals in *3xflag::ccf-1; gfp::fbf-1* than in the control (**Figure 4-4D**; *P*<0.0001, **Table 4-2**). By contrast, PLA foci density in mitotic germ cells of *3xflag::ccf-1; gfp::fbf-2* was not different from the control (**Figure 4-4D; Table 4-2**), although the expression of GFP::FBFs or GFP alone in mitotic germ cells appeared similar (data not shown). Together, these data suggest that FBF-1, but not FBF-2, colocalizes with CCR4-NOT in SPCs, in agreement with the dependence of FBF-1 function on CCR4-NOT.

Table 4-2 Proximity Ligation Assay detects association of FBF-1 with CCR4-NOT complex component CCF-1

Genotype	PLA density in SPC zone (/um^2) x 10^{-2}	P value, vs. control	*N*
3xflag::ccf-1; gfp::fbf-1	5.2±2.4	<0.0001	32
3xflag::ccf-1; gfp::fbf-2	1.1 ±0.8	ns	27
3xflag::ccf-1; gfp	0.6±0.2	n/a	12

PLA foci density was determined in maximal intensity projections of confocal image stacks encompassing germline SPC zones of the indicated strains. Reported values are mean ± SD derived from three

independent biological replicates (*3xflag::ccf-1; gfp::fbf-1* and *3xflag::ccf-1; gfp::fbf-2*) or a single replicate (*3xflag::ccf-1; gfp*), all reared at 24°C. Differences in PLA density between *3xflag::ccf-1; gfp::fbf-1* or *3xflag::ccf-1; gfp::fbf-2* and the control *3xflag::ccf-1; gfp* were analyzed by one-way ANOVA with Dunnett's post-test. *N*, number of germline images analyzed.

FBF-1 PROMOTES DEADENYLATION OF ITS TARGET MRNA

Since a knockdown of CCR4-NOT deadenylase compromises FBF-1-mediated target repression, we hypothesized that FBF-1 promotes deadenylation of target mRNAs. To test this hypothesis, we compared the length of the poly(A) tail of two FBF target mRNAs among the wild type, *fbf-1(lf)*, and *fbf-2(lf)* genetic backgrounds by Poly(A) tail (PAT)-PCR. We selected the targets associated with cell cycle (*cyb-2.1;* (Kershner and Kimble, 2010; Porter et al., 2019; Prasad et al., 2016)) and with meiotic entry (*htp-1*; (Merritt and Seydoux, 2010)) and used an mRNA not associated with FBFs (*unc-54*) as a control. RNA samples were extracted from animals of *glp-1 (gain-of-function, gf)* mutant background, which produces germlines with a large number of mitotic cells at the restrictive temperature (Pepper et al., 2003a; Figure 5 – figure supplement 1A), thus allowing us to focus on the mRNAs in the mitotic cell population.

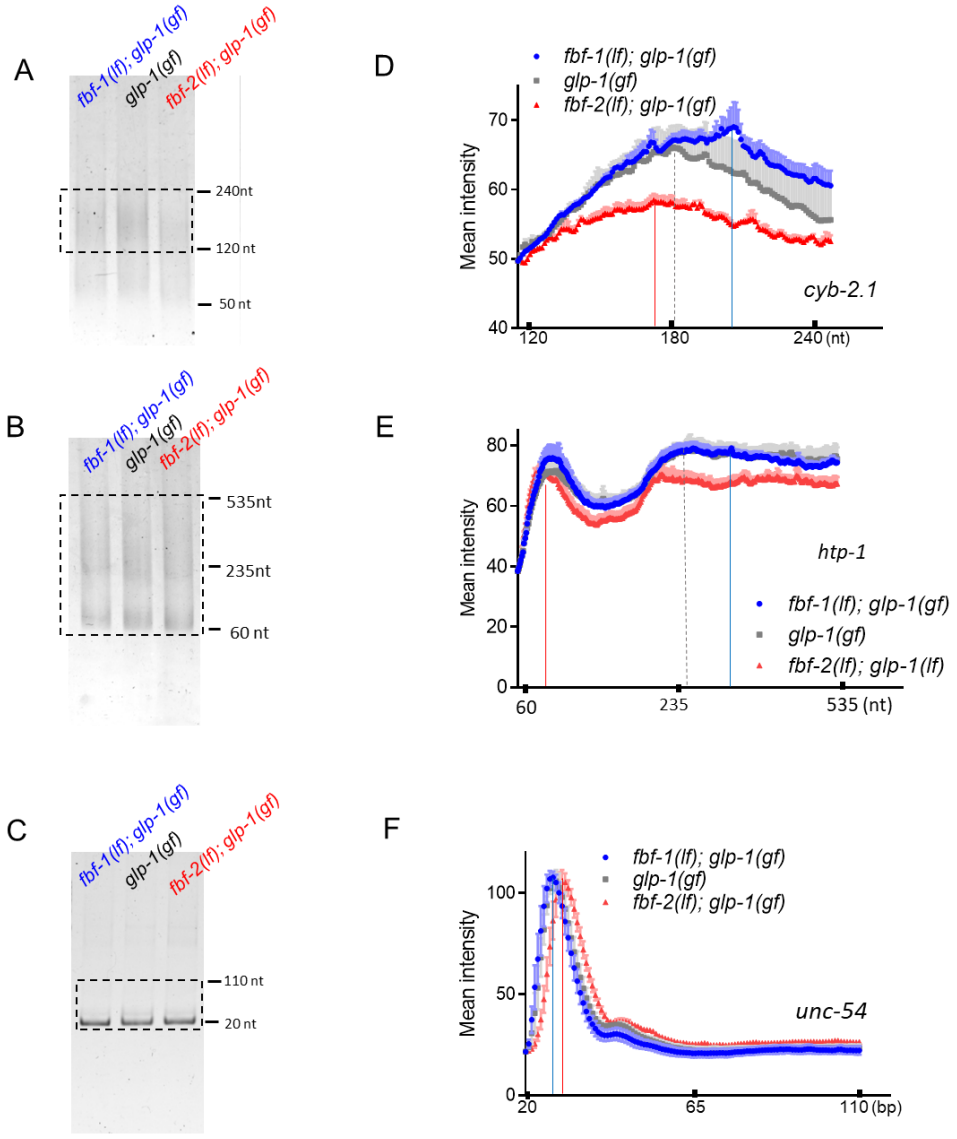

Figure 4-5. FBF-1 promotes deadenylation of FBF targets *cyb-2.1* and *htp-1* (A-C) Representative PAT-PCR analysis of the poly(A) tail length of *cyb-2.1* (A), *htp-1* (B) and control *unc-54* (C) in *fbf-1(lf); glp-1(gf)*, *glp-1(gf)*, and *fbf-2(lf); glp-1(gf)* genetic backgrounds at 25°C. The positions of size markers are indicated on the left. The areas boxed by dotted lines were quantified by densitometry in ImageJ. (D-F) Densitometric quantification of PAT-PCR amplification products (boxed in A-C). Y-axis, mean intensity (arbitrary units) represents the average of PAT-PCR reactions from three independent biological replicates. X-axis, estimated sizes of poly(A) tails. Values are arithmetical means ± SD. Vertical dashed lines in (D-F) mark the sizes of the peak of poly(A) tail length distribution for each mRNA in each *fbf* mutant background.

PAT-PCR assays using RNA samples extracted from *fbf-1(lf); glp-1(gf)*, *glp-1(gf)*, and *fbf-2(lf); glp-1(gf)* revealed that *fbf* mutations led to changes in the poly(A) tail lengths of FBF targets. The poly(A) tail lengths distributions of *cyb-2.1* and *htp-1* mRNAs in *fbf-2(lf)* were both shifted to shorter lengths compared to the wild type background (**Figure 4-5A, B, D, E**). In *fbf-1(lf)* background, the predominant *cyb-2.1* mRNA species appeared to have a longer poly(A) tail than in the wild type background, while the poly(A) tail length distribution of *htp-1* mRNA appeared qualitatively similar to the wild type although the peak of the distribution appeared to shift to longer species (**Figure 4-5A, B, D, E**). By contrast, the poly(A) tail length of *unc-54* mRNA did not decrease in *fbf-2(lf)* background compared to both wild type and *fbf-1(lf)* (**Figure 4-5C, F**). We conclude that FBF-1 promotes deadenylation of target mRNAs, while FBF-2 might protect some targets from deadenylation presumably by competing for binding with FBF-1.

Cytoplasmic deadenylation of mRNA frequently leads to its decay (Mugridge et al., 2018). To test whether differential polyadenylation of FBF targets in *fbf-1(lf)* and *fbf-2(lf)* resulted in changes in their steady-state amounts relative to the wild type, we compared the mRNA abundance of selected FBF targets among *fbf-1(lf); glp-1(gf)*, *glp-1(gf)*, and *fbf-2(lf); glp-1(gf)* genetic backgrounds by qPCR (data not shown). We determined steady-state levels of both meiotic entry associated transcripts, *him-3, htp-1,* and *htp-2* (Merritt and Seydoux, 2010) and cell cycle regulators, *cyb-1, cyb-2.1, cyb-2.2* and *cyb-3* (Kershner and Kimble, 2010; Porter et al., 2019; Prasad et al., 2016), and used *unc-54* as a control. All transcript levels were normalized to a housekeeping gene actin (*act-1*). Surprisingly, we found that the steady-state abundance of all FBF targets decreased to a variable degree in both *fbf* mutants relative to the wild type background (data not shown). By contrast, the abundance of *unc-54* mRNA did not show a similar decrease. We conclude that differential polyadenylation of FBF targets in *fbf* mutants do not lead to unequal mRNA accumulation.

THREE VARIABLE REGIONS OUTSIDE OF FBF-2 RNA BINDING DOMAIN ARE NECESSARY TO PREVENT COOPERATION WITH CCR4-NOT

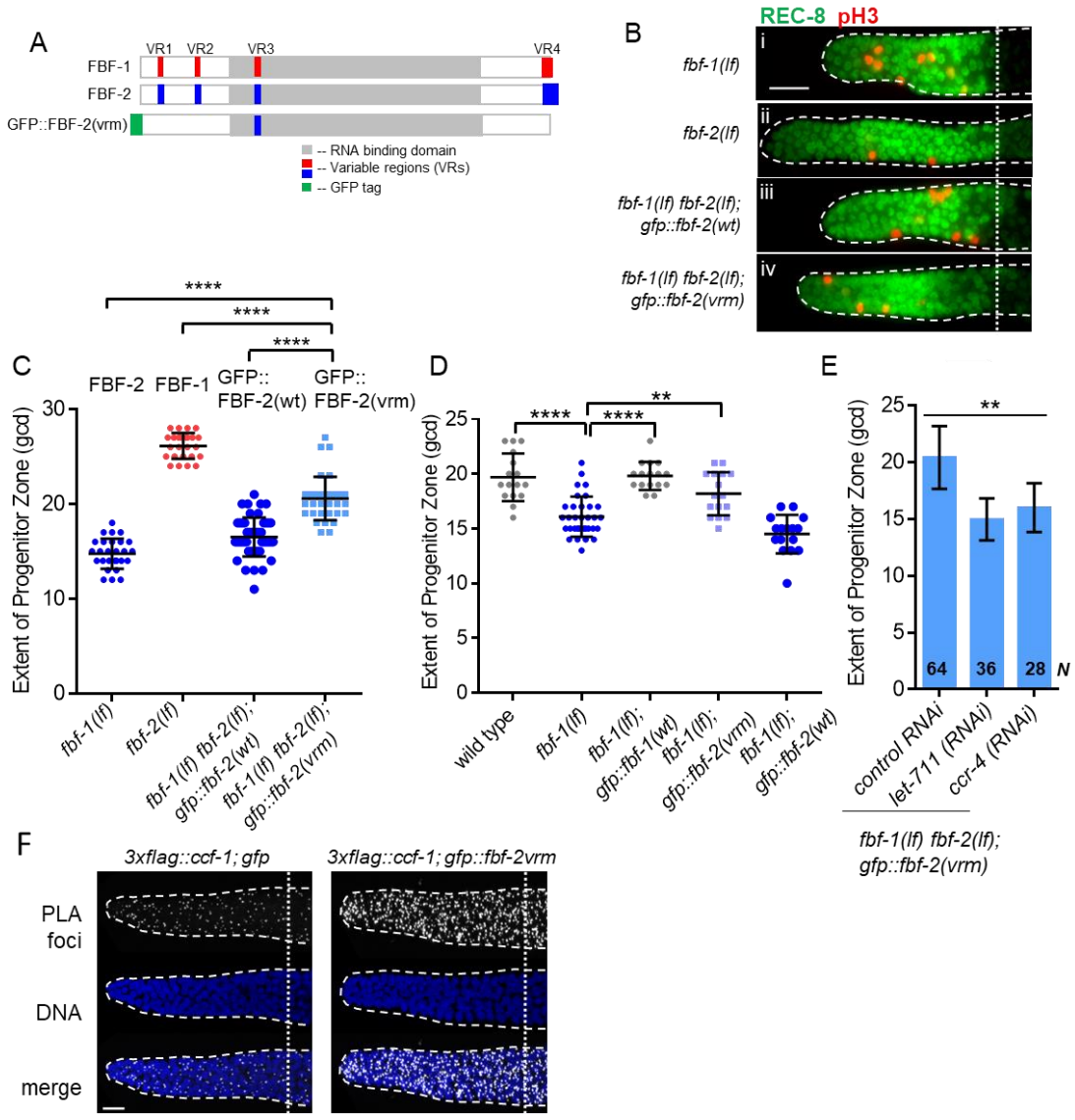

Figure 4-6. Three variable regions of FBF-2 prevent its cooperation with CCR4-NOT. (A) Schematics of FBF-1, FBF-2 and GFP::FBF-2(vrm) mutant transgene (Wang et al., 2016). Red and blue colors indicate variable regions distinguishing FBF-1 and FBF-2 respectively, grey box indicates the RNA binding domain, and green box indicates GFP tag. (B) Distal germlines of the indicated genetic backgrounds stained with anti-REC-8 (green) and anti-pH3 (red). Germlines are outlined with the dashed lines, and the vertical dotted line marks the beginning of transition zone. Scale bar: 10 µm. (C) The extent of SPC zone in the indicated genetic backgrounds (on the X-axis). FBF protein(s) present in each genetic background are

noted above each data set. Plotted values are individual data points and arithmetical means ± SD. Differences in SPC zone length between *fbf-1(lf) fbf-2(lf); gfp::fbf-2(vrm)* and the other strains were evaluated by one-way ANOVA test with Dunnett's post-test; asterisks mark statistically significant differences (P<0.0001). Data were collected from 3 independent experiments and 24-28 germlines were scored for each genotype. (D) The extent of SPC zone was measured after crossing the GFP::FBF-2(vrm), GFP::FBF-1(wt) and GFP::FBF-2(wt) transgenes into *fbf-1(lf)* genetic background. As controls, SPC zone length was also measured in *fbf-1(lf)* and the wild type. Plotted values are individual data points and arithmetical means ± SD. Differences in SPC zone length between *fbf-1(lf)* and all other strains were evaluated by one-way ANOVA test with Dunnett's post-test; asterisks mark statistically significant differences (****, *P*<0.0001; ***P*<0.01). (E) The extent of SPC zone after knocking down CCR4-NOT subunits in the *fbf-1(lf) fbf-2(lf); gfp::fbf-2(vrm)* genetic background. RNAi treatments are indicated on the X-axis and average length of SPC zone ± SD on the Y-axis. Differences in SPC zone length between CCR4-NOT knockdowns and control were evaluated by one-way ANOVA (asterisks, *P*<0.01). Data were collected from 3 independent experiments. *N*, the number of independent germlines scored. (B-D): All experiments were performed at 24°C.

Our findings suggest that FBF-1-mediated SPC maintenance depends on CCR4-NOT deadenylase complex, while FBF-2 can function independent of CCR4-NOT. Since FBF proteins are very similar in primary sequence except for the four variable regions (VRs, **Figure 4-6A**), we next investigated whether the VRs were necessary for FBF-2-specific maintenance of germline SPCs and prevented FBF-2 dependence on CCR4-NOT. We previously found that mutations/deletions of the VRs outside of FBF-2 RNA-binding domain (VR1, 2 and 4, **Figure 4-6A**) produced GFP::FBF-2(vrm) protein with a disrupted localization and compromised function (Wang et al., 2016). We hypothesized that these three VRs might contribute to FBF-2-specific effects on the extent of SPC zone as well as prevent FBF-2 from cooperating with CCR4-NOT.

We first tested whether the three VRs are required for FBF-2-specific SPC zone length. To test this hypothesis, the extent of SPC zone was determined after crossing the GFP::FBF-2(vrm) transgene into *fbf* double mutant background. We found that the SPC zone maintained by GFP::FBF-2(vrm) (**Figure 4-6Biv**) is significantly longer than that maintained by GFP::FBF-2(wt) (**Figure 4-6Biii**) and the endogenous FBF-2 (**Figure 4-6Bi**) and significantly shorter than that maintained by FBF-1 (P<0.01, **Figure 4-6C**), suggesting that the GFP::FBF-2(vrm) effect on SPC

zone length is distinct from that of FBF-2. Western blot analysis indicated that expression of GFP::FBF-2(vrm) is comparable to that of GFP::FBF-2(wt), so their distinct effects on SPC zone length are likely due to functional differences (data not shown). To test whether GFP::FBF-2(vrm) can rescue either of *fbf* single mutants, we determined the extent of SPC zone after crossing GFP::FBF-2(vrm) into *fbf-1(lf)* and *fbf-2(lf)* genetic backgrounds. As controls, the lengths of SPC zones were also measured after crossing the wild type GFP::FBF-2(wt) and GFP::FBF-1(wt) transgenes into each *fbf* single mutant. As expected, the SPC zone length of *fbf-2(lf); gfp::fbf-2(wt)* is significantly shorter than *fbf-2(lf)* ($P<0.01$) while the SPC zone of *fbf-2(lf); gfp::fbf-1(wt)* is similar to *fbf-2(lf)* (data not shown), suggesting that GFP::FBF-2(wt), but not GFP::FBF-1(wt), rescues *fbf-2(lf)*. Likewise, GFP::FBF-1(wt), but not GFP::FBF-2(wt), rescues *fbf-1(lf)* ($P<0.01$, **Figure 4-6D**). Interestingly, we found that the extent of SPC zone of *fbf-2(lf); gfp::fbf-2(vrm)* is similar to that of *fbf-2(lf)* (data not shown), suggesting that GFP::FBF-2(vrm) does not rescue *fbf-2(lf)*. By contrast, the SPC zone of *fbf-1(lf); gfp::fbf-2(vrm)* is significantly longer than that of *fbf-1(lf)* ($P<0.01$, **Figure 4-6D**) and there is no significant difference in the SPC zone length between *fbf-1(lf); gfp::fbf-2(vrm)* and the wild type, suggesting that the GFP::FBF-2(vrm) completely rescues *fbf-1(lf)*. We conclude that the three VRs outside of FBF-2 RNA-binding domain (VR1, 2, and 4) are important for FBF-2-specific effect on the extent of germline SPC zone and mutation or deletion of these VRs resulted in a mutant protein FBF-2(vrm) that functions similar to FBF-1.

Since FBF-1 function requires CCR4-NOT complex and FBF-2(vrm) appears similar to FBF-1, we hypothesized that CCR4-NOT is required for FBF-2(vrm) function. To test this hypothesis, we measured SPC zone length after knockdown of CCR4-NOT subunits in *fbf-1(lf) fbf-2(lf); gfp::fbf-2(vrm)* animals by RNAi. We found that SPC zone of *fbf-1(lf) fbf-2(lf); gfp::fbf-2(vrm)* after RNAi of CCR4-NOT subunits becomes significantly shorter than the control ($P<0.01$, **Figure 4-6E**), suggesting that GFP::FBF-2(vrm) function requires CCR4-NOT. If GFP::FBF-2(vrm) cooperates with CCR4-NOT, we expect that it might associate with CCF-1 by proximity ligation assay. Indeed, PLA foci density in the mitotic cells of *3xflag::ccf-1; gfp::fbf-2(vrm)* was significantly greater than in the control (**Figure 4-6F**; **Table 4-3**; $P<0.0001$). We conclude that the VRs outside of FBF-2 RNA-binding domain are required for FBF-2-specific effect on the extent of SPC zone and to prevent FBF-2 from cooperation with CCR4-NOT.

Table 4-3 Proximity Ligation Assay detects association of FBF-2(vrm) with CCR4-NOT complex component CCF-1

Genotype	PLA density in SPC zone (/um^2) x 10^{-2}	P value, vs. control	*N*
3xflag::ccf-1; gfp::fbf-2vrm	2.3±0.7	<0.0001	58
3xflag::ccf-1; gfp	1.1±0.5	n/a	48

THE VARIABLE REGION 4 (VR4) OF FBF-2 IS SUFFICIENT TO PREVENT COOPERATION WITH CCR4-NOT

To test whether one of the three VRs outside of FBF-2 RNA-binding domain (VR1, 2, and 4) is sufficient to support FBF-2-specific effects on the length of SPC zone, we established a transgenic FBF-1 chimera with VR4 swapped from FBF-2 (GFP::FBF-1(FBF-2vr4); **Figure 4-7A**) and crossed it into *fbf* double mutant. Since VR3 residing in FBF-2 RNA-binding domain was not sufficient for FBF-2-specific function, *gfp::fbf-1(fbf-2vr3)* (with VR3 swapped from FBF-2; **Figure 4-7A**) chimeric transgene was made for comparison. SPC zone length assessment showed that the SPC zone maintained by GFP::FBF-1(FBF-2vr4) (**Figure 4-7Biii**) is significantly shorter than that maintained by GFP::FBF-1(wt) (**Figure 4-7Bv**) and endogenous FBF-1 (P<0.0001; **Figure 4-7Bii, C**). By contrast, the SPC zone maintained by GFP::FBF-1(FBF-2vr3) (**Figure 4-7Biv**) is similar to that maintained by the GFP::FBF-1(wt) (**Figure 4-7Biv, C**). This finding suggested that GFP::FBF-1(FBF-2vr4) might function similarly to FBF-2. Western blot analysis revealed that the protein expression levels of GFP::FBF-1, GFP::FBF-1(FBF-2vr3), and GFP::FBF-1(FBF-2vr4) were comparable, so the observed effects on SPC zone length are likely due to functional differences (data not shown). To test whether GFP::FBF-1(FBF-2vr4) rescues FBF-1- or FBF-2-specific function, we measured the extent of SPC zones after crossing GFP::FBF-1(FBF-2vr4) into *fbf-1(lf)* and *fbf-2(lf)* genetic backgrounds. For comparison, GFP::FBF-1(FBF-2vr3) was also crossed into each *fbf* single mutant. We found that the SPC zone of *fbf-1(lf); gfp::fbf-1(fbf-2vr4)* is similar to that of *fbf-1(lf)* (data not shown),

suggesting that GFP::FBF-1(FBF-2vr4) does not rescue *fbf-1(lf)*. Interestingly, SPC zone of *fbf-2(lf); gfp::fbf-1(fbf-2vr4)* is significantly shorter than that of *fbf-2(lf)* (P<0.01, data not shown), suggesting that GFP::FBF-1(FBF-2vr4) rescues *fbf-2(lf)*. By contrast, GFP::FBF-1(FBF-2vr3) rescues *fbf-1(lf),* but not *fbf-2(lf)* (data not shown). We conclude that the presence of VR4 from FBF-2 in a chimeric GFP::FBF-1(FBF-2vr4) protein is sufficient to impart FBF-2-specific effect on the extent of SPC zone.

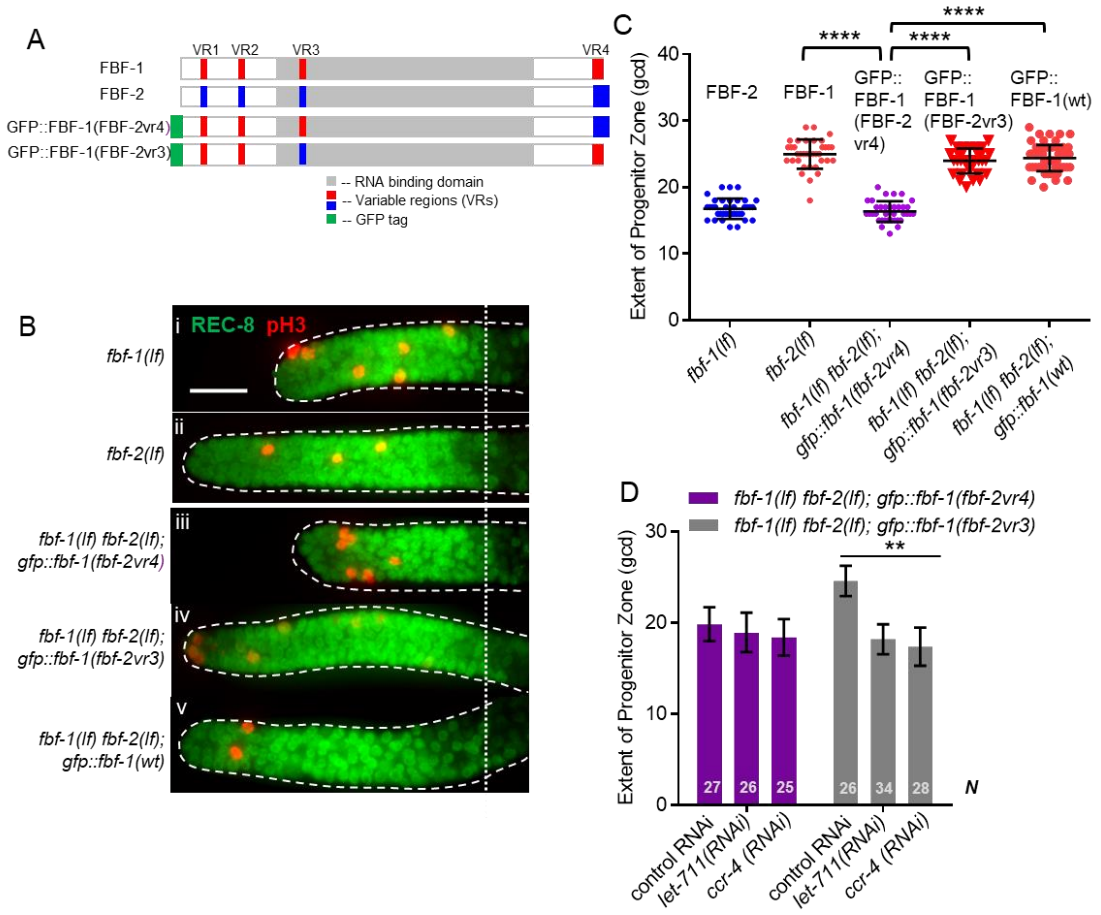

Figure 4-7. Variable region 4 (VR4) from FBF-2 is sufficient to prevent FBF-1 chimera from cooperation with CCR4-NOT. (A) Schematics of FBF-1, FBF-2, transgenic GFP::FBF-1(FBF-2vr4) chimera (with VR4 swapped from FBF-2) and transgenic GFP::FBF-1(FBF-2vr3) chimera (with VR3 swapped from FBF-2). Red and blue colors indicate variable regions distinguishing FBF-1 and FBF-2 respectively, grey box indicates RNA binding domain, and green box indicates GFP tag. (B) Distal germlines dissected from the indicated genetic backgrounds stained with anti-REC-8 (green) and anti-pH3 (red). Germlines are outlined with the

dashed lines and the vertical dotted line marks the beginning of the transition zone. Scale bar: 10 μm. (C) The extent of SPC zone in the indicated genetic backgrounds (on the X-axis). FBF protein present in each genetic background is noted above each data set. Plotted values are individual data points and arithmetical means ± SD. Differences in SPC zone length between *fbf-1(lf) fbf-2(lf); gfp::fbf-1(fbf-2vr4)* and the other strains were evaluated by one-way ANOVA test with Dunnett's post-test; asterisks mark statistically significant differences (P<0.0001). Data were collected from 2 independent experiments and 31-60 germlines were scored for each genotype. (D) SPC zone length after knocking down CCR4-NOT subunits in the *fbf-1(lf) fbf-2(lf); gfp::fbf-1(fbf-2vr4)* and *fbf-1(lf) fbf-2(lf); gfp::fbf-1(fbf-2vr3)* genetic backgrounds (as indicated on the X-axis). Plotted values are arithmetical means ± SD. Differences in the extent of SPC zone between CCR4-NOT RNAi and control RNAi were evaluated by one-way ANOVA. Asterisks mark the group with significant changes in SPC zone length after CCR4-NOT knockdown (P<0.01). Data was collected from 2 independent experiments. *N*, the number of hermaphrodite germlines scored. (B-D) All experiments were performed at 24°C.

To test whether VR4 is sufficient to inhibit cooperation of GFP::FBF-1(FBF-2vr4) with CCR4-NOT, we measured the length of SPC zone after knockdown of CCR4-NOT subunits in *fbf-1(lf) fbf-2(lf); gfp::fbf-1(fbf-2vr4)* animals by RNAi. As a control, CCR4-NOT knockdown was also performed on *fbf-1(lf) fbf-2(lf); gfp::fbf-1(fbf-2vr3).* We found that the SPC zone of *fbf-1(lf) fbf-2(lf); gfp::fbf-1(fbf-2vr4)* after RNAi of CCR4-NOT subunits is similar to the control (**Figure 4-7D**), suggesting that GFP::FBF-1(FBF-2vr4) function in SPCs does not rely on CCR4-NOT. By contrast, the SPC zone of *fbf-1(lf) fbf-2(lf); gfp::fbf-1(fbf-2vr3)* is significantly shortened after RNAi of CCR4-NOT subunits compared to the control (P<0.01, **Figure 4-7D**), indicating that GFP::FBF-1(FBF-2vr3) maintains dependence on CCR4-NOT. We conclude that FBF-2 VR4 in a chimeric GFP::FBF-1(FBF-2vr4) protein is sufficient to support FBF-2-specific effect on the extent of germline SPC zone and to prevent the chimera's cooperation with CCR4-NOT.

Discussion

This manuscript focuses on the roles of PUF family FBF proteins in the control of rates of cell cycle progression and meiotic entry of *C. elegans* germline stem and progenitor cells. Our results support three main conclusions. First, FBF proteins affect SPC cell cycle and meiotic entry through translational control of FBF target mRNAs required for both processes. Second, FBF-mediated repression of cyclin B affects SPC cell division rate. Third, distinct effects of FBF homologs on SPC

development and their target mRNAs are mediated by differential cooperation of FBFs with deadenylation machinery. In turn, activation of deadenylation machinery by FBFs depends on the protein sequences outside of the conserved PUF RNA-binding domain. Collectively, our results support a model where two paralogous FBF proteins have complementary effects on SPC cell division and meiotic entry achieved through distinct regulatory mechanisms (**Figure 4-8**).

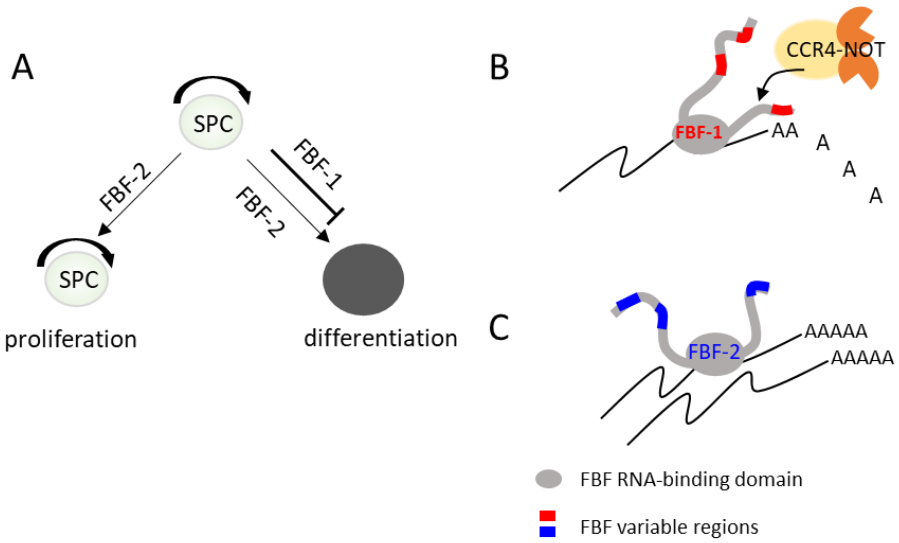

Figure 4-8. Distinct effects of FBF-1 and FBF-2 on germline SPC dynamics are mediated by their effects on target mRNAs in *C. elegans*. (A) Complementary activities of FBFs in maintaining germline SPC homeostasis: FBF-1 promotes SPC self-renewal by inhibiting differentiation, while FBF-2 facilitates both proliferation and differentiation of SPCs. (B, C) FBFs differentially control target mRNAs that regulate both stem cell proliferation and differentiation, and FBFs differential cooperation with CCR4-NOT is determined by their variable regions, VRs, outside of the RNA binding domain of FBFs. (B) FBF-1 cooperates with CCR4-NOT deadenylase and destabilizes target mRNAs. FBF-1-dependent RNA regulation is required to restrict the rate of germline stem cell differentiation. (C) FBF-2 does not rely on CCR4-NOT and promotes accumulation of target mRNAs. FBF-2-dependent accumulation of mRNAs is required to sustain both wild type rates of germline stem cell proliferation and of meiotic entry.

FBFS AFFECT THE RATES OF BOTH STEM CELL MITOTIC DIVISIONS AND MEIOTIC ENTRY

Here we provide evidence that loss-of-function mutation of *fbf* homologs change the rates of both cell cycle and meiotic entry in *C. elegans* germline SPC. We find that slow proliferation of

SPCs in *fbf-2(lf)* is associated with a slower rate of progenitor meiotic entry (differentiation), while the progenitors of *fbf-1(lf)* mutant have a faster rate of meiotic entry (**Figure 4-8A**). We propose that differentiation and proliferation are simultaneously affected by FBF-mediated control of target mRNAs encoding key molecular regulators of meiotic entry and cell cycle. According to our model, post-transcriptional regulation by both FBFs is required to promote the wild type balance of cell cycle progression and meiotic entry. Therefore, changes in the rate of cell divisions and/or meiotic entry in the individual *fbf* mutants might lead to changes in SPC zone size. One alternative mechanism for SPC zone size changes in *fbf* mutants is through changes in the number of uncommitted stem cells through altered accumulation of SYGL-1 and LST-1. SYGL-1 and LST-1 are common cofactors of FBFs that promote FBF-dependent regulation (Haupt et al., 2019a; Shin et al., 2017). The abundance of SYGL-1 and LST-1 plays a key role in determining the number of uncommitted stem cells and thus the overall size of SPC zone (Haupt et al., 2019a; Shin et al., 2017). Since both SYGL-1 and LST-1 are also FBF targets (Kershner and Kimble, 2010; Kershner et al., 2014; Prasad et al., 2016), it would be interesting to see whether FBF effects on SPC zone size might be mediated through changes in SYGL-1 and/or LST-1 levels.

Slow meiotic entry rate in *fbf-2(lf)* likely results from enhanced translational repression of FBF targets that regulate differentiation; indeed, slower accumulation of FBF target GLD-1 has been documented in this genetic background (Brenner and Schedl, 2016). In a similar fashion, mutations of FBF targets *gld-2* and *gld-3* lead to a decrease in meiotic entry rate and to accumulation of excessive numbers of SPCs (Eckmann et al., 2004; Fox and Schedl, 2015). Conversely, higher meiotic entry rate of *fbf-1(lf)* SPCs might be explained by partial derepression of FBF targets. FBF-2 represses FBF target transcripts in *fbf-1(lf)* background, while sequestering them in large cytoplasmic aggregates (Voronina et al., 2012). However, this repression is less effective than FBF-1-dependent mRNA deadenylation since partial derepression of GLD-1 has been previously observed in *fbf-1(lf)* (Brenner and Schedl, 2016; Crittenden et al., 2002).

We find that FBF-2 promotes SPC cell division through facilitating progression of SPCs through the G2-phase of cell cycle. Thus, SPCs of the *fbf-2(lf)* mutant are characterized by longer median

G2-phase length. By contrast, the G2-phase of *fbf-1(lf)* SPCs is the same as in the wild type, even though this genetic background shows an increase in the mitotic index. There are several possible explanations for a higher mitotic index in *fbf-1(lf)* background. One is slow progression through the M-phase of the cell cycle. We tested for activation of mitotic checkpoints in *fbf-1(lf)* genetic background, but found no difference with the wild type in the prevalence of inactivated NCC-1/CDK-1 (pTyr15) (data not shown). Another possibility for the change in mitotic index is the difference in the proportion of cycling-competent versus non-cycling cells in *fbf-1(lf)*. The proximal SPC zone contains non-cycling cells in meiotic S-phase, estimated to comprise 30-40% of total SPC zone cells in the wild type germlines (Crittenden et al., 2006; Jaramillo-Lambert et al., 2007; Fox et al., 2011). Faster meiotic entry rate of *fbf-1(lf)* SPCs might be associated with faster progenitor transit through the meiotic S-phase. As a result, the number of non-cycling premeiotic cells (and consequently the total number of SPC zone cells) would be lower, leading to an inflated SPC mitotic index. We could not address whether *fbf-1(lf)* germlines have a lower number of progenitors in meiotic S-phase since there are no specific molecular markers for this developmental stage. Finally, we find that disruption of FBF-mediated regulation of a single B-type cyclin in slowly proliferating and slowly differentiating *fbf-2(lf)* SPCs is sufficient to disturb stem cell homeostasis and leads to excessive SPC accumulation. This result also supports the idea that the rate of meiotic entry is not a direct consequence of the rate of SPC proliferation, but is controlled separately.

REGULATION OF CYCLIN B BY PUF-FAMILY PROTEINS IN STEM CELLS

PUF mRNA targets have been studied in multiple organisms including *C. elegans*, mouse and human identifying thousands of target mRNAs (Chen et al., 2012; Galgano et al., 2008; Kershner and Kimble, 2010; Morris et al., 2008; Porter et al., 2019; Prasad et al., 2016). One highly conserved group of PUF regulatory targets is related to the control of cell cycle progression. In several developmental contexts stem cells undergo rapid G1/S transitions and spend an extended time in G2, as observed for *C. elegans* germline stem cells as well as mouse and human embryonic stem cells (Fox et al., 2011; Lange and Calegari, 2010; Orford and Scadden, 2008). Human, mouse, and *C. elegans* PUF proteins repress cell cycle inhibitors such as Cip/Kip family cyclin-dependent

kinase inhibitors (Kalchhauser et al., 2011; Kedde et al., 2010; Lin et al., 2019). This repression was found important for cell cycle progression of human and mouse cells through G1 (Kedde et al., 2010; Lin et al., 2019). Additionally, mitotic cyclins B and A are among the core targets of PUF proteins across species including nematode FBFs (Kershner and Kimble, 2010; Porter et al., 2019; Prasad et al., 2016), *Drosophila* Pumilio (Asaoka-Taguchi et al., 1999), human and mouse PUM1 and PUM2 (Chen et al., 2012; Galgano et al., 2008; Hafner et al., 2010; Morris et al., 2008), and yeast Puf proteins (Gerber et al., 2004; Wilinski et al., 2015). Cyclin B regulation by PUFs contributes to cell cycle control of *Drosophila* embryonic cell divisions (Asaoka-Taguchi et al., 1999; Vardy and Orr-Weaver, 2007) and to the control of meiotic resumption during *Xenopus* and zebrafish oocyte maturation (Kotani et al., 2013; Nakahata et al., 2003; Ota et al., 2011). Here, we report the function of PUF-mediated regulation of mitotic cyclins in the germline stem cells of *C. elegans*. A recent report suggests that regulation of cyclin B by PUFs is also observed in mouse embryonic stem cells
(Uyhazi et al., 2020).

MRNA DEADENYLATION AND PUF-MEDIATED REPRESSION

Multiple studies indicate that deadenylation contributes to PUF-mediated translational repression (Goldstrohm et al., 2006; Kadyrova et al., 2007; Van Etten et al., 2012; Weidmann et al., 2014). CCR4-NOT deadenylation machinery is conserved in evolution from yeast to humans (Collart et al., 2017; Wahle and Winkler, 2013). Although deadenylation is required for germline stem cell maintenance in flies, nematodes and mice (Berthet et al., 2004; Fu et al., 2015; Joly et al., 2013; Nakamura et al., 2004; Nousch et al., 2019; Shan et al., 2017; Suh et al., 2009), the contribution of deadenylation to PUF translational repression *in vivo* is still controversial (Weidmann et al., 2014). Previous studies of CCR4-NOT component CCF-1 in *C. elegans* suggested that paralogous PUF proteins FBF-1 and FBF-2 might employ both CCF-1-dependent and CCF-1-independent regulatory modes (Suh et al., 2009). Here, we find that FBF-1 and FBF-2 differentially cooperate with CCR4-NOT deadenylation machinery in *C. elegans* germline SPCs.

Multiple lines of evidence suggest that FBF-1's function *in vivo* is supported by the CCR4-NOT deadenylation. First, the size of germline SPC zone maintained by FBF-1 in the absence of FBF-2

is significantly reduced by a knock-down of CCR4-NOT deadenylase components. Second, FBF-1-mediated repression of FBF target reporter *in vivo* requires CCR4-NOT deadenylase. By contrast, SPC zone maintained by FBF-2 and the reporter repression by FBF-2 in the absence of FBF-1 are not affected by CCR4-NOT component knock down. Taken together, these observations provide genetic evidence that CCR4-NOT promotes FBF-1 function in germline SPCs. The increase in FBF-1 protein levels that we observed after knocking down the CCR4-NOT subunit *ccf-1* (data not shown) might result from the relief of FBF-1 auto-regulation (Lamont et al., 2004). Third, both endogenous FBF-1 and GFP::FBF-1 colocalize with a core CCR4-NOT subunit 3xFLAG::CCF-1 *in vivo* by co-immunostaining. Additionally, an *in vivo* test of protein interaction between GFP::FBF-1 and 3xFLAG::CCF-1 using proximity ligation assay detects positive signal suggesting that these proteins reside in the same complex. By contrast, there's significantly less *in vivo* colocalization and proximity between GFP::FBF-2 and 3xFLAG::CCF-1. These data are consistent with the idea that FBF-1 and FBF-2 form distinct RNP complexes, of which FBF-1 complex preferentially includes CCR4-NOT deadenylase. Finally, we assessed the length of FBF target poly(A) tail length in the nematodes mutant for each *fbf*, and found that the poly(A) tail length of FBF target *cyb-2.1* was relatively shorter in *fbf-2(lf)* background than in *fbf-1(lf)*. We conclude that FBF-1 selectively cooperates with deadenylation machinery to promote translational repression of target mRNAs (**Figure 4-8**).

The two FBF proteins are 91% identical in primary sequence (Zhang et al., 1997). If FBFs have distinct abilities to engage deadenylation machinery, what are the features of FBF-2 that prevent it from cooperating with CCR4-NOT? PUF RNA-binding domain is sufficient for a direct interaction with the CCF-1 subunit of CCR4-NOT and its homologs in multiple species, including *C. elegans* (Goldstrohm et al., 2006; Hook et al., 2007; Kadyrova et al., 2007; Suh et al., 2009; Van Etten et al., 2012). However, protein sequences outside of the well-structured RNA-binding domain can promote PUF-induced deadenylation, and are hypothesized to function either through improved recruitment of CCR4-NOT complex or through allosteric activation of CCR4-NOT (Webster et al., 2019). We find that the Variable Region (VR) sequences outside of the RNA-binding domain of FBF-1 and FBF-2 play a key role in determining whether these proteins are able to cooperate with

CCR4-NOT (**Table 4-4**). Mutations of three VRs (VR1, 2, and 4) in FBF-2 result in a protein that now cooperates with CCR4-NOT, suggesting that these regions are necessary to prevent the wild type FBF-2 from engaging with the deadenylase. Conversely, swapping the VR4 of FBF-2 onto FBF-1 renders resulting the chimeric protein FBF-1(FBF-2vr4) insensitive to CCR4-NOT knockdown, indicating that VR4 of FBF-2 is sufficient to prevent cooperation with CCR4-NOT. By contrast, swapping VR3 residing within FBF-2 RNA-binding domain into FBF-1 does not affect the FBF-1(FBF-2vr3) chimera's cooperation with CCR4-NOT, supporting the importance of protein sequences outside of the RNA-binding domain affecting cooperation with CCR4-NOT. Overall, we conclude that the protein regions outside of the conserved PUF RNA-binding domain regulate the repressive action mediated by each PUF protein homolog. As a result, distinct sequences flanking the RNA-binding domain may lead to differential preference of regulatory mechanisms exerted by individual PUF-family proteins (**Figure 4-8B, C**). Identifying the sequences outside of FBF-1 RNA-binding domain that promote its cooperation with CCR4-NOT remains a subject for future studies to understand regulatory impact of PUF domain flanking sequences.

Table 4-4 Variable regions outside of RNA-binding domain regulate FBF function

Transgene	Mutated variable region (VR) sequence	Rescues *fbf-1(lf)?*	Rescues *fbf-2(lf)?*	Dependent on CCR4-NOT
GFP::FBF-2wt	N/A	No	Yes	No[a]
GFP::FBF-1wt	N/A	Yes	No	Yes[a]
GFP::FBF-2(vrm)	mutated VR1, 2; VR4 deleted	Yes	No	Yes[b]
GFP::FBF-1(FBF-2vr4)	VR4 swapped with FBF-2	No	Yes	No[b]
GFP::FBF-1(FBF-2vr3)	VR3 swapped with FBF-2	Yes	No	Yes[b]

Rescue assays were performed by crossing transgenic GFP::FBFs into loss of function mutant of each *fbf*, followed by SPC zone length measurement (data not shown). Dependence on CCR4-NOT was defined as a decrease in the length of SPC zone after knocking down CCR4-NOT subunits. [a] – analyzed in single *fbf*

loss-of-function mutants, **Figure 4-3B**. [b] – analyzed in the strains containing GFP::FBF transgenes in *fbf-1 fbf-2* double-mutant background, **Figures 4-6D** and **4-7D**.

CONCLUSIONS

Our results suggest a new mechanism contributing to balancing stem cell self-renewal with differentiation at a population level in *C. elegans* germline. We propose that antagonistic regulation of key mRNA targets by PUF family FBF proteins modulates SPC cell division rate together with the rate of meiotic entry or differentiation. Complementary activities of FBF-1 and FBF-2 combine to fine tune SPC proliferation and meiotic entry coordinately regulating both processes. PUF proteins are conserved stem cell regulators in a variety of organisms, and their control of target mRNAs that affect proliferation and differentiation is wide spread as well. The future challenge will be to determine whether PUF-dependent RNA regulation in other stem cell systems might be modulated to adjust stem cell division rate in concert with changing the rate of differentiation.

Acknowledgements

We thank the members of Voronina laboratory for insightful discussions and Geraldine Seydoux for comments on our manuscript. We are grateful to Ella Baumgarten and Jessica Bailey for help with cloning and crosses. We appreciate Ariz Mohammad for sharing the modified R script (originally from the Kimble lab) and instructions on using R for cell counts. Confocal microscopy was performed in the University of Montana BioSpectroscopy Core Research Laboratory operated with support from NIH awards P20GM103546 and S10OD021806. This work was supported by the NIH grants GM109053 to EV and P20GM103546 (S. Sprang, PI; EV Pilot Project PI), American Heart Association Fellowship 18PRE34070028 to XW, and Montana Academy of Sciences award to XW.

Chapter 5. Conclusions and future directions

Balance of stem cell proliferation and differentiation is pivotal for maintaining body homeostasis because stem cell overproliferation can cause tumor formation and excess differentiation can cause tissue degeneration. Still, the mechanisms balancing stem cell proliferation and differentiation remain one of the open and intriguing questions in stem cell biology. Pumilio and FBF (PUF) family RNA-binding proteins that are highly conserved among eukaryotes share evolutionarily conserved roles in regulating stem cell maintenance (Quenault et al., 2011; Wickens et al., 2002). FBF-1 and FBF-2, two PUF family translational repressors in *C. elegans*, are expressed in the mitotic region of the germline and are important for maintaining germline stem cells. FBF-1 and FBF-2 (or FBFs) are about 89% identical to each other in primary sequence but have different effects on the stem cell pool size, which might be linked to distinct modes of regulation of their target mRNAs, indicating that FBFs may have unique roles. In the course of my dissertation, I set out to investigate whether and how FBF homologs differentially regulate the balance of stem cell proliferation and differentiation and to elucidate molecular mechanisms contributing to the differences between FBFs. This dissertation identified that FBF-1 and FBF-2 have distinct effects on stem cell dynamics: FBF-1 restricts the rate of stem cell meiotic entry, while FBF-2 promotes both rates of proliferation and meiotic entry. This work also identified several FBF-1- or FBF-2-specific cofactors that contribute to the unique functions of FBFs. FBF-1's function relies on cooperation with CCR4-NOT deadenylation machinery, while FBF-2-dependent regulation requires interaction with other cofactors, such as dynein light chain DLC-1. Splicing machinery appears to promote the function of both FBF-1 and FBF-2, but might cooperate with each FBF through different mechanisms. In this chapter, I first focus on the unique roles of FBFs in regulation of stem cell proliferation and differentiation, and then discuss possible mechanisms behind functional divergence of FBFs.

5.1 FBF-1 and FBF-2 differentially regulate germline stem cell proliferation and differentiation.

In *C. elegans* germline, the number of stem cells is controlled at a population level (Kimble and Crittenden, 2007), where loss of some stem cells through differentiation is balanced by proliferation of remaining cells, and the rates of differentiation and proliferation are similar. FBF homologs are redundantly required for maintaining germline stem cell pool, but loss-of-function (lf) mutations in each *fbf* result in different sizes of stem cell pool: *fbf-1(lf)* mutation results in a smaller stem cell pool compared to the wild type whereas *fbf-2(lf)* results in a larger stem cell pool compared to the wild type (Lamont et al., 2004). Although the two FBF homologs have been recognized as redundant regulators of germline stem cell maintenance, the effects of FBFs on stem cell proliferation and differentiation have not been examined. This dissertation demonstrats that *fbf-1(lf)* mutation leads to a faster rate of stem cell meiotic entry while *fbf-2(lf)* mutation leads to slower rates of both cell cycle and meiotic entry. This finding suggests a model where FBFs coordinately regulate cell cycle and meiotic entry rates of stem cells, and loss of either *fbf* would disrupt the balance of stem cell proliferation and differentiation, causing a change in stem cell pool size. Our findings of differential roles of FBFs in stem cell proliferation and differentiation are consistent with recently published studies regarding the function of two FBF homologs, PUM1 and PUM2, in mouse embryonic stem cells (ESCs), where PUM1 promotes differentiation while PUM2 promotes self-renewal of mouse ESCs (Uyhazi et al., 2020).

We further concluded that FBFs' effects on cell cycle rate are mediated by repression of a cyclin B family gene, one of the conserved regulators of the cell cycle. A previous study by Lin et al. (Lin et al., 2019) in the mouse demonstrated that binding of PUM1 or PUM2 to the mRNA of cell cycle regulator *Cdkn1b* promotes G1-S transition and cell proliferation, and thus controls mouse organ and body size. Our study found that loss of *fbf-2* resulted in significantly longer median G2-phase of germline stem cells, suggesting that FBF-2 promotes progression through G2 phase of the cell cycle. We hypothesized that FBFs' effects on cell cycle were mediated by regulating the mRNAs affecting G2 progression. Cell cycle regulators, including cyclin B genes, are among the mRNAs co-isolated with FBF proteins (Porter et al., 2019; Prasad et al., 2016). We tested whether disruption of PUF-mediated control of one member of cyclin B gene family could impact cell cycle progression. We found that removal of all canonical FBF binding sites from *cyb-2.1* 3'UTR results in increased expression of CYB-2.1 protein and faster cell cycle rate of germline stem cells in *fbf-*

2 mutant background. In the future, it would be interesting to test whether the faster cell cycle of stem cells resulting from elevated expression of CYB-2.1 in *fbf-2(lf)* is associated with a rescue of G2 phase progression. Additionally, since mRNAs encoding several other members of cyclin B family have also been co-isolated with FBFs, it would be interesting to test whether disruption of FBF-mediated regulation of other cyclin B genes in *fbf-2(lf)* would similarly rescue the extended G2 phase length and cell cycle rate.

FBFs largely bind to the same target RNAs and the same elements within those RNAs (Porter et al., 2019; Prasad et al., 2016), suggesting that FBFs may be competitively binding to the same target mRNAs. Why do the two FBF homologs produce distinct regulatory effects on stem cell maintenance? It is possible that FBFs' function is modulated by association with different cofactors. Our findings regarding such cofactors specific for FBF-1 or FBF-2 function are discussed in the following sections.

5.2 CCR4-NOT deadenylase machinery is an FBF-1-specific cofactor

As reported in Chapter 4, I identified that FBF-1 and -2 have different reliance on CCR4-NOT deadenylase machinery, suggesting that CCR4-NOT might be one of the factors contributing to distinct roles of FBFs in stem cell maintenance.

PUF family translational regulators don't have enzymatic activity and typically recruit specific cofactors to their target mRNAs to mediate regulatory outcomes (Cho et al., 2006; Cho et al., 2005; Eckmann et al., 2002; Friend et al., 2012; Goldstrohm et al., 2006; Kadyrova et al., 2007; Sonoda and Wharton, 1999; Sonoda and Wharton, 2001; Suh et al., 2009). The repressive function of PUF proteins in *C. elegans* and other species can be mediated by the CCR4-NOT deadenylase complex that promotes RNA deadenylation and decay. *In vitro*, both FBF-1 and FBF-2 bind CCF-1, one of the enzymatic subunits of CCR4-NOT (Suh et al., 2009). Our study, for the first time, demonstrated that FBF-1-mediated regulation was more dependent on CCR4-NOT than FBF-2-mediated regulation. This conclusion was supported by three lines of evidence. First, a knockdown of CCR4-NOT resulted in a decrease of the stem cell pool size in *fbf-2(lf)* mutant, but did not affect the stem cell pool size in *fbf-1(lf)* and the wild type backgrounds. Second, knockdown of CCR4-NOT caused derepression of a transgenic reporter of FBF target *htp-2* in the

stem cell region in *fbf-2(lf)* background. Finally, poly(A) tail length of FBF target mRNAs in *fbf-1(lf)* mutant animals was longer than in the wild type and shorter in *fbf-2(lf)* than in the wild type, suggesting that FBF-1 promoted deadenylation of target RNA while FBF-2 protected targets from deadenylation *in vivo*. To test whether FBF-1-dependent deadenylation is mediated by CCR4-NOT enzyme, in the future it would be interesting to analyse the poly(A) tail length in *fbf-2(lf)* after knocking down CCR4-NOT. Deadenylated mRNA in the cytoplasm can become a target of RNA decay (Łabno et al., 2016), and one mode of PUF-mediated repression is through promoting decay of target mRNAs (Goldstrohm et al., 2006; Olivas and Parker, 2000; Ulbricht and Olivas, 2008). Interestingly, our qPCR analysis showed that for most of FBF targets, mRNA abundance in *fbf-1(lf)* mutant is not significantly different from the wild type background, suggesting that FBF-1 cooperating with CCR4-NOT may promote translational repression rather than mRNA decay. To connect these findings to the regulation of stem cell pool dynamics, it would be interesting to test whether CCR4-NOT is required for FBF-1-mediated restriction of stem cell meiotic entry.

Interestingly, our *in vivo* results contradict the conclusions of an earlier *in vitro* study, which found that both FBF proteins interact with CCR4-NOT subunit CCF-1 and FBF-2 can promote *in vitro* deadenylation of a target RNA mediated by CCR4-NOT (Suh et al., 2009). We propose that the differences between *in vivo* and *in vitro* results might be explained by selective interaction of CCR4-NOT with FBF-1 *in vivo*. How would this selective interaction be achieved? One possible mechanism could be that CCR4-NOT and FBF-1 localize to the same cytoplasmic RNA-protein complex, which is different from the compartment that FBF-2 localizes to. In support of this possibility, we found that *in vivo* CCR4-NOT colocalizes with FBF-1, but not FBF-2. An alternative mechanism could be inhibition of FBF-2/CCR4-NOT interaction mediated by a cofactor of FBF-2; that is, the binding site for CCR4-NOT in FBF-2 might be occupied by other cofactor(s) of FBF-2 *in vivo*.

5.3 Splicing machinery facilitates function of both FBF-1 and FBF-2, but in different ways

As described in **Chapter 2**, we identified several splicing factors as potential cofactors for both FBF-1 and FBF-2 in *C. elegans* germline. Interestingly, there are differences in phenotypes observed after knocking down a subset of these splicing factors in *fbf-1(lf)* and *fbf-2(lf)*

backgrounds, suggesting that some splicing factors might preferentially promote the function of one of FBFs, and that the same splicing factors can promote FBF-mediated translational regulation during different stages of germline development. First, individual knockdowns of five splicing factors (*rsp-3, teg-1, gut-2, lsm-4, and lsm-7*) produced synthetic sterility only with the *fbf-1* mutant, but not with *fbf-2*, suggesting that these five splicing factors are FBF-2-specific cofactors. Second, individual knockdowns of the remaining two splicing factors (*prp-17* and *mtr-4)* in *fbf-1* mutant resulted in derepression of FBF target reporter in mitotic cells. By contrast, the same knockdowns in *fbf-2* mutant did not cause derepression of the target reporter in mitotic cells, but instead resulted in overexpression of the target reporter in meiotic cells. These observations suggest that PRP-17 and MTR-4 promote FBF-2-mediated target repression during stem cell development and FBF-1-mediated target repression during meiotic entry. To better understand cooperation between FBFs and splicing machinery, we might pursue the following directions discussed below.

Is splicing machinery required for FBF-2 or FBF-1 function in stem cell pool maintenance? Our observations suggest that stem cell pool sizes in *fbf* mutants were affected by splicing factor knockdowns. Quantification of stem cell pool sizes after individual knockdowns of all splicing factors in *fbf* mutants would determine whether the splicing factor knockdowns are affecting *fbf* mutants differently. If some splicing factors are found to selectively promote FBF-1 or FBF-2 function in stem cell maintenance, we could further test whether they are required for FBF-dependent regulation of the cell cycle or meiotic entry rate.

Our study suggested that five splicing factors are cofactors specific for FBF-2. Several core components of the splicesome such as Sm proteins have been found to be constitutive P granule components in *C. elegans* (Barbee et al., 2002). Interestingly, FBF-2 function depends on its localization to P granules (Voronina et al., 2012). It is possible that the five splicing factors that cooperate with FBF-2 colocalize with FBF-2 at P granules. To test this, co-immunolocalization of individual of the five splicing factors with P granules or GFP tagged FBF-2 could be performed. If commercial antibodies against these endogenous splicing factors are not available, we would need to tag these gene with affinity tags (such as 3xFLAG) by CRISPR or transgenesis. Since other PUF family proteins, such as PUF-8, can also localize to P granules, we propose that splicing

factors might also cooperate with other PUF family regulators. Additionally, antibodies against Sm proteins can stain germ granules (like P granules in *C. elegans*) in mouse (Moussa et al., 1994), suggesting that splicing factors as germ granule components might be a conserved structure in germ cells of diverse species.

5.4 Dynein light chain DLC-1 is an FBF-2-specific cofactor

From the list of genes co-immunoprecipitated with GFP tagged FBF-2, I identified an LC8 dynein light chain DLC-1 as a specific cofactor for FBF-2. As shown in **Chapter 3**, our study suggests that DLC-1 is required for FBF-2-specific target regulation as well as for FBF-2 localization in germline stem cells, and that DLC-1 directly binds to FBF-2. These results lead to two further questions: 1. Is DLC-1 required for FBF-2 to promote stem cell proliferation and/or differentiation? To test this possibility, measurement of cell cycle rate and differentiation rate scoring could be performed after knocking down *dlc-1* in *fbf-1* mutant. 2. Does DLC-1 presence affect FBF-2 target RNA binding preference? This question could be investigated through several possible directions. First, we could employ fluorescence polarization RNA-binding assay to test whether the presence of DLC-1 changes FBF-2's RNA-binding affinity to a few known target mRNAs compared to FBF-2 alone. Second, using SEQRS (in vitro selection, integrating high-throughput sequencing of RNA and sequence specificity landscapes, Campbell et al., 2012), RNA-binding preferences of FBF-2 bound to DLC-1 versus FBF-2 alone could be compared to uncover any variant RNA-binding specificity of the FBF-2/DLC-1 complex. Lastly, using iCLIP-seq, we could determine whether FBF-2/DLC-1 has distinct RNA-binding specificity *in vivo* by comparing the mRNAs bound to FBF-2 in *dlc-1* mutant compared to the mRNAs bound to FBF-2 in wild type genetic background.

FBF proteins are very similar in primary sequence except for four variable regions (VRs). As described in **Chapter 3**, our work identified that DLC-1 physically interacts with FBF-2 protein *in vitro* at three of those VRs (VR1, 2, 4) and that these DLC-1 binding sites are required for FBF-2 localization and function *in vivo*. We further found (**Chapter 4**) that the same three VRs are necessary for FBF-2-specific function in stem cell pool maintenance and a chimeric FBF-1 protein with swapped VR4 of FBF-2 gains the ability to rescue *fbf-2* function in stem cell maintenance. Together, these data suggest a possibility that VRs 1, 2, and 4 might be the key regions mediating

functional differences between FBF-1 and FBF-2. However, it is still important to tease apart whether the ability of these VRs to bind DLC-1 or other properties are the key factors that contribute to the functional differences between FBFs. In the future, more experiments could be performed to test this question. First, our study found that VR4 can rescue FBF-2-specific function, but we still don't know whether the individual VR1 and 2 would similarly be able to rescue FBF-2-specific function in stem cell maintenance. To test this, stem cell pool sizes of the germlines expressing FBF-1 chimeras with swapped VR1 or VR2 of FBF-2 could be measured and compared to that of the germlines expressing wild type FBF-1 or FBF-2 alone. If the experiments show that both VR1 and VR2 can promote FBF-2-specific function, it would suggest that DLC-1 binding might be the factor contributing to functional divergence between FBFs. But it is still possible that these effects are mediated by some unknown factor that can bind to the same regions in FBF-2 as DLC-1. Alternatively, if either none, or only VR1 or VR2 rescues FBF-2-function, it would suggest that DLC-1 binding is not important for functional divergence between FBFs. Finally, we could test whether either VR1, 2, or 4 mediates FBF-2-specific functions in stem cell proliferation and differentiation. To test this, measurement of cell cycle and meiotic entry rates could be performed in the animals expressing either FBF-2vrm mutant (with mutated VR1, 2, and 4) or any of FBF-1 chimeras with single FBF-2 VRs for comparison with the animals expressing only FBF-2wt and only FBF-1wt.

The studies in **Chapter 4** suggest that VRs 1, 2, and 4 in FBF-2 are necessary to prevent FBF-2 from cooperating with CCR4-NOT deadenylase. How do these VRs prevent FBF-2 from interacting with CCR4-NOT? We have already found that FBF-1 and CCR4-NOT colocalize to the same RNA granules while FBF-2 and CCR4-NOT localize to different RNA granules in stem cells. It is possible that the VRs bring FBF-2 to a cytoplasmic compartment that is different from where CCR4-NOT localizes. We found that the FBF-2vrm mutant, where the relevant VRs are mutated, can colocalize with CCR4-NOT, which supports the localization hypothesis. To determine whether either of VRs 1, 2, and 4 is sufficient to prevent FBF-2 from colocalizing with CCR4-NOT, we could test whether FBF-1 chimera mutants with swapped VR1 (or 2, or 4) can still colocalize with CCR4-NOT. Alternatively, it is possible that DLC-1 and CCR4-NOT might be competitive interactors of FBF-2, or DLC-1 binding might hinder the interaction between FBF-2 and CCR4-NOT complex.

Previously, Suh et al (Suh et al., 2009) using pull-down showed that the CCR4-NOT subunit CCF-1 interacts with FBF-2 *in vitro*. To test our hypothesis, GST pull-down could be employed to test whether CCF-1 can only pull down FBF-2 or the complex of FBF-2/DLC-1. If CCF-1 can only pull down FBF-2, it would suggest that CCF-1 and DLC-1 are competitive in binding to the same region of FBF-2, supporting our hypothesis that DLC-1 binding prevents FBF-2 from cooperation with CCR4-NOT. Alternatively, if CCF-1 can pull down the FBF-2/DLC-1 complex, it would suggest that CCF-1 and DLC-1 bind to different regions of FBF-2, and DLC-1 binding is not the reason that disrupts FBF-2's dependence on CCR4-NOT.

5.5 Summary

This dissertation, for first time, identified clear functional differences between FBF-1 and FBF-2 in controlling stem cell proliferation and differentiation in *C. elegans* germline. Our results support a model where FBF-2 promotes both cell cycle progression and meiotic entry of stem cells while FBF-1 inhibits meiotic entry. We propose that FBFs' coordinate regulation contributes to maintaining the balance of stem cell proliferation and differentiation in the germline. We identified CCR4-NOT deadenylation machinery as an FBF-1-specific cofactor, DLC-1 as an FBF-2-specific cofactor, and five splicing factors as potential specific cofactors for FBF-2. However, it is still unknown whether all the identified cofactors contribute to the functional divergence between FBF-1 and FBF-2 in regulating stem cell proliferation and differentiation. DLC-1 binding is required for FBF-2 RNP localization to P granules and the VRs containing DLC-binding sites prevent FBF-2 from localizing to the same compartment as CCR4-NOT deadenylase machinery. This allows for an exciting possibility that DLC-1 binding could be a key factor that inhibits interaction of FBF-2 with FBF-1-specific cofactors and therefore causes functional divergence between FBF-1 and FBF-2.

PUF proteins are conserved stem cell regulators in eukaryotes, from yeast to humans, and they share conserved mechanisms that affect stem cell proliferation and differentiation. Our studies give new mechanistic insight into PUF function in *C. elegans* that is likely relevant for other organisms.

References

Ahringer, J. and Kimble, J. (1991). Control of the sperm-oocyte switch in Caenorhabditis elegans hermaphrodites by the fem-3 3' untranslated region. *Nature* **349**, 346-348.

Aleem, E., Kiyokawa, H. and Kaldis, P. (2005). Cdc2-cyclin E complexes regulate the G1/S phase transition. *Nat Cell Biol* **7**, 831-836.

Ariz, M., Mainpal, R. and Subramaniam, K. (2009). C. elegans RNA-binding proteins PUF-8 and MEX-3 function redundantly to promote germline stem cell mitosis. *Dev Biol* **326**, 295-304.

Arur, S., Ohmachi, M., Berkseth, M., Nayak, S., Hansen, D., Zarkower, D. and Schedl, T. (2011). MPK-1 ERK controls membrane organization in C. elegans oogenesis via a sex-determination module. *Dev Cell* **20**, 677-688.

Arvola, R. M., Weidmann, C. A., Tanaka Hall, T. M. and Goldstrohm, A. C. (2017). Combinatorial control of messenger RNAs by Pumilio, Nanos and Brain Tumor Proteins. *RNA Biol* **14**, 1445-1456.

Asaoka-Taguchi, M., Yamada, M., Nakamura, A., Hanyu, K. and Kobayashi, S. (1999). Maternal Pumilio acts together with Nanos in germline development in Drosophila embryos. *Nat Cell Biol* **1**, 431-437.

Austin, J. and Kimble, J. (1987). glp-1 is required in the germ line for regulation of the decision between mitosis and meiosis in C. elegans. *Cell* **51**, 589-599.

Barbee, S. A., Lublin, A. L. and Evans, T. C. (2002). A novel function for the Sm proteins in germ granule localization during C. elegans embryogenesis. *Curr Biol* **12**, 1502-1506.

Barton, M. K. and Kimble, J. (1990). fog-1, a regulatory gene required for specification of spermatogenesis in the germ line of Caenorhabditis elegans. *Genetics* **125**, 29-39.

Becker, K. A., Ghule, P. N., Therrien, J. A., Lian, J. B., Stein, J. L., van Wijnen, A. J. and Stein, G. S. (2006). Self-renewal of human embryonic stem cells is supported by a shortened G1 cell cycle phase. *J Cell Physiol* **209**, 883-893.

Belfiore, M., Pugnale, P., Saudan, Z. and Puoti, A. (2004). Roles of the C. elegans cyclophilin-like protein MOG-6 in MEP-1 binding and germline fates. *Development* **131**, 2935-2945.

Bernet, J. D., Doles, J. D., Hall, J. K., Kelly Tanaka, K., Carter, T. A. and Olwin, B. B. (2014). p38 MAPK signaling underlies a cell-autonomous loss of stem cell self-renewal in skeletal muscle of aged mice. *Nat Med* **20**, 265-271.

Bernstein, D., Hook, B., Hajarnavis, A., Opperman, L. and Wickens, M. (2005). Binding specificity and mRNA targets of a C. elegans PUF protein, FBF-1. *RNA* **11**, 447-458.

Berry, L. W., Westlund, B. and Schedl, T. (1997). Germ-line tumor formation caused by activation of glp-1, a Caenorhabditis elegans member of the Notch family of receptors. *Development* **124**, 925-936.

Berthet, C., Morera, A. M., Asensio, M. J., Chauvin, M. A., Morel, A. P., Dijoud, F., Magaud, J. P., Durand, P. and Rouault, J. P. (2004). CCR4-associated factor CAF1 is an essential factor for spermatogenesis. *Mol Cell Biol* **24**, 5808-5820.

Boag, P. R., Nakamura, A. and Blackwell, T. K. (2005). A conserved RNA-protein complex component involved in physiological germline apoptosis regulation in C. elegans. *Development* **132**, 4975-4986.

Boward, B., Wu, T. and Dalton, S. (2016). Concise Review: Control of Cell Fate Through Cell Cycle and Pluripotency Networks. *Stem Cells* **34**, 1427-1436.

Brenner, J. L. and Schedl, T. (2016). Germline Stem Cell Differentiation Entails Regional Control of Cell Fate Regulator GLD-1 in Caenorhabditis elegans. *Genetics* **202**, 1085-1103.

Brenner, S. (1974). The genetics of Caenorhabditis elegans. *Genetics* **77**, 71-94.

Buck, S. H., Chiu, D. and Saito, R. M. (2009). The cyclin-dependent kinase inhibitors, cki-1 and cki-2, act in overlapping but distinct pathways to control cell cycle quiescence during C. elegans development. *Cell Cycle* **8**, 2613-2620.

Burdon, T., Stracey, C., Chambers, I., Nichols, J. and Smith, A. (1999). Suppression of SHP-2 and ERK signalling promotes self-renewal of mouse embryonic stem cells. *Dev Biol* **210**, 30-43.

Butuči, M., Williams, A. B., Wong, M. M., Kramer, B. and Michael, W. M. (2015). Zygotic Genome Activation Triggers Chromosome Damage and Checkpoint Signaling in C. elegans Primordial Germ Cells. *Dev Cell* **34**, 85-95.

Byrd, D. T., Knobel, K., Affeldt, K., Crittenden, S. L. and Kimble, J. (2014). A DTC niche plexus surrounds the germline stem cell pool in Caenorhabditis elegans. *PLoS One* **9**, e88372.

Campbell, Z. T., Bhimsaria, D., Valley, C. T., Rodriguez-Martinez, J. A., Menichelli, E., Williamson, J. R., Ansari, A. Z. and Wickens, M. (2012). Cooperativity in RNA-protein interactions: global analysis of RNA binding specificity. *Cell Rep* **1**, 570-581.

Campbell, Z. T., Valley, C. T. and Wickens, M. (2014). A protein-RNA specificity code enables targeted activation of an endogenous human transcript. *Nat Struct Mol Biol* **21**, 732-738.

Cao, Q., Padmanabhan, K. and Richter, J. D. (2010). Pumilio 2 controls translation by competing with eIF4E for 7-methyl guanosine cap recognition. *RNA* **16**, 221-227.

Casper, A. and Van Doren, M. (2006). The control of sexual identity in the Drosophila germline. *Development* **133**, 2783-2791.

Ceron, J., Rual, J. F., Chandra, A., Dupuy, D., Vidal, M. and van den Heuvel, S. (2007). Large-scale RNAi screens identify novel genes that interact with the C. elegans retinoblastoma pathway as well as splicing-related components with synMuv B activity. *BMC Dev Biol* **7**, 30.

Chao, H. X., Fakhreddin, R. I., Shimerov, H. K., Kedziora, K. M., Kumar, R. J., Perez, J., Limas, J. C., Grant, G. D., Cook, J. G., Gupta, G. P., et al. (2019). Evidence that the human cell cycle is a series of uncoupled, memoryless phases. *Mol Syst Biol* **15**, e8604.

Chen, C., Fingerhut, J. M. and Yamashita, Y. M. (2016). The ins(ide) and outs(ide) of asymmetric stem cell division. *Curr Opin Cell Biol* **43**, 1-6.

Chen, D., Zheng, W., Lin, A., Uyhazi, K., Zhao, H. and Lin, H. (2012). Pumilio 1 suppresses multiple activators of p53 to safeguard spermatogenesis. *Curr Biol* **22**, 420-425.

Cheong, C. G. and Hall, T. M. (2006). Engineering RNA sequence specificity of Pumilio repeats. *Proc Natl Acad Sci U S A* **103**, 13635-13639.

Cho, P. F., Gamberi, C., Cho-Park, Y. A., Cho-Park, I. B., Lasko, P. and Sonenberg, N. (2006). Cap-dependent translational inhibition establishes two opposing morphogen gradients in Drosophila embryos. *Curr Biol* **16**, 2035-2041.

Cho, P. F., Poulin, F., Cho-Park, Y. A., Cho-Park, I. B., Chicoine, J. D., Lasko, P. and Sonenberg, N. (2005). A new paradigm for translational control: inhibition via 5'-3' mRNA tethering by Bicoid and the eIF4E cognate 4EHP. *Cell* **121**, 411-423.

Chuykin, I. A., Lianguzova, M. S., Pospelova, T. V. and Pospelov, V. A. (2008). Activation of DNA damage response signaling in mouse embryonic stem cells. *Cell Cycle* **7**, 2922-2928.

Collart, M. A., Kassem, S. and Villanyi, Z. (2017). Mutations in the. *Front Genet* **8**, 61.

Costes, S. V., Daelemans, D., Cho, E. H., Dobbin, Z., Pavlakis, G. and Lockett, S. (2004). Automatic and quantitative measurement of protein-protein colocalization in live cells. *Biophys J* **86**, 3993-4003.

Cotsarelis, G., Sun, T. T. and Lavker, R. M. (1990). Label-retaining cells reside in the bulge area of pilosebaceous unit: implications for follicular stem cells, hair cycle, and skin carcinogenesis. *Cell* **61**, 1329-1337.

Crittenden, S. L., Bernstein, D. S., Bachorik, J. L., Thompson, B. E., Gallegos, M., Petcherski, A. G., Moulder, G., Barstead, R., Wickens, M. and Kimble, J. (2002). A conserved RNA-binding protein controls germline stem cells in Caenorhabditis elegans. *Nature* **417**, 660-663.

Crittenden, S. L., Leonhard, K. A., Byrd, D. T. and Kimble, J. (2006). Cellular analyses of the mitotic region in the Caenorhabditis elegans adult germ line. *Mol Biol Cell* **17**, 3051-3061.

Day, N. J., Wang, X. and Voronina, E. (2020). In Situ Detection of Ribonucleoprotein Complex Assembly in the *C. elegans* Germline using Proximity Ligation Assay. Journal of Visualized Experiments.

Degrauwe, N., Suvà, M. L., Janiszewska, M., Riggi, N. and Stamenkovic, I. (2016). IMPs: an RNA-binding protein family that provides a link between stem cell maintenance in normal development and cancer. *Genes Dev* **30**, 2459-2474.

Dickinson, D. J., Ward, J. D., Reiner, D. J. and Goldstein, B. (2013). Engineering the Caenorhabditis elegans genome using Cas9-triggered homologous recombination. *Nat Methods* **10**, 1028-1034.

Dubnau, J., Chiang, A. S., Grady, L., Barditch, J., Gossweiler, S., McNeil, J., Smith, P., Buldoc, F., Scott, R., Certa, U., et al. (2003). The staufen/pumilio pathway is involved in Drosophila long-term memory. *Curr Biol* **13**, 286-296.

Eckmann, C. R., Crittenden, S. L., Suh, N. and Kimble, J. (2004). GLD-3 and control of the mitosis/meiosis decision in the germline of Caenorhabditis elegans. *Genetics* **168**, 147-160.

Eckmann, C. R., Kraemer, B., Wickens, M. and Kimble, J. (2002). GLD-3, a bicaudal-C homolog that inhibits FBF to control germline sex determination in C. elegans. *Dev Cell* **3**, 697-710.

Ellenbecker, M., Osterli, E., Wang, X., Day, N. J., Baumgarten, E., Hickey, B. and Voronina, E. (2019). Dynein Light Chain DLC-1 Facilitates the Function of the Germline Cell Fate Regulator GLD-1 in. *Genetics* **211**, 665-681.

Fernandez, A. G., Mis, E. K., Lai, A., Mauro, M., Quental, A., Bock, C. and Piano, F. (2014). Uncovering buffered pleiotropy: a genome-scale screen for mel-28 genetic interactors in Caenorhabditis elegans. *G3 (Bethesda)* **4**, 185-196.

Forbes, A. and Lehmann, R. (1998). Nanos and Pumilio have critical roles in the development and function of Drosophila germline stem cells. *Development* **125**, 679-690.

Fox, P. M. and Schedl, T. (2015). Analysis of Germline Stem Cell Differentiation Following Loss of GLP-1 Notch Activity in Caenorhabditis elegans. *Genetics* **201**, 167-184.

Fox, P. M., Vought, V. E., Hanazawa, M., Lee, M. H., Maine, E. M. and Schedl, T. (2011). Cyclin E and CDK-2 regulate proliferative cell fate and cell cycle progression in the C. elegans germline. *Development* **138**, 2223-2234.

Francis, R., Barton, M. K., Kimble, J. and Schedl, T. (1995). gld-1, a tumor suppressor gene required for oocyte development in Caenorhabditis elegans. *Genetics* **139**, 579-606.

Fredriksson, S., Gullberg, M., Jarvius, J., Olsson, C., Pietras, K., Gústafsdóttir, S. M., Ostman, A. and Landegren, U. (2002). Protein detection using proximity-dependent DNA ligation assays. *Nat Biotechnol* **20**, 473-477.

Friend, K., Campbell, Z. T., Cooke, A., Kroll-Conner, P., Wickens, M. P. and Kimble, J. (2012). A conserved PUF-Ago-eEF1A complex attenuates translation elongation. *Nat Struct Mol Biol* **19**, 176-183.

Frøkjaer-Jensen, C., Davis, M. W., Hopkins, C. E., Newman, B. J., Thummel, J. M., Olesen, S. P., Grunnet, M. and Jorgensen, E. M. (2008). Single-copy insertion of transgenes in Caenorhabditis elegans. *Nat Genet* **40**, 1375-1383.

Frøkjær-Jensen, C., Jain, N., Hansen, L., Davis, M. W., Li, Y., Zhao, D., Rebora, K., Millet, J. R. M., Liu, X., Kim, S. K., et al. (2016). An Abundant Class of Non-coding DNA Can Prevent Stochastic Gene Silencing in the C. elegans Germline. *Cell* **166**, 343-357.

Fu, Z., Geng, C., Wang, H., Yang, Z., Weng, C., Li, H., Deng, L., Liu, L., Liu, N., Ni, J., et al. (2015). Twin Promotes the Maintenance and Differentiation of Germline Stem Cell Lineage through Modulation of Multiple Pathways. *Cell Rep* **13**, 1366-1379.

Furuta, T., Joo, H. J., Trimmer, K. A., Chen, S. Y. and Arur, S. (2018). GSK-3 promotes S-phase entry and progression in. *Development* **145**.

Galgano, A., Forrer, M., Jaskiewicz, L., Kanitz, A., Zavolan, M. and Gerber, A. P. (2008). Comparative analysis of mRNA targets for human PUF-family proteins suggests extensive interaction with the miRNA regulatory system. *PLoS One* **3**, e3164.

Gallegos, M., Ahringer, J., Crittenden, S. and Kimble, J. (1998). Repression by the 3' UTR of fem-3, a sex-determining gene, relies on a ubiquitous mog-dependent control in Caenorhabditis elegans. *EMBO J* **17**, 6337-6347.

Garcia-Muse, T. and Boulton, S. J. (2005). Distinct modes of ATR activation after replication stress and DNA double-strand breaks in Caenorhabditis elegans. *EMBO J* **24**, 4345-4355.

García-Rodríguez, L. J., Gay, A. C. and Pon, L. A. (2007). Puf3p, a Pumilio family RNA binding protein, localizes to mitochondria and regulates mitochondrial biogenesis and motility in budding yeast. *J Cell Biol* **176**, 197-207.

Gerber, A. P., Herschlag, D. and Brown, P. O. (2004). Extensive association of functionally and cytotopically related mRNAs with Puf family RNA-binding proteins in yeast. *PLoS Biol* **2**, E79.

Gerber, A. P., Luschnig, S., Krasnow, M. A., Brown, P. O. and Herschlag, D. (2006). Genome-wide identification of mRNAs associated with the translational regulator PUMILIO in Drosophila melanogaster. *Proc Natl Acad Sci U S A* **103**, 4487-4492.

Ghosh, S., Marchand, V., Gáspár, I. and Ephrussi, A. (2012). Control of RNP motility and localization by a splicing-dependent structure in oskar mRNA. *Nat Struct Mol Biol* **19**, 441-449.

Ghosh, S., Obrdlik, A., Marchand, V. and Ephrussi, A. (2014). The EJC binding and dissociating activity of PYM is regulated in Drosophila. *PLoS Genet* **10**, e1004455.

Glisovic, T., Bachorik, J. L., Yong, J. and Dreyfuss, G. (2008). RNA-binding proteins and post-transcriptional gene regulation. *FEBS Lett* **582**, 1977-1986.

Goldstrohm, A. C., Hook, B. A., Seay, D. J. and Wickens, M. (2006). PUF proteins bind Pop2p to regulate messenger RNAs. *Nat Struct Mol Biol* **13**, 533-539.

Graham, P. L. and Kimble, J. (1993). The mog-1 gene is required for the switch from spermatogenesis to oogenesis in Caenorhabditis elegans. *Genetics* **133**, 919-931.

Grishok, A., Hoersch, S. and Sharp, P. A. (2008). RNA interference and retinoblastoma-related genes are required for repression of endogenous siRNA targets in Caenorhabditis elegans. *Proc Natl Acad Sci U S A* **105**, 20386-20391.

Grishok, A. and Sharp, P. A. (2005). Negative regulation of nuclear divisions in Caenorhabditis elegans by retinoblastoma and RNA interference-related genes. *Proc Natl Acad Sci U S A* **102**, 17360-17365.

Guevara, C., Korver, W., Mahony, D., Parry, D., Seghezzi, W., Shanahan, F. and Lees, E. (1999). Regulation of G1/S transition in mammalian cells. *Kidney Int* **56**, 1181-1192.

Hachet, O. and Ephrussi, A. (2004). Splicing of oskar RNA in the nucleus is coupled to its cytoplasmic localization. *Nature* **428**, 959-963.

Hafner, M., Landthaler, M., Burger, L., Khorshid, M., Hausser, J., Berninger, P., Rothballer, A., Ascano, M., Jungkamp, A. C., Munschauer, M., et al. (2010). Transcriptome-wide identification of RNA-binding protein and microRNA target sites by PAR-CLIP. *Cell* **141**, 129-141.

Hall, T. M. (2016). De-coding and re-coding RNA recognition by PUF and PPR repeat proteins. *Curr Opin Struct Biol* **36**, 116-121.

Hamill, D. R., Severson, A. F., Carter, J. C. and Bowerman, B. (2002). Centrosome maturation and mitotic spindle assembly in C. elegans require SPD-5, a protein with multiple coiled-coil domains. *Dev Cell* **3**, 673-684.

Hansen, D., Hubbard, E. J. and Schedl, T. (2004a). Multi-pathway control of the proliferation versus meiotic development decision in the Caenorhabditis elegans germline. *Dev Biol* **268**, 342-357.

Hansen, D. and Schedl, T. (2013). Stem cell proliferation versus meiotic fate decision in Caenorhabditis elegans. *Adv Exp Med Biol* **757**, 71-99.

Hansen, D., Wilson-Berry, L., Dang, T. and Schedl, T. (2004b). Control of the proliferation versus meiotic development decision in the C. elegans germline through regulation of GLD-1 protein accumulation. *Development* **131**, 93-104.

Haupt, K. A., Enright, A. L., Ferdous, A. S., Kershner, A. M., Shin, H., Wickens, M. and Kimble, J. (2019a). The molecular basis of LST-1 self-renewal activity and its control of stem cell pool size. *Development* **146**.

Haupt, K. A., Law, K. T., Enright, A. L., Kanzler, C. R., Shin, H., Wickens, M. and Kimble, J. (2019b). A PUF Hub Drives Self-Renewal in. *Genetics*.

Henderson, S. T., Gao, D., Christensen, S. and Kimble, J. (1997). Functional domains of LAG-2, a putative signaling ligand for LIN-12 and GLP-1 receptors in Caenorhabditis elegans. *Mol Biol Cell* **8**, 1751-1762.

Hirsh, D., Oppenheim, D. and Klass, M. (1976). Development of the reproductive system of Caenorhabditis elegans. *Dev Biol* **49**, 200-219.

Hodgkin, J. (1987). A genetic analysis of the sex-determining gene, tra-1, in the nematode Caenorhabditis elegans. *Genes Dev* **1**, 731-745.

Hook, B. A., Goldstrohm, A. C., Seay, D. J. and Wickens, M. (2007). Two yeast PUF proteins negatively regulate a single mRNA. *J Biol Chem* **282**, 15430-15438.

Hubbard, E. J., Korta, D. Z. and Dalfó, D. (2013). Physiological control of germline development. *Adv Exp Med Biol* **757**, 101-131.

Hubbard, E. J. A. and Schedl, T. (2019). Biology of the. *Genetics* **213**, 1145-1188.

Hubstenberger, A., Cameron, C., Shtofman, R., Gutman, S. and Evans, T. C. (2012). A network of PUF proteins and Ras signaling promote mRNA repression and oogenesis in C. elegans. *Dev Biol* **366**, 218-231.

Hubstenberger, A., Courel, M., Bénard, M., Souquere, S., Ernoult-Lange, M., Chouaib, R., Yi, Z., Morlot, J. B., Munier, A., Fradet, M., et al. (2017). P-Body Purification Reveals the Condensation of Repressed mRNA Regulons. *Mol Cell* **68**, 144-157.e145.

Jaramillo-Lambert, A., Ellefson, M., Villeneuve, A. M. and Engebrecht, J. (2007). Differential timing of S phases, X chromosome replication, and meiotic prophase in the C. elegans germ line. *Dev Biol* **308**, 206-221.

Jin, S. W., Arno, N., Cohen, A., Shah, A., Xu, Q., Chen, N. and Ellis, R. E. (2001a). In Caenorhabditis elegans, the RNA-binding domains of the cytoplasmic polyadenylation element binding protein FOG-1 are needed to regulate germ cell fates. *Genetics* **159**, 1617-1630.

Jin, S. W., Kimble, J. and Ellis, R. E. (2001b). Regulation of cell fate in Caenorhabditis elegans by a novel cytoplasmic polyadenylation element binding protein. *Dev Biol* **229**, 537-553.

Joly, W., Chartier, A., Rojas-Rios, P., Busseau, I. and Simonelig, M. (2013). The CCR4 deadenylase acts with Nanos and Pumilio in the fine-tuning of Mei-P26 expression to promote germline stem cell self-renewal. *Stem Cell Reports* **1**, 411-424.

Kadyk, L. C. and Kimble, J. (1998). Genetic regulation of entry into meiosis in Caenorhabditis elegans. *Development* **125**, 1803-1813.

Kadyrova, L. Y., Habara, Y., Lee, T. H. and Wharton, R. P. (2007). Translational control of maternal Cyclin B mRNA by Nanos in the Drosophila germline. *Development* **134**, 1519-1527.

Kalchhauser, I., Farley, B. M., Pauli, S., Ryder, S. P. and Ciosk, R. (2011). FBF represses the Cip/Kip cell-cycle inhibitor CKI-2 to promote self-renewal of germline stem cells in C. elegans. *EMBO J* **30**, 3823-3829.

Kamath, R. S. and Ahringer, J. (2003). Genome-wide RNAi screening in Caenorhabditis elegans. *Methods* **30**, 313-321.

Kareta, M. S., Sage, J. and Wernig, M. (2015). Crosstalk between stem cell and cell cycle machineries. *Curr Opin Cell Biol* **37**, 68-74.

Kasturi, P., Zanetti, S., Passannante, M., Saudan, Z., Müller, F. and Puoti, A. (2010). The C. elegans sex determination protein MOG-3 functions in meiosis and binds to the CSL co-repressor CIR-1. *Dev Biol* **344**, 593-602.

Kataoka, N., Yong, J., Kim, V. N., Velazquez, F., Perkinson, R. A., Wang, F. and Dreyfuss, G. (2000). Pre-mRNA splicing imprints mRNA in the nucleus with a novel RNA-binding protein that persists in the cytoplasm. *Mol Cell* **6**, 673-682.

Kawano, T., Kataoka, N., Dreyfuss, G. and Sakamoto, H. (2004). Ce-Y14 and MAG-1, components of the exon-exon junction complex, are required for embryogenesis and germline sexual switching in Caenorhabditis elegans. *Mech Dev* **121**, 27-35.

Kaye, J. A., Rose, N. C., Goldsworthy, B., Goga, A. and L'Etoile, N. D. (2009). A 3'UTR pumilio-binding element directs translational activation in olfactory sensory neurons. *Neuron* **61**, 57-70.

Kedde, M., van Kouwenhove, M., Zwart, W., Oude Vrielink, J. A., Elkon, R. and Agami, R. (2010). A Pumilio-induced RNA structure switch in p27-3' UTR controls miR-221 and miR-222 accessibility. *Nat Cell Biol* **12**, 1014-1020.

Kerins, J. A., Hanazawa, M., Dorsett, M. and Schedl, T. (2010). PRP-17 and the pre-mRNA splicing pathway are preferentially required for the proliferation versus meiotic development decision and germline sex determination in Caenorhabditis elegans. *Dev Dyn* **239**, 1555-1572.

Kershner, A. M. and Kimble, J. (2010). Genome-wide analysis of mRNA targets for Caenorhabditis elegans FBF, a conserved stem cell regulator. *Proc Natl Acad Sci U S A* **107**, 3936-3941.

Kershner, A. M., Shin, H., Hansen, T. J. and Kimble, J. (2014). Discovery of two GLP-1/Notch target genes that account for the role of GLP-1/Notch signaling in stem cell maintenance. *Proc Natl Acad Sci U S A* **111**, 3739-3744.

Kimble, J. and Crittenden, S. L. (2007). Controls of germline stem cells, entry into meiosis, and the sperm/oocyte decision in Caenorhabditis elegans. *Annu Rev Cell Dev Biol* **23**, 405-433.

Kimble, J. and Page, D. C. (2007). The mysteries of sexual identity. The germ cell's perspective. *Science* **316**, 400-401.

Kimble, J. E. and White, J. G. (1981). On the control of germ cell development in Caenorhabditis elegans. *Dev Biol* **81**, 208-219.

Kocsisova, Z., Kornfeld, K. and Schedl, T. (2019). Rapid population-wide declines in stem cell number and activity during reproductive aging in. *Development* **146**.

Kocsisova, Z., Mohammad, A., Kornfeld, K. and Schedl, T. (2018). Cell Cycle Analysis in the C. elegans Germline with the Thymidine Analog EdU. *J Vis Exp*.

Koh, Y. Y., Opperman, L., Stumpf, C., Mandan, A., Keles, S. and Wickens, M. (2009). A single C. elegans PUF protein binds RNA in multiple modes. *RNA* **15**, 1090-1099.

Konishi, T., Uodome, N. and Sugimoto, A. (2008). The Caenorhabditis elegans DDX-23, a homolog of yeast splicing factor PRP28, is required for the sperm-oocyte switch and differentiation of various cell types. *Dev Dyn* **237**, 2367-2377.

Kotani, T., Yasuda, K., Ota, R. and Yamashita, M. (2013). Cyclin B1 mRNA translation is temporally controlled through formation and disassembly of RNA granules. *J Cell Biol* **202**, 1041-1055.

Kraemer, B., Crittenden, S., Gallegos, M., Moulder, G., Barstead, R., Kimble, J. and Wickens, M. (1999). NANOS-3 and FBF proteins physically interact to control the sperm-oocyte switch in Caenorhabditis elegans. *Curr Biol* **9**, 1009-1018.

Kumsta, C. and Hansen, M. (2012). C. elegans rrf-1 mutations maintain RNAi efficiency in the soma in addition to the germline. *PLoS One* **7**, e35428.

Kwon, S. C., Yi, H., Eichelbaum, K., Föhr, S., Fischer, B., You, K. T., Castello, A., Krijgsveld, J., Hentze, M. W. and Kim, V. N. (2013). The RNA-binding protein repertoire of embryonic stem cells. *Nat Struct Mol Biol* **20**, 1122-1130.

Lamont, L. B., Crittenden, S. L., Bernstein, D., Wickens, M. and Kimble, J. (2004). FBF-1 and FBF-2 regulate the size of the mitotic region in the C. elegans germline. *Dev Cell* **7**, 697-707.

Lamont, L. B. and Kimble, J. (2007). Developmental expression of FOG-1/CPEB protein and its control in the Caenorhabditis elegans hermaphrodite germ line. *Dev Dyn* **236**, 871-879.

Lange, C. and Calegari, F. (2010). Cdks and cyclins link G1 length and differentiation of embryonic, neural and hematopoietic stem cells. *Cell Cycle* **9**, 1893-1900.

Langenfeld, J., Kiyokawa, H., Sekula, D., Boyle, J. and Dmitrovsky, E. (1997). Posttranslational regulation of cyclin D1 by retinoic acid: a chemoprevention mechanism. *Proc Natl Acad Sci U S A* **94**, 12070-12074.

Lawrence, K. S., Chau, T. and Engebrecht, J. (2015). DNA damage response and spindle assembly checkpoint function throughout the cell cycle to ensure genomic integrity. *PLoS Genet* **11**, e1005150.

Le Hir, H., Izaurralde, E., Maquat, L. E. and Moore, M. J. (2000). The spliceosome deposits multiple proteins 20-24 nucleotides upstream of mRNA exon-exon junctions. *EMBO J* **19**, 6860-6869.

Le Hir, H. and Séraphin, B. (2008). EJCs at the heart of translational control. *Cell* **133**, 213-216.

Lechler, M. C., Crawford, E. D., Groh, N., Widmaier, K., Jung, R., Kirstein, J., Trinidad, J. C., Burlingame, A. L. and David, D. C. (2017). Reduced Insulin/IGF-1 Signaling Restores the Dynamic Properties of Key Stress Granule Proteins during Aging. *Cell Rep* **18**, 454-467.

Lee, M. H., Hook, B., Lamont, L. B., Wickens, M. and Kimble, J. (2006). LIP-1 phosphatase controls the extent of germline proliferation in Caenorhabditis elegans. *EMBO J* **25**, 88-96.

Lee, M. H., Hook, B., Pan, G., Kershner, A. M., Merritt, C., Seydoux, G., Thomson, J. A., Wickens, M. and Kimble, J. (2007a). Conserved regulation of MAP kinase expression by PUF RNA-binding proteins. *PLoS Genet* **3**, e233.

Lee, M. H., Ohmachi, M., Arur, S., Nayak, S., Francis, R., Church, D., Lambie, E. and Schedl, T. (2007b). Multiple functions and dynamic activation of MPK-1 extracellular signal-regulated kinase signaling in Caenorhabditis elegans germline development. *Genetics* **177**, 2039-2062.

Lee, Y. and Rio, D. C. (2015). Mechanisms and Regulation of Alternative Pre-mRNA Splicing. *Annu Rev Biochem* **84**, 291-323.

Lin, H. and Spradling, A. C. (1997). A novel group of pumilio mutations affects the asymmetric division of germline stem cells in the Drosophila ovary. *Development* **124**, 2463-2476.

Lin, K., Qiang, W., Zhu, M., Ding, Y., Shi, Q., Chen, X., Zsiros, E., Wang, K., Yang, X., Kurita, T., et al. (2019). Mammalian Pum1 and Pum2 Control Body Size via Translational Regulation of the Cell Cycle Inhibitor Cdkn1b. *Cell Rep* **26**, 2434-2450.e2436.

Lindqvist, A., Rodríguez-Bravo, V. and Medema, R. H. (2009). The decision to enter mitosis: feedback and redundancy in the mitotic entry network. *J Cell Biol* **185**, 193-202.

Liu, Q., Stumpf, C., Thomas, C., Wickens, M. and Haag, E. S. (2012). Context-dependent function of a conserved translational regulatory module. *Development* **139**, 1509-1521.

Lu, G., Dolgner, S. J. and Hall, T. M. (2009). Understanding and engineering RNA sequence specificity of PUF proteins. *Curr Opin Struct Biol* **19**, 110-115.

Luitjens, C., Gallegos, M., Kraemer, B., Kimble, J. and Wickens, M. (2000). CPEB proteins control two key steps in spermatogenesis in C. elegans. *Genes Dev* **14**, 2596-2609.

Maciejowski, J., Ugel, N., Mishra, B., Isopi, M. and Hubbard, E. J. (2006). Quantitative analysis of germline mitosis in adult C. elegans. *Dev Biol* **292**, 142-151.

Maheshwari, R., Pushpa, K. and Subramaniam, K. (2016). A role for post-transcriptional control of endoplasmic reticulum dynamics and function in C. elegans germline stem cell maintenance. *Development* **143**, 3097-3108.

Malik, S., Jang, W., Park, S. Y., Kim, J. Y., Kwon, K. S. and Kim, C. (2019). The target specificity of the RNA binding protein Pumilio is determined by distinct co-factors. *Biosci Rep* **39**.

Mantina, P., MacDonald, L., Kulaga, A., Zhao, L. and Hansen, D. (2009). A mutation in teg-4, which encodes a protein homologous to the SAP130 pre-mRNA splicing factor, disrupts the balance between proliferation and differentiation in the C. elegans germ line. *Mech Dev* **126**, 417-429.

Mee, C. J., Pym, E. C., Moffat, K. G. and Baines, R. A. (2004). Regulation of neuronal excitability through pumilio-dependent control of a sodium channel gene. *J Neurosci* **24**, 8695-8703.

Menichelli, E., Wu, J., Campbell, Z. T., Wickens, M. and Williamson, J. R. (2013). Biochemical characterization of the Caenorhabditis elegans FBF.CPB-1 translational regulation complex identifies conserved protein interaction hotspots. *J Mol Biol* **425**, 725-737.

Merritt, C., Rasoloson, D., Ko, D. and Seydoux, G. (2008). 3' UTRs are the primary regulators of gene expression in the C. elegans germline. *Curr Biol* **18**, 1476-1482.

Merritt, C. and Seydoux, G. (2010). The Puf RNA-binding proteins FBF-1 and FBF-2 inhibit the expression of synaptonemal complex proteins in germline stem cells. *Development* **137**, 1787-1798.

Mesa, K. R., Kawaguchi, K., Cockburn, K., Gonzalez, D., Boucher, J., Xin, T., Klein, A. M. and Greco, V. (2018). Homeostatic Epidermal Stem Cell Self-Renewal Is Driven by Local Differentiation. *Cell Stem Cell* **23**, 677-686.e674.

Michaelson, D., Korta, D. Z., Capua, Y. and Hubbard, E. J. (2010). Insulin signaling promotes germline proliferation in C. elegans. *Development* **137**, 671-680.

Millonigg, S., Minasaki, R., Nousch, M., Novak, J. and Eckmann, C. R. (2014). GLD-4-mediated translational activation regulates the size of the proliferative germ cell pool in the adult C. elegans germ line. *PLoS Genet* **10**, e1004647.

Morgan, C. T., Lee, M. H. and Kimble, J. (2010). Chemical reprogramming of Caenorhabditis elegans germ cell fate. *Nat Chem Biol* **6**, 102-104.

Morris, A. R., Mukherjee, N. and Keene, J. D. (2008). Ribonomic analysis of human Pum1 reveals cis-trans conservation across species despite evolution of diverse mRNA target sets. *Mol Cell Biol* **28**, 4093-4103.

Morrison, S. J. and Kimble, J. (2006). Asymmetric and symmetric stem-cell divisions in development and cancer. *Nature* **441**, 1068-1074.

Moser, S. C., von Elsner, S., Büssing, I., Alpi, A., Schnabel, R. and Gartner, A. (2009). Functional dissection of Caenorhabditis elegans CLK-2/TEL2 cell cycle defects during embryogenesis and germline development. *PLoS Genet* **5**, e1000451.

Moussa, F., Oko, R. and Hermo, L. (1994). The immunolocalization of small nuclear ribonucleoprotein particles in testicular cells during the cycle of the seminiferous epithelium of the adult rat. *Cell Tissue Res* **278**, 363-378.

Mugridge, J. S., Coller, J. and Gross, J. D. (2018). Structural and molecular mechanisms for the control of eukaryotic 5'-3' mRNA decay. *Nat Struct Mol Biol* **25**, 1077-1085.

Nadarajan, S., Govindan, J. A., McGovern, M., Hubbard, E. J. and Greenstein, D. (2009). MSP and GLP-1/Notch signaling coordinately regulate actomyosin-dependent cytoplasmic streaming and oocyte growth in C. elegans. *Development* **136**, 2223-2234.

Nakahata, S., Kotani, T., Mita, K., Kawasaki, T., Katsu, Y., Nagahama, Y. and Yamashita, M. (2003). Involvement of Xenopus Pumilio in the translational regulation that is specific to cyclin B1 mRNA during oocyte maturation. *Mech Dev* **120**, 865-880.

Nakamura, T., Yao, R., Ogawa, T., Suzuki, T., Ito, C., Tsunekawa, N., Inoue, K., Ajima, R., Miyasaka, T., Yoshida, Y., et al. (2004). Oligo-astheno-teratozoospermia in mice lacking Cnot7, a regulator of retinoid X receptor beta. *Nat Genet* **36**, 528-533.

Naudin, C., Hattabi, A., Michelet, F., Miri-Nezhad, A., Benyoucef, A., Pflumio, F., Guillonneau, F., Fichelson, S., Vigon, I., Dusanter-Fourt, I., et al. (2017). PUMILIO/FOXP1 signaling drives expansion of hematopoietic stem/progenitor and leukemia cells. *Blood* **129**, 2493-2506.

Noble, S. L., Allen, B. L., Goh, L. K., Nordick, K. and Evans, T. C. (2008). Maternal mRNAs are regulated by diverse P body-related mRNP granules during early Caenorhabditis elegans development. *J Cell Biol* **182**, 559-572.

Nott, A., Meislin, S. H. and Moore, M. J. (2003). A quantitative analysis of intron effects on mammalian gene expression. *RNA* **9**, 607-617.

Nousch, M., Techritz, N., Hampel, D., Millonigg, S. and Eckmann, C. R. (2013). The Ccr4-Not deadenylase complex constitutes the main poly(A) removal activity in C. elegans. *J Cell Sci* **126**, 4274-4285.

Nousch, M., Yeroslaviz, A. and Eckmann, C. R. (2019). Stage-specific combinations of opposing poly(A) modifying enzymes guide gene expression during early oogenesis. *Nucleic Acids Res* **47**, 10881-10893.

Novak, P., Wang, X., Ellenbecker, M., Feilzer, S. and Voronina, E. (2015). Splicing Machinery Facilitates Post-Transcriptional Regulation by FBFs and Other RNA-Binding Proteins in Caenorhabditis elegans Germline. *G3 (Bethesda)* **5**, 2051-2059.

Okano, H., Kawahara, H., Toriya, M., Nakao, K., Shibata, S. and Imai, T. (2005). Function of RNA-binding protein Musashi-1 in stem cells. *Exp Cell Res* **306**, 349-356.

Olivas, W. and Parker, R. (2000). The Puf3 protein is a transcript-specific regulator of mRNA degradation in yeast. *EMBO J* **19**, 6602-6611.

Opperman, L., Hook, B., DeFino, M., Bernstein, D. S. and Wickens, M. (2005). A single spacer nucleotide determines the specificities of two mRNA regulatory proteins. *Nat Struct Mol Biol* **12**, 945-951.

Orford, K. W. and Scadden, D. T. (2008). Deconstructing stem cell self-renewal: genetic insights into cell-cycle regulation. *Nat Rev Genet* **9**, 115-128.

Ota, R., Kotani, T. and Yamashita, M. (2011). Biochemical characterization of Pumilio1 and Pumilio2 in Xenopus oocytes. *J Biol Chem* **286**, 2853-2863.

Parisi, M. and Lin, H. (1999). The Drosophila pumilio gene encodes two functional protein isoforms that play multiple roles in germline development, gonadogenesis, oogenesis and embryogenesis. *Genetics* **153**, 235-250.

Pazdernik, N. and Schedl, T. (2013). Introduction to germ cell development in Caenorhabditis elegans. *Adv Exp Med Biol* **757**, 1-16.

Pepper, A. S., Killian, D. J. and Hubbard, E. J. (2003a). Genetic analysis of Caenorhabditis elegans glp-1 mutants suggests receptor interaction or competition. *Genetics* **163**, 115-132.

Pepper, A. S., Lo, T. W., Killian, D. J., Hall, D. H. and Hubbard, E. J. (2003b). The establishment of Caenorhabditis elegans germline pattern is controlled by overlapping proximal and distal somatic gonad signals. *Dev Biol* **259**, 336-350.

Peters, J. M. (2002). The anaphase-promoting complex: proteolysis in mitosis and beyond. *Mol Cell* **9**, 931-943.

Popp, M. W. and Maquat, L. E. (2014). The dharma of nonsense-mediated mRNA decay in mammalian cells. *Mol Cells* **37**, 1-8.

Porter, D. F., Prasad, A., Carrick, B. H., Kroll-Connor, P., Wickens, M. and Kimble, J. (2019). Toward Identifying Subnetworks from FBF Binding Landscapes in. *G3 (Bethesda)* **9**, 153-165.

Prasad, A., Porter, D. F., Kroll-Conner, P. L., Mohanty, I., Ryan, A. R., Crittenden, S. L., Wickens, M. and Kimble, J. (2016). The PUF binding landscape in metazoan germ cells. *RNA* **22**, 1026-1043.

Puoti, A. and Kimble, J. (1999). The Caenorhabditis elegans sex determination gene mog-1 encodes a member of the DEAH-Box protein family. *Mol Cell Biol* **19**, 2189-2197.

---- (2000). The hermaphrodite sperm/oocyte switch requires the Caenorhabditis elegans homologs of PRP2 and PRP22. *Proc Natl Acad Sci U S A* **97**, 3276-3281.

Qiu, C., Bhat, V. D., Rajeev, S., Zhang, C., Lasley, A. E., Wine, R. N., Campbell, Z. T. and Hall, T. M. T. (2019). A crystal structure of a collaborative RNA regulatory complex reveals mechanisms to refine target specificity. *Elife* **8**.

Quenault, T., Lithgow, T. and Traven, A. (2011). PUF proteins: repression, activation and mRNA localization. *Trends Cell Biol* **21**, 104-112.

Ratti, A., Fallini, C., Cova, L., Fantozzi, R., Calzarossa, C., Zennaro, E., Pascale, A., Quattrone, A. and Silani, V. (2006). A role for the ELAV RNA-binding proteins in neural stem cells: stabilization of Msi1 mRNA. *J Cell Sci* **119**, 1442-1452.

Reinke, V., Gil, I. S., Ward, S. and Kazmer, K. (2004). Genome-wide germline-enriched and sex-biased expression profiles in Caenorhabditis elegans. *Development* **131**, 311-323.

Rezza, A., Skah, S., Roche, C., Nadjar, J., Samarut, J. and Plateroti, M. (2010). The overexpression of the putative gut stem cell marker Musashi-1 induces tumorigenesis through Wnt and Notch activation. *J Cell Sci* **123**, 3256-3265.

Roy, D., Michaelson, D., Hochman, T., Santella, A., Bao, Z., Goldberg, J. D. and Hubbard, E. J. A. (2016). Cell cycle features of C. elegans germline stem/progenitor cells vary temporally and spatially. *Dev Biol* **409**, 261-271.

Salvetti, A., Rossi, L., Lena, A., Batistoni, R., Deri, P., Rainaldi, G., Locci, M. T., Evangelista, M. and Gremigni, V. (2005). DjPum, a homologue of Drosophila Pumilio, is essential to planarian stem cell maintenance. *Development* **132**, 1863-1874.

Schindelin, J., Arganda-Carreras, I., Frise, E., Kaynig, V., Longair, M., Pietzsch, T., Preibisch, S., Rueden, C., Saalfeld, S., Schmid, B., et al. (2012). Fiji: an open-source platform for biological-image analysis. *Nat Methods* **9**, 676-682.

Schmidt, D. J., Rose, D. J., Saxton, W. M. and Strome, S. (2005). Functional analysis of cytoplasmic dynein heavy chain in Caenorhabditis elegans with fast-acting temperature-sensitive mutations. *Mol Biol Cell* **16**, 1200-1212.

Schultz, E. (1974). A quantitative study of the satellite cell population in postnatal mouse lumbrical muscle. *Anat Rec* **180**, 589-595.

---- (1985). Satellite cells in normal, regenerating and dystrophic muscle. *Adv Exp Med Biol* **182**, 73-84.

Seidel, H. S. and Kimble, J. (2015). Cell-cycle quiescence maintains Caenorhabditis elegans germline stem cells independent of GLP-1/Notch. *Elife* **4**.

Shan, L., Wu, C., Chen, D., Hou, L., Li, X., Wang, L., Chu, X., Hou, Y. and Wang, Z. (2017). Regulators of alternative polyadenylation operate at the transition from mitosis to meiosis. *J Genet Genomics* **44**, 95-106.

Shigunov, P., Sotelo-Silveira, J., Kuligovski, C., de Aguiar, A. M., Rebelatto, C. K., Moutinho, J. A., Brofman, P. S., Krieger, M. A., Goldenberg, S., Munroe, D., et al. (2012). PUMILIO-2 is involved in the positive regulation of cellular proliferation in human adipose-derived stem cells. *Stem Cells Dev* **21**, 217-227.

Shiimori, M., Inoue, K. and Sakamoto, H. (2013). A specific set of exon junction complex subunits is required for the nuclear retention of unspliced RNAs in Caenorhabditis elegans. *Mol Cell Biol* **33**, 444-456.

Shin, H., Haupt, K. A., Kershner, A. M., Kroll-Conner, P., Wickens, M. and Kimble, J. (2017). SYGL-1 and LST-1 link niche signaling to PUF RNA repression for stem cell maintenance in Caenorhabditis elegans. *PLoS Genet* **13**, e1007121.

Sijen, T., Fleenor, J., Simmer, F., Thijssen, K. L., Parrish, S., Timmons, L., Plasterk, R. H. and Fire, A. (2001). On the role of RNA amplification in dsRNA-triggered gene silencing. *Cell* **107**, 465-476.

Simons, B. D. and Clevers, H. (2011). Strategies for homeostatic stem cell self-renewal in adult tissues. *Cell* **145**, 851-862.

Snow, M. H. (1977). The effects of aging on satellite cells in skeletal muscles of mice and rats. *Cell Tissue Res* **185**, 399-408.

Sonoda, J. and Wharton, R. P. (1999). Recruitment of Nanos to hunchback mRNA by Pumilio. *Genes Dev* **13**, 2704-2712.

---- (2001). Drosophila Brain Tumor is a translational repressor. *Genes Dev* **15**, 762-773.

Sorokin, E. P., Gasch, A. P. and Kimble, J. (2014). Competence for chemical reprogramming of sexual fate correlates with an intersexual molecular signature in Caenorhabditis elegans. *Genetics* **198**, 561-575.

Stead, E., White, J., Faast, R., Conn, S., Goldstone, S., Rathjen, J., Dhingra, U., Rathjen, P., Walker, D. and Dalton, S. (2002). Pluripotent cell division cycles are driven by ectopic Cdk2, cyclin A/E and E2F activities. *Oncogene* **21**, 8320-8333.

Strome, S. and Wood, W. B. (1982). Immunofluorescence visualization of germ-line-specific cytoplasmic granules in embryos, larvae, and adults of Caenorhabditis elegans. *Proc Natl Acad Sci U S A* **79**, 1558-1562.

Stumpf, C. R., Kimble, J. and Wickens, M. (2008). A Caenorhabditis elegans PUF protein family with distinct RNA binding specificity. *RNA* **14**, 1550-1557.

Suh, N., Crittenden, S. L., Goldstrohm, A., Hook, B., Thompson, B., Wickens, M. and Kimble, J. (2009). FBF and its dual control of gld-1 expression in the Caenorhabditis elegans germline. *Genetics* **181**, 1249-1260.

Sönnichsen, B., Koski, L. B., Walsh, A., Marschall, P., Neumann, B., Brehm, M., Alleaume, A. M., Artelt, J., Bettencourt, P., Cassin, E., et al. (2005). Full-genome RNAi profiling of early embryogenesis in Caenorhabditis elegans. *Nature* **434**, 462-469.

Thompson, B. E., Bernstein, D. S., Bachorik, J. L., Petcherski, A. G., Wickens, M. and Kimble, J. (2005). Dose-dependent control of proliferation and sperm specification by FOG-1/CPEB. *Development* **132**, 3471-3481.

Timmons, L. and Fire, A. (1998). Specific interference by ingested dsRNA. *Nature* **395**, 854.

Ulbricht, R. J. and Olivas, W. M. (2008). Puf1p acts in combination with other yeast Puf proteins to control mRNA stability. *RNA* **14**, 246-262.

Uyhazi, K. E., Yang, Y., Liu, N., Qi, H., Huang, X. A., Mak, W., Weatherbee, S. D., de Prisco, N., Gennarino, V. A., Song, X., et al. (2020). Pumilio proteins utilize distinct regulatory mechanisms to achieve complementary functions required for pluripotency and embryogenesis. *Proc Natl Acad Sci U S A* **117**, 7851-7862.

van der Voet, M., Lorson, M. A., Srinivasan, D. G., Bennett, K. L. and van den Heuvel, S. (2009). C. elegans mitotic cyclins have distinct as well as overlapping functions in chromosome segregation. *Cell Cycle* **8**, 4091-4102.

Van Etten, J., Schagat, T. L., Hrit, J., Weidmann, C. A., Brumbaugh, J., Coon, J. J. and Goldstrohm, A. C. (2012). Human Pumilio proteins recruit multiple deadenylases to efficiently repress messenger RNAs. *J Biol Chem* **287**, 36370-36383.

Vardy, L. and Orr-Weaver, T. L. (2007). The Drosophila PNG kinase complex regulates the translation of cyclin B. *Dev Cell* **12**, 157-166.

Voronina, E., Paix, A. and Seydoux, G. (2012). The P granule component PGL-1 promotes the localization and silencing activity of the PUF protein FBF-2 in germline stem cells. *Development* **139**, 3732-3740.

Voronina, E., Seydoux, G., Sassone-Corsi, P. and Nagamori, I. (2011). RNA granules in germ cells. *Cold Spring Harb Perspect Biol* **3**.

Wahle, E. and Winkler, G. S. (2013). RNA decay machines: deadenylation by the Ccr4-not and Pan2-Pan3 complexes. *Biochim Biophys Acta* **1829**, 561-570.

Wang, C., Wilson-Berry, L., Schedl, T. and Hansen, D. (2012). TEG-1 CD2BP2 regulates stem cell proliferation and sex determination in the C. elegans germ line and physically interacts with the UAF-1 U2AF65 splicing factor. *Dev Dyn* **241**, 505-521.

Wang, M., Ogé, L., Perez-Garcia, M. D., Hamama, L. and Sakr, S. (2018). The PUF Protein Family: Overview on PUF RNA Targets, Biological Functions, and Post Transcriptional Regulation. *Int J Mol Sci* **19**.

Wang, X., McLachlan, J., Zamore, P. D. and Hall, T. M. (2002). Modular recognition of RNA by a human pumilio-homology domain. *Cell* **110**, 501-512.

Wang, X., Olson, J. R., Rasoloson, D., Ellenbecker, M., Bailey, J. and Voronina, E. (2016). Dynein light chain DLC-1 promotes localization and function of the PUF protein FBF-2 in germline progenitor cells. *Development* **143**, 4643-4653.

Wang, X., Zamore, P. D. and Hall, T. M. (2001). Crystal structure of a Pumilio homology domain. *Mol Cell* **7**, 855-865.

Webster, M. W., Stowell, J. A. and Passmore, L. A. (2019). RNA-binding proteins distinguish between similar sequence motifs to promote targeted deadenylation by Ccr4-Not. *Elife* **8**.

Weidmann, C. A. and Goldstrohm, A. C. (2012). Drosophila Pumilio protein contains multiple autonomous repression domains that regulate mRNAs independently of Nanos and brain tumor. *Mol Cell Biol* **32**, 527-540.

Weidmann, C. A., Qiu, C., Arvola, R. M., Lou, T. F., Killingsworth, J., Campbell, Z. T., Tanaka Hall, T. M. and Goldstrohm, A. C. (2016). Drosophila Nanos acts as a molecular clamp that modulates the RNA-binding and repression activities of Pumilio. *Elife* **5**.

Weidmann, C. A., Raynard, N. A., Blewett, N. H., Van Etten, J. and Goldstrohm, A. C. (2014). The RNA binding domain of Pumilio antagonizes poly-adenosine binding protein and accelerates deadenylation. *RNA* **20**, 1298-1319.

White, J. and Dalton, S. (2005). Cell cycle control of embryonic stem cells. *Stem Cell Rev* **1**, 131-138.

Wickens, M., Bernstein, D. S., Kimble, J. and Parker, R. (2002). A PUF family portrait: 3'UTR regulation as a way of life. *Trends Genet* **18**, 150-157.

Wilinski, D., Qiu, C., Lapointe, C. P., Nevil, M., Campbell, Z. T., Tanaka Hall, T. M. and Wickens, M. (2015). RNA regulatory networks diversified through curvature of the PUF protein scaffold. *Nat Commun* **6**, 8213.

Wreden, C., Verrotti, A. C., Schisa, J. A., Lieberfarb, M. E. and Strickland, S. (1997). Nanos and pumilio establish embryonic polarity in Drosophila by promoting posterior deadenylation of hunchback mRNA. *Development* **124**, 3015-3023.

Wu, J., Campbell, Z. T., Menichelli, E., Wickens, M. and Williamson, J. R. (2013). A protein.protein interaction platform involved in recruitment of GLD-3 to the FBF.fem-3 mRNA complex. *J Mol Biol* **425**, 738-754.

Zamore, P. D., Williamson, J. R. and Lehmann, R. (1997). The Pumilio protein binds RNA through a conserved domain that defines a new class of RNA-binding proteins. *RNA* **3**, 1421-1433.

Zanetti, S., Grinschgl, S., Meola, M., Belfiore, M., Rey, S., Bianchi, P. and Puoti, A. (2012). The sperm-oocyte switch in the C. elegans hermaphrodite is controlled through steady-state levels of the fem-3 mRNA. *RNA* **18**, 1385-1394.

Zanetti, S., Meola, M., Bochud, A. and Puoti, A. (2011). Role of the C. elegans U2 snRNP protein MOG-2 in sex determination, meiosis, and splice site selection. *Dev Biol* **354**, 232-241.

Zanetti, S. and Puoti, A. (2013). Sex determination in the Caenorhabditis elegans germline. *Adv Exp Med Biol* **757**, 41-69.

Zhang, B., Gallegos, M., Puoti, A., Durkin, E., Fields, S., Kimble, J. and Wickens, M. P. (1997). A conserved RNA-binding protein that regulates sexual fates in the C. elegans hermaphrodite germ line. *Nature* **390**, 477-484.

Zhang, M., Chen, D., Xia, J., Han, W., Cui, X., Neuenkirchen, N., Hermes, G., Sestan, N. and Lin, H. (2017). Post-transcriptional regulation of mouse neurogenesis by Pumilio proteins. *Genes Dev* **31**, 1354-1369.

Zhong, W. and Sternberg, P. W. (2006). Genome-wide prediction of C. elegans genetic interactions. *Science* **311**, 1481-1484.

Łabno, A., Tomecki, R. and Dziembowski, A. (2016). Cytoplasmic RNA decay pathways - Enzymes and mechanisms. *Biochim Biophys Acta* **1863**, 3125-3147.